University of Alberta

# Systematics of an Oligocene-Aged Fossil Snake Assemblage from the White River Formation, Wyoming.

by

Jasmine Croghan

A thesis submitted to the Faculty of Graduate Studies and Research
in partial fulfillment of the requirements for the degree of

Master of Science
in
Systematics and Evolution

Department of Biological Sciences

Spring 2014
Edmonton, Alberta

# ABSTRACT

Extinct snake taxa are primarily recognized from isolated vertebrae. A new specimen from the Oligocene of Wyoming provides a rare opportunity to examine four nearly complete and articulated fossil snakes. Informally assigned previously to the 'erycine' vertebral form taxa *Ogmophis* and *Calamagras,* a comparison reveals that the diagnostic morphology of both genera are present in a single individual of the new specimen, invalidating these assignments. A new taxon, *Congerophis lego* is described and erected, and its phylogenetic relationships are tested using two existing morphological datasets of all snakes and of the 'Erycinae.' *Congerophis lego* is found to be in the sister-group position to the New World 'erycine' *Charina.* When *Charina* and the Old World 'erycine' *Eryx* are scored separately and analyzed with relevant outgroup taxa, the subfamily is found to be non-monophyletic. The new subfamily Charininae, inclusive of *Charina* and *Congerophis,* is erected, and the 'Erycinae' is redefined as monogeneric.

# Acknowledgements

First and foremost, I would like to extend my deepest thanks to my advisor and friend, Dr. Michael Caldwell, for his continual support (academically and non-), deep, informative discussions, the funding for this venture, and maybe a little bit of whip-cracking as well.

I cannot thank enough, my colleague and good friend Dr. Alessandro Palci, for his tireless aid and companionship.  I would be a lot farther from where I am without his help, his incredible knowledge of modern and fossil Squamata, the answering of my many millions of questions, his companionship on all of my travels, and his function as a wonderful and informative sounding board for my ideas.  Your patience is deep, my friend, and you will make a wonderful advisor soon enough!

Of course, without the incredible support of my fellow graduate students at the University of Alberta, my ladies and honorary ladies, I may not be as sane, healthy, or happy as I am, a large contributing factor to my success as a graduate student.  So I thank, in no particular order, Hallie Street, Gavin Bradley, Michelle Campbell, Betsy Kruk, Stephanie Blais, Kelly Grieve, Thodoris Argyriou, Paulina Jimenez Huidobro, and Tiago Simoes.

Finally, I would like to thank my partner through it all, Shad Bauer. Your constant support of my dreams and goals as well as your own is a rare thing to have, and I feel very lucky to have you in my life.

# TABLE OF CONTENTS

## SUMMARY OF FIGURES

# CHAPTER 1

# INTRODUCTION

The Cenozoic of North America has yielded a bounty of fossil snakes. Although isolated or short strings of vertebrae are common in the North American record of fossil snakes, cranial material and complete specimens are exceedingly rare. A new specimen from the exposures of the Oligocene-aged White River Formation in Converse County Wyoming, University of Wyoming specimen UW11120, consists of four spectacularly preserved, nearly complete individuals, preserved articulated in three dimensional, life-like positions. This specimen provides a unique opportunity to study the rarely preserved whole cranial and whole vertebral column morphology of four individual Palaeogene snakes.

Henophidian snakes dominated the snake fauna of North America prior to the middle Miocene colubroid expansion (Savitzky, 1980; Holman, 2000), and the majority of that earlier diversity is among the so-called "erycine boas". The extinct North American erycines s.l. are represented by seven genera divided into twenty four species, known only from isolated vertebrae to short strings of articulated vertebra (~6): *Ogmophis, Calamagras, Tregophis, Helagras, Huberophis, Geringophis, Pterygoboa* (Holman, 2000). Of these, *Ogmophis* (Cope,

1884) and *Calamagras* (Cope, 1873) are the most common, well known, and speciose, containing, respectively, six and seven species in North America.

The term "erycine boa" implies that the extinct taxa are both part of the subfamily 'Erycinae' (Bonaparte, 1831) and the broader family 'Boidae', Gray, 1825. The current fluid nature of snake systematics requires that both the 'Erycinae' and the 'Boidae' be referred to informally, and given meaning outside of a phylogenetic context. A 'boid' refers to a medium-to-exceedingly large non-venomous snake of predominantly New World distribution. They are characterized as relatively primitive, possessing vestigial hind limbs and a robust, basal macrostomatan skull. They do not possess premaxillary teeth or a supraorbital ossification and are live-bearers, all features that distinguish the boids from the closely related 'pythonids', which also fall under the 'Booidea' (Greene, 1997). The modern Erycinae sensu lato are medium sized, non-venomous, semi-fossorial snakes with distinct Old World and New World populations. They possess a unique, fused "club-tail" consisting of several bony elaborations of the caudal vertebrae. Their semi-fossorial habit is linked to several morphological features, such as a broadened and reinforced rostrum for burrowing, and low neural spines of the vertebrae (Greene, 1997).

Named the Erycina by Bonaparte, 1831, to classify several members of the Old World genus *Eryx*, Daudin, 1803, the Erycinae sensu lato did not see the addition of the extant New World taxa until the suggestion of Hoffstetter (1962) who hypothesized a close relationship between the Old World genus *Eryx* and the New World genus *Charina* on the basis of the unique elaborations and additional apophyses in the caudal vertebrae. Underwood (1967), though accepting of Hoffstetter's (1962) placement of *C. bottae,* placed *C. trivirgata*, somewhere within the boines, though caudal vertebrae had not yet been studied for the taxon.

All familial assignments prior to Hoffstetter (1962) had been based entirely on quantitative measures and phenetic measures of overall similarity. The Erycinae s.l. was finally diagnosed by synapomorphies by Hoffstetter and Rage (1972). This synapomorphy list was created out of the need for osteological characteristics for the assignment of several European fossils postulated to be part of the Erycinae s.l. Hoffstetter and Rage's (1972) synapomorphies include: the lacrimal foramen is not entirely surrounded by the prefrontal; the palatine foramen is not entirely surrounded by the palatine, the neural arch is flattened; the neural spine of the trunk vertebrae is usually low; the prezygapophyseal process is very reduced but not absent; the neural spines of the caudal vertebra are swollen.

The Erycinae s.l. was not the subject of a detailed phylogenetic treatment until Kluge (1993) who argued for the assignment of *Calabaria reinhardtii* (initially a species of *Eryx,* Schlegel, 1851) to the subfamily. Kluge (1993) also went on to explore the relationships of the fourteen accepted species of erycines s.l., and assessed the monophyly of the subfamily as a whole. The synapomorphies recovered by Kluge (1993) are as follows: the loss of the lateral and medial heads on the anterior end of the ectopterygoid; the palatine contacting a wide ledge of bone projecting medially from the pterygoid; the maxillary process of the palatine lying posteriorly, at the level of the palatine-pterygoid contact; the right posterior opening for the vidian canal being larger than the left; caudal neural spines that are grooved dorsally; an accessory process on the neural arch of a caudal vertebra. Since Kluge (1993), the subfamily has been considered monophyletic, and morphological phylogenetic analyses tend to treat it as a single terminal taxon (e.g., Cundall, 1993; Tchernov et al., 2000; Lee and Scanlon, 2002; Gauthier et al., 2012; Longrich et al., 2012; and Zaher and Scanferla, 2012).

Concerning UW11120 specifically, there has been very little formal published work completed on the specimen in order to address phylogenetic and evolutionary questions. The first, and to date, only published manuscript is that of Breithaupt and Duvall (1986) who described the unique mode of preservation of UW11120, but did not describe the specimens nor formally assign them to a taxon. Instead, they gave a brief description of the find and informally designated the larger individual *Ogmophis* sp. and the smaller individuals *Calamagras* sp., "based on vertebral characteristics". They summarized the taphonomy of the specimen, hypothesizing that these individuals died while over-wintering in a burrow, as suggested by their life-like positions, after which they were buried relatively rapidly.

Caldwell, Breithaupt, and Bamforth (2007) in an unpublished poster abstract examined the probable synonomy of several species of *Ogmophis* and *Calamagras*. Using UW11120, the authors compared the variability of the vertebral form along the columns of these complete individuals to the variable morphologies observed on the isolated vertebrae of species of *Ogmophis* and *Calamagras*, including *O. oregonensis, O. compactus, O. platyspondyla, C. murivorus, C. weigeli,* and *C. angulatus.* The authors recommended *Ogmophis* be considered a junior synonym of *Calamagras*, and that *Calamagras* be retained for nomenclatural stability. The as yet undiscovered caudal vertebrae left open the question of whether the specimen was to be considered an erycine.

Croghan, Caldwell, and Breithaupt (2012), in another poster abstract, provided some of the first views of the cranial material of UW11120 to the scientific community. The authors compiled a list of erycine s.l. synapomorphies from three well-respected sources: Rage (1984), Kluge (1993), and Gauthier et al. (2012), scoring UW11120 in the first test of whether or not the specimens could be considered erycine s.l. According to their analysis, the cranial material was most likely erycine s.l., but the problem of the absent caudal vertebrae prevented a definitive assignment. Additionally, the material was compared to non-erycines s.l., and it was discovered that nearly every synapomorphy listed could be found in closely related snakes outside of the Erycinae s.l., casting doubt on the monophyly of the subfamily.

In this thesis, I will expand on previous works by examining the specific affinities of the White River specimens (UW11120) in order to then address broader questions in snake systematics. For example, does the Erycinae s.l. represent a monophyletic group, or has convergence led to the independent evolution of caudal vertebral elaborations, and thus contributed to the long-standing assumption of their monophyly? The White River specimen allows a deeper inquiry into the evolutionary history of this enigmatic group by providing erycine features in the absence of caudal elaborations. I also will consider more theoretical problems, such as the question of whether a single trunk vertebra is sufficient for making a species diagnosis. Using the nearly complete individuals in UW11120, it is possible to explore the amount of overlap between this specimen and the 24 species of erycine s.l. found in the Cenozoic of North America.

In Chapter 2 I will describe a new fossil snake taxon based on the nearly complete material of UW11120. Once described and compared to similar taxa, I will place the new taxon in phylogenetic context, utilizing two recent, relevant character matrices, one in the broad context of Serpentes (Palci et al., 2013), and one that is specific to the subfamily Erycinae s.l. (Kluge, 1993). I will then modify the Kluge (1993) data matrix to include closely related taxa, based on the results of the analysis of Palci et al. (2013), as a test of Kluge's (1993) hypothesis of a monophyletic Erycinae s.l.

In Chapter 3, I intend to make progress towards the form taxon problem dominating North American snake paleontology. The vertebrae comprising the vertebral column of UW11120 will be compared with similar fossil snake vertebrae that have been assigned to the subfamily Erycinae s.l., e.g., various species of *Ogmophis* and *Calamagras*. The vertebrae of several modern taxa will also be compared to UW 11120 and to *Ogmophis* and *Calamagras*. On the basis of their morphological similarity, and non-diagnostic nature, to parts of the vertebral column of UW11120, various species of *Ogmophis* and *Calamagras* will be referred to the taxon erected for UW11120. All species of these genera not reassigned to the taxon of UW11120 are considered *nomina dubia*.

# LITERATURE CITED

Bonaparte, C.L. 1831. Saggio di una distribuzione metodica degli animali vertebrati. Rome, 86 pp.

Breithaupt, B.H., and D. Duvall, 1986. The oldest record of serpent aggregation. Lethaia 19:181-185.

Caldwell, M.W., B.H. Breithaupt, and E. Bamforth. 2007. The Oligocene erycine snakes, *Ogmophis* and *Calamagras*: New material clarifies vertebral-form species. Journal of Vertebrate Paleontology 27(3):55A.

Cope, E.D., 1873. Synopsis of new vertebrata from the Tertiary of Colorado, obtained during the summer of 1873. Washington, D.C. U.S. Government Printing Office 1-19.

Cope, E.D., 1883. The Vertebrata of the Tertiary formations of the West. Book I. Reports of the United States Geological Survey of the Territories, F. V. Hayden, United States Geologist-in-Charge 3:1-1002.

Croghan, J.A., M.W. Caldwell, and B.H. Breithaupt. 2012. *Ogmophis, Calamagras* and the 32 million year old aggregation of snakes from the White River Formation: Are they erycines? 32:82A.

Cundall, D., V. Wallach, and D.A. Rossman. 1993. The systematic relationships of the snake genus *Anomochilus.* Zoological Journal of the Linnean Society, 109(3):275-299.

Gauthier, J.A., M. Kearney, J.A. Maisano, O. Rieppel, and A.D.B. Behlke. 2012. Assembling the squamate tree of life: Perspectives from the phenotype and the fossil record. Bulletin of the Peabody Museum of Natural History 53(1):3–308.

Greene, H. W. 1997. Snakes: The Evolution of Mystery In Nature. University of California Press, 356p.

Hoffstetter, R., 1962. Revue des recéntes acquisitions concernant l'histoire et la systématique des Squamates. Colloques Internationaux du Centre National de la Recherche Scientifique 104:243-278.

Hoffstetter, R., J.-C. Rage. 1972. .Les Erycinae fossiles de France (Serpentes, Boidae): compréhension et histoire de la sous-famille. Annales de Paléontologie (Vértebrés) 58:82–124, pl.I–II.

Holman, J. A., 2000. Fossil Snakes of North America: Origin, Evolution, Distribution, Paleoecology. Indiana University Press, Bloomington, Indiana, 376p.

Kluge, A. G. 1993. *Calabaria* and the phylogeny of erycine snakes. Zoological Journal of the Linnean Society 107:293-351.

Lee, M. S. Y., and J. D. Scanlon. 2002. Snake phylogeny based on osteology, soft anatomy and ecology. Biological Reviews 77:333-401.

Longrich, N. R., B.-A. S. Bhullar, and J. A. Gauthier. 2012. A transitional snake from the Late Cretaceous period of North America. Nature 488:205-208.

Palci, A., M. W. Caldwell, and R. L. Nydam. 2013. Reevaluation of the anatomy of the Cenomanian (Upper Cretaceous) hind-limbed marine fossil snakes *Pachyrhachis*, *Haasiophis* and *Eupodophis.* Journal of Vertebrate Paleontology, 33:1328-1342.

Rage, J.-C. 1984. Serpentes. Handbuch der Paläoherpetologie, v. 11, Gustav Fischer Verlag, Stuttgart, 80pp.

Savitzky, A. H. 1980. The role of venom delivery strategies in snake evolution. Evolution 34(6):1194-1204.

Schlegel, H. 1851. Description d'une nouvelle espèce du genre *Eryx*, *Eryx reinhardtii.* Bijdragen tot de Dierkunde, Amsterdam 1:1-3.

Tchernov, E., O. Rieppel, H. Zaher, M. J. Polcyn, and L. L. Jacobs. 2000. A fossil snake with limbs. Science, 287(5460):2010-2012.

Underwood, G. 1967. A Contribution to the Classification of Snakes. British Museum of Natural History, London. 179pp.

Zaher, H., and C. A. Scanferla. 2012. The skull of the Upper Cretaceous snake *Dinilysia patagonica* Smith-Woodward, 1901, and its phylogenetic position revisited. Zoological Journal of the Linnean Society, 164:194-238.

# CHAPTER 2

# A NEW FOSSIL GENUS AND SPECIES OF NORTH AMERICAN ‘ERYCINE’ SNAKE, AND A PHYLOGENETIC ANALYSIS OF THE ‘ERYCINAE’

Manuscript to be submitted to Systematic Paleontology as: Croghan, J., Caldwell, M.W., & Breithaupt, B.B., “A New Fossil Genus and Species of North American ‘Erycine’ Snake, and a Phylogenetic Analysis of the ‘Erycinae’

# INTRODUCTION

The existence of complete, well preserved fossil snake skeletons, including three dimensionally preserved skulls, is exceedingly rare (see Breithaupt and Duvall, 1986, for a list). To find an assemblage of three exceptionally well preserved fossil snakes with articulated skeletons and skulls, and an associated second block with a fourth equally well preserved individual snake, UW11120, is singularly unique. Using this execptional specimen, a new fossil snake taxon is described from four articulated individuals from the early Orellan White River Formation exposures of Converse County, Wyoming. Instead of a single holotype, we designate three syntypes (Article 73.2 of the ICZN): three nearly complete skulls (A, B, and C) and their articulated, nearly complete vertebral columns in a single block of rock broken into two pieces (blocks 2 and 3). Referred materials include a partial skull (D) with its nearly complete, articulated postcrania on a second block of rock (block 1). The cranial details of the new taxon are derived from Skull A and Skull B, while details of the axial skeleton are derived from all four individuals. Skulls C and D were less complete than A and B and showed no details of cranial architecture for matching elements that were different than those observed in A and B.

Breithaupt and Duvall (1986), in the only previous work on these specimens described only their unique mode of preservation. Three individuals

(Skulls A, B, and C and their skeletons) were interpreted as the earliest evidence of snake aggregation, loosely coiled around one another in life-like positions on a roughly horizontal plane, in what was considered to be a burrow structure (Breithaupt and Duvall, 1986). Though isolated or short strings of snake vertebrae are often found in the White River Fm., these nearly complete, exceptionally preserved individuals represent the most complete record found to date of a snake from this formation. The exceptional preservation of the delicate cranial bones in three dimensions presents a unique opportunity to study these fossil snakes in unprecedented detail.

Breithaupt and Duvall (1986) speculated, based on their relative size and the low neural spines present on the vertebrae, that the larger individual, Skull B, might be assigned to the vertebral form taxon *Ogmophis* Cope, 1884, and the smaller, Skull A, might be assigned to the vertebral form taxon *Calamagras* Cope, 1873. These two fossil vertebral form taxa are commonly recognized in the North American Cenozoic record, with two putative species found in Poland and France (Rage, 1984). Breithaupt and Duvall (1986) made no formal assignment of these specimens to the aforementioned genera, but speculated they belonged to the subfamily 'Erycinae' as *Ogmophis* and *Calamagras* had been referred to the subfamily 'Erycinae'. This referral was based on their general booid-like vertebral morphology, possessing low neural spines and depressed neural arches, despite the lack of any truly diagnostic features for the modern subfamily 'Erycinae'.

The subfamily 'Erycinae' has a long history of assumed monophyly. Hoffstetter (1962) was the first to suggest a close relationship between the Old World genus *Eryx* and the New World genus *Charina* on the basis of the unique elaborations and additional apophyses in the caudal vertebrae. Underwood (1967), accepted Hoffstetter's (1962) placement of *C. bottae,* but placed *C. trivirgata* somewhere within the boines, though caudal vertebrae had not yet been studied for the taxon. Though neither of these hypotheses were tested using methods similar to modern cladistics, subsequent studies of snake phylogeny using morphological data sets have assumed erycine monophyly ever since without testing ingroup relationships (see Cundall, 1993; Tchernov et al., 2000; Lee and Scanlon, 2002; Gauthier et al., 2012; Longrich et al., 2012; Zaher and Scanferla, 2012). Recent studies using molecular data sets, have found the Erycinae s.l. to be non-monoplyletic. The Old World and one New World erycines s.l. group into two distinct clades bounded by their geography (Vidal and Hedges, 2002; Slowinski and Lawson, 2002; Noonan and Chippendale, 2006; Weins, et al., 2012; Pyron, Burbrink, and Weins, 2013). While molecular systematists were not explicitly testing erycine monophyly, the methods of obtaining molecular data from individual snakes, and using them as terminal taxa in the analysis, meant that erycine monophyly was not assumed in the same manner as it has been assumed for so long by morphological systematists.

Examinations of ingroup relationships have been few in number, with Hoffstetter and Rage (1972) creating the first set of diagnostic characters for the group, and Kluge (1993), who ran a phylogenetic analysis of the modern species with the addition of the Calabar Ground Python (*Calabaria reinhardtii*), creating the first synapomorphy list for the group. Kluge's (1993) starting assumption was that the python *Calabaria reinhardtii* was an 'erycine', and he set out to demonstrate that assumption by including it in his ingroup of typical erycines without including other taxa outside of the usual concept of erycines s.l.. The problem with Kluge's (1993) analysis is that if *Calabaria* is indeed not an erycine s.l., not a boine, and is in fact a python, then the presumed test of erycine interrelationships accomplished nothing at all. However, as Kluge's (1993) study remains the only ingroup analysis of accepted erycine taxa, it is a critical study to test assumptions that the fossil snakes represented by UW11120 are erycines.

The opposing hypotheses from morphological systematics, and mounting evidence from the molecular studies, have created doubt on the monophyly of the Erycinae s.l. This analysis will therefore test the monophyly of erycines s.l. in a global study of snakes to evaluate New and Old World erycines s.l. separately, and an ingroup analysis of erycines s.l.. In this analysis, we will test the informal assignment of the new specimens to the ‘erycine’ subfamily by including the two most accessible skulls (A and B) in a phylogenetic analyses, using two separate data matrices, one encompassing all modern snakes and fossil relatives (Palci et al., 2013) and one specific to the subfamily ‘Erycinae’ (Kluge, 1993).

## GEOLOGIC SETTING

The blocks of rock containing the four fossil snakes were collected by Mr. Kent Sundell in 1976 at University of Wyoming (UW) Locality V-75004, Converse County, Wyoming.  The White River Formation in the area of collection is early Orellan in age, radioisotopically dated using volcanic ash units elsewhere in the formation to a minimum age of 32 million years (Breithaupt and Duvall, 1986). The matrix surrounding the specimens is a buff-grey, fine sandy mudstone, likely deposited during a small flood episode, part of the cyclic fluvial deposits of mudstone, siltstone, and sandstone typical of the White River Fm. in the area of collection (Breithaupt and Duvall, 1986).

## INSTITUTIONAL ABBREVIATONS

American Museum of Natural History, New York, NY (AMNH); Field Museum of Natural History, Chicago, IL (FMNH); Muséum National d’Histoire Naturelle, Paris, France (MNHN), National History Museum, London, England

(NHML); Smithsonian Museum of Natural History, Washington D.C. (SMNH), Texas Natural History Collections at the University of Texas at Austin, Austin, TX (TNHC), University of Alberta Museum of Zoology (UAMZ), National Museum of Natural History, Washington, DC (USNM), University of Texas, Arlington, Arlington, TX (UTA), University of Wyoming, Laramie, WY (UW), Yale Peabody Museum (YPM).

## MATERIALS AND METHODS

For morphological comparisons, a series of skeletonized and computed tomography (CT)-scanned specimens were examined that belong to both living and fossil taxa for a total of 36 species of snakes (86 specimens).

Photographs of figured specimens were taken using a NIKON D300S. The CT-scan data for *Anilius scytale* (USNM 204078), *Boa constrictor* (FMNH 31182), *Calabaria reinhardtii* (FMNH 117833), *Casarea dussumieri* (TNHC 190285), *Charina* (*Lichanura*) *trivirgata* (YPM 12869), *Cylindrophis ruffus* (FMNH 60958), *Eryx colubrinus* (FMNH 63117), *Python molurus* (to be accessioned TNHC), *Tropidophis haetianus* (TNHCxxxx (JCO0011)), and *Ungaliophis continentalis* (UTA 50569) were acquired under the Deep Scaly Project (NSF grant EF-0334961) and kindly provided by M. Kearney and O. Rieppel.

One specimen of *Charina trivirgata* (UAMZ 3819) was CT-scanned using a Skyscan 1174 at the University of Alberta. The new fossil specimens, UW11120, were CT-scanned at the High-Resolution X-Ray Computed Tomography Facility at The University of Texas at Austin using an Xradia MicroXCT source for Skull A and an ACTIS ultra-high-resolution subsystem source for the remaining blocks. Scanning parameters were individually optimized and thus varied across specimens. The datasets were rendered in three dimensions using Avizo 7.1 (Visualization Sciences Group). The CT data and detailed scan parameters will be made available from the Digital Morphology database.

Modern, skeletonized material examined in this study, organized systematically, include: *Boa constrictor* NHML 59.7.30.35; *Epicrates cenchria* NHML 62.6.18.1; *Casarea dussumieri* MNHN 1993.3383; *Python molurus* NHML 1940.4.28.2, NHML 1971.2168; *Python reticulatus* NHML 1972.21.69; *Morelia spilota* NHML 88.10.27.2, NHML 1964.934, NHML 1987.2108; *Liasis amethistinus* NHML 77.3.3.1, NHML 85.6.30.61, NHML 1988.604; *Calabaria reinhardtii* NHML 96.3.9.3, NHML 1911.10.28.17; *Eryx (Gongylophis) conicus* NHML 52.11.3.1, NHML 1930.58.12, NHML 1930.5.8.14, NHML 1964.1224; *Eryx colubrinus* FMNH 223196, MNHN no number; *Eryx jaculus* FMNH 19624, MNHN no number, NHML 152G.VIII, NHML 1930.5.8.18; *Eryx jayakari* NHML 1909.10.15.8; *Eryx johnii* MNHN RH11, NHML 1930.5.8.25, NHML 1964.1227;

*Charina bottae* FMNH 1218, FMNH 22348, FMNH 31300, NHML 78.5.23, NHML 1969.2948; *Charina (Lichanura) trivirgata* UAMZ 3819, *C. t. roseofusca* NHML 94.3.24.4; *Tropidophis canus* AMNH R-45839, AMNH R-73066; *Ungaliophis panamensis* AMNH R-58845, AMNH R-62639; *Loxocemus bicolor* AMNH R-19393, AMNH R-4402, AMNH R-110151, NHML 82.8.17.16; *Xenopeltis unicolor* AMNH R-29969, AMNH R-71531, NHML 1947.1.1.10, NHML 1947.1.1.12, SMNH 287277; *Acrochordus javanicus* AMNH R-46251, AMNH R-89839; *Pareas carinatus* NHML 1964.1092, NHML 1964.1094; *Xenodermus javanicus* FMNH 67427.

Fossil material examined in this study, in alphabetical order, include: *Albaneryx dipereti* MNHN LGA1, MNHN LGA2, MNHN LGA3, MNHN LGA8, MNHN LGA9; *Bransateryx vireti* MNHN Cod 1, MNHN Cod 2, MNHN Cod 3, MNHN Cod 4, MNHN Cod 9, MNHN Cod 10; *Bransateryx* sp. MNHN Qu16311, MNHN Qu16312, MNHN Qu16314, MNHN Qu16315, MNHN Sg. 15; *Calamagras angulatus* AMNH 1654; *Calamagras murivorus* AMNH 1603; *Messelophis ermannorum* SMFME 759; *Messelophis variatus* SMFME 1828 a and b, SMFME 2379; *Paleopython* sp. NHML 11271; *Paraepicrates brevispondylus* AMNH 3829.

Data on the Erycinae s.l. were complimented by the works of Rieppel (1978) and Holman (2000). The many CT-derived animations available on DigiMorph.org for snakes also proved to be a useful resource.

## SYSTEMATIC PALEONTOLOGY

### REPTILIA Linnaeus, 1758

### SQUAMATA Oppel, 1811

### OPHIDIA Brongniart, 1800

### *Congerophis*, gen. nov.

**Etymology**–From the Latin ‘congeries’ (fem., an accumulation, a hill, pile, or heap), after the unique mode of preservation of the type specimen of three individuals together and the locality, named Snake Hill, and from the Greek ‘ophis’ (masc., serpent).

**Type Species**—*Congerophis lego,* sp. nov.

**Diagnosis**—As for the type and only known species.

### *Congerophis lego* sp. nov.

Figs. 2.1-2.7

**Etymology**–From the latin verb ‘lego’, (verb, in this instance meaning ‘to collect’), referring to the latin root of the word ‘coil’, the resting state of many modern snakes and the positions of the type specimens implying that they were at rest at the time of death.

**Syntypes**—Three complete to very complete individual snakes, designated A, B and C, on the two part specimen (Blocks 2 and 3) bearing the single specimen number UW11120.

**Type Locality**—University of Wyoming locality V-75004, Converse County, Wyoming.

**Referred Materials**—One relatively complete snake skeleton, designated specimen D, on Block 1, also bearing specimen number UW11120.

**Diagnosis**—Apomorphies of the taxon: Nearly absent crista tuberalis, subrectangular prootic that is anteroposteriorly more elongate than tall; a single foramen for the vomeronasal nervepresent in the vomer, high on the median wall forming the posterior wall of the vomeronasal capsule; low, smooth parasphenoid wings obscuring the anterior opening of the vidian canal; medially located foramen for the mandibular branch of the trigeminal nerve in the adductor fossa. Differs from *Charina* in having: a narrower maxillary process of the palatine; the lateral wall of the adductor fossa of the compound bone is higher than the medial wall; a transversely straight nasofrontal joint; a small, but present, parasphenoid wing; a forked anterior end of the ectopterygoid; a deep ventromedial groove in the quadrate ramus of the pterygoid; lack of distinct coronoid eminence; presence of a lateral foramen in the maxilla on at least one side.

## DESCRIPTION AND COMPARISONS

### General

The specimen consists of three blocks, two of which are associated (Blocks 2 and 3). Block 1 (Fig. 2.1) contains a single largely articulated individual, including a partial skull, in a burrow cast of gray mudstone. The partial skull, here referred to as Skull D, preserves large portions of the bones associated with the orbit and the nasals, but both the anterior and posterior thirds of the skull have been lost. From the preserved portion, Skull D was assigned to the same taxon as Skulls A and B. Blocks 2 and 3 (Fig. 2.2) preserve three largely articulated individuals, including three very complete skulls; the two blocks are associated and can be fitted back together, having only been broken during collection. One skull has been prepared loose from Block 2, and is here referred to as Skull A (Fig. 2.3). Skull A is from a smaller individual, and was disarticulated from its postcrania, but there is an associated postcranium that likely belongs to this individual in the surrounding matrix. The largest individual is preserved in nearly its entirety, articulated on Block 3, and here is referred to as Skull B (Fig. 2.4). This individual can be followed along and just under the prepared surface of

Block 3, with only one small loop of midtrunk vertebrae and the very distal tip of the caudal series missing, likely as a result of exposure and erosion and weathering of the specimen prior to collection. A third individual was discovered from CT scans of Block 3. The skull, referred to as Skull C, is median in size between Skulls A and B and completely enclosed by matrix under the midbody of Skull B, near the articulation between Blocks 2 and 3. Upon inspection, Skull C was assigned to the same taxon as the more accessible associated skull; it also has a good portion of anterior trunk vertebrae preserved in articulation with the largely complete skull.

The following description refers only to Skulls A and B, because they are the most complete and accessible of the four skulls.

## Skull and Mandible

**Premaxilla**— The premaxilla is present only on Skull B (Fig. 2.4c/d). The transverse processes make up the majority of what is preserved; they describe a shallow arc that is concave posteriorly, similar to boines and to *Charina*. Two small, blunt eminences are located posteromedially along the transverse processes, these are the poorly preserved vomerine processes. All other traces of articulation with the snout are not visible and likely have not been preserved.

**Vomer**—Only the left vomer is present in Skull A, but it is well preserved in articulation with the septomaxilla (Fig. 2.3g/h). Both vomers are present, but harder to discern and slightly displaced in Skull B (Fig. 2.4g/h, only left vomer figured). In ventral view (Fig. 2.3g/h), the medial edge of the vomer is longitudinally straight until it angles slightly laterally into a relatively long, narrow posterior process (the palatine process of Kluge, 1993), similar to *Charina,* making up the posterior third of the element. The anterior third is developed into a broad, rounded, spatulate extension that likely approached the premaxilla. The posterolateral edge of this extension forms the anteromedial bony border of the vomeronasal fenestra. The medial edge of the vomeronasal fenestra is a wide v-shape, with the posterior edge formed by the medial, triangular portion of the vomer. The posterior edge of the medial third is uneven, and, on its dorsal surface, supports a medial, transverse wall, forming the posterior wall of the vomeronasal vacuity. The posterior wall also supports the septomaxilla on the lateral side, and is pierced by a single, small foramen located near the top of the wall (Fig. 2.3i/j). There is a large vertical wall extending the length of the medial side of the vomer, forming the medial wall of the vomeronasal vacuity anteriorly, and supporting the dorsal lappet of the septomaxilla along the anterior two thirds of the vomer (Fig. 2.5). The wall thins anteriorly, until it is truncated by the anterior sweep of the septomaxilla. The posterior edge of the vertical wall is concave posteriorly and a small foramen pierces the vertical wall just above the ventral border, surrounded by a shallow depression that extends anteroposteriorly (Fig. 2.5).

**Septomaxilla**—In Skull A, only the left septomaxilla is preserved in life position, while the dorsoposterior process is broken and floating in the matrix just dorsal to the snout complex (Fig. 2.3g/h). Both septomaxillae are preserved in Skull B but the right septomaxilla is poorly preserved, and the left is rotated laterally, but very well preserved (Fig. 2.4g/h). The left septomaxilla of Skull B is the only one with the dorsoposterior process preserved; the dorsoposterior process of *Charina* is long, but does not reach posterior to the end of the septomaxilla; the process in *Congerophis lego* is somewhat shorter but is still quite distinct. The process arises from the flattened anterior tip of the septomaxilla, which projects just past the anterior-most extent of the vomer, cupping the tip of the vomer anteriorly. Just posterior to the spatulate tip, the septomaxilla bulges dorsolaterally, forming a dome that is the roof, lateral, and anterior wall of the vomeronasal cavity, which is lenticular in shape (Fig. 2.3g/h). The posterior end of the dome is supported by the median wall of the vomer, at which point a lappet wraps the medial side of the vertical wall of the vomer for half of the remaining length of the vomer, tapering posteriorly (Fig. 2.5). The lateral-most edge of the septomaxilla forms the lateral border of the vomeronasal fenestra, continuing posteriorly for a short distance before terminating at approximately the level of the second tooth position of the palatine. The posterior border of the septomaxilla is a broad arch, describing the outline of the dorsolateral border of the vomeronasal cavity, and is broadly concave posteriorly.

**Maxilla**—The left and right maxillae are well preserved in Skull A, though both are broken into several pieces posterior to the palatine process. The right maxilla has been lost in Skull B, but the left is present and very well preserved (Fig. 2.4a/b). There are 14 dental alveoli on the right maxilla of Skull B, and one lateral foramen. There are 16 alveoli on the right maxilla of Skull A and one lateral foramen, but only 15 alveoli on the left maxilla and no lateral foramina. The teeth gradually increase in size and recurvature anteriorly, excepting the most anterior tooth, which is slightly shorter than the following tooth.

In lateral view (Fig. 2.4a/b), anterior to the origin of the palatine process, the maxilla increases in height to become taller than it is wide, whereas posterior to the palatine process, it flattens to become slightly wider than it is tall. In dorsal view (Fig. 2.3e/f), the lateral edge of the maxilla bows medially at the base of the palatine process, located just posterior to the halfway point of the length of the maxilla. The anterior portion of the maxilla curves slightly medially, terminating just before the presumed end of the snout. The posterior portion terminates just posterior to the postorbital process of the parietal.

The palatine process projects ventromedially, supporting the palatine at its most medial extent (Fig. 2.6f). The medial fork of the prefrontal contacts the maxilla on the anterior portion of the palatine process, just anterolateral to the palatine. The lateral foot process of the prefrontal loosely contacts the dorsal surface of the maxilla just anterior to the origin of the palatine process of the maxilla. There are two foramina associated with the palatine process: the posterior foramen is located on the surface just dorsal to the joint of the posterior edge of the palatine process and the posterior half of the body of the maxilla (Fig. 2.4e); the anterior foramen is located on the anteromedial surface of the anterior portion of the main body of the maxilla, just at the anterior point of origin of the palatine process (Fig. 2.4g). It is likely that the anterior foramen is the opening for the maxillary branch of the trigeminal nerve (cranial nerve V) because the opening leads into the interior of the main body of the maxilla, the destination of the fifth cranial nerve. It is unknown what function the posterior foramen served.

**Ectopterygoid**—Only one ectopterygoid, the right, is present in Skull A and is displaced dorsomedially in the orbit (Fig. 2.3a/b; Fig. 2.6h). Both are missing from Skull B. The lateral edge of the element gently curves medially. The anterior end overlaps a point near the posterior end of the maxilla, and is extremely shallowly forked, with small lateral and medial heads separated by a short, anteriorly concave edge (Fig. 2.6h). This forked state is common in Booidea but is usually much more pronounced, though the ectopterygoid in *C. lego* most resembles that of Ungaliophiinae; the lateral and medial heads are lost in Tropidophiinae, *Eryx* and *Charina.* The posterior end joins the ectopterygoid process of the pterygoid on its anterolateral surface. The element is dorsoventrally flattened at the anterior end and slightly thicker at the contact with the pterygoid. It is a short gracile bone, approximately one fifth of the snout-occiput length.

**Palatine**—There are seven alveoli on the dentigerous processes of both palatines in Skull A, with five teeth remaining in their alveoli on the right palatine, and four remaining on the left (Fig. 2.3g/h). There are six alveoli and four teeth present on both palatines in Skull B (Fig. 2.6a/b). In all four palatines, the first (most anterior) tooth is quite recurved, but the teeth progress to much less recurved posteriorly. There is only a slight decrease in tooth length from anterior to posterior.

The choanal process of the palatine presents as a broad sheet of bone, rising in a dorsomedial direction, with a ventromedial curve along its length, which originates from the posterior half of the dentigerous process (Fig. 2.6a). This is the same state seen in *Charina*; the choanal process is nearly lost in *Eryx*, and is much more robust and narrow in the majority of Booidea; anilioids also possess a broad sheet-like process, but theirs is lower and does not possess the finger-like anterior projection.

The maxillary process extends slightly ventrolaterally in a rounded, triangular tongue that overlaps the palatine process of the maxilla immediately posterior to the medial contact of the prefrontal and maxilla (Fig. 2.6f). The pterygoid processes of the palatine derived from the maxillary process anteriorly and a ventral continuation of the posterior edge of the choanal process that descends to the level of the tooth row. These two processes clasp the anterior border and the dorsomedial third of the pterygoid, respectively (Fig. 2.6b). There is no palatine foramen; instead, this area is a slight excavation at the meeting of the dentigerous and maxillary processes.

**Pterygoid**—Both pterygoids are preserved on both skulls, though the posterior portion of the quadrate ramus is broken off of the left pterygoid of Skull A and it seems to be missing the anterior-most few tooth positions as well. There are 12 alveoli, every other one filled with a tooth, on the right pterygoid of Skull A, but only 10 are discernible on the left pterygoid, though it is incomplete (Fig. 2.3g/h).

There are 10-12 tooth positions in either pterygoid of Skull B, though the resolution is too coarse to discern the exact count due to the small size of the pterygoid teeth (Fig. 2.4g/h). The pterygoid teeth only slightly decrease in both size and recurvature posteriorly, but at their longest are approximately the size of the smallest maxillary tooth.

The pterygoid extends along the base of the skull for approximately two thirds of the snout-occiput length. There is an oblique expansion at approximately the mid-point of the length of the pterygoid which forms, medially and a bit posteriorly, the basipterygoid wing, and laterally and a bit anteriorly, the ectopterygoid process. The ectopterygoid process is a pronounced, subrectangular lateral eminence that, at the articulation with the ectopterygoid, thickens dorsoventrally to form a gracile subrectangular facet (Fig. 2.6b). This process is relatively more pronounced in Skull B than in Skull A and is much like the even more pronounced ectopterygoid process of *Charina,* but never reaches the more robust state found in other Booidea; this in contrast to the state in *Eryx* in which the process is reduced to a smooth bulge in the lateral edge only. The basipterygoid wing loosely cups the low mound of the basipterygoid process as it presents in these specimens. The two basipterygoid wings closely approach each other in both specimens, and are preserved as overlapping slightly in Skull A (Fig. 2.3g/h). The quadrate ramus of the pterygoid gradually tapers to a rounded posterior point. The medial surface is folded into a deep groove that continues until the posterior end of the swelling that represents the basipterygoid wing, such that, in cross section, the quadrate forms a flattened c-shape that is concave medially (Fig. 2.4k/l). This groove is present in all Booidea and Ungaliophiinae, but not *Charina.* Along the medial surface of the dentigerous process of the pterygoid, a narrow shelf emerges anteriorly, approximately half way through the depth of the anterior portion of the process, on which the medial pterygoid process of the palatine fits (Fig. 2.6b).

**Nasal**— Only one nasal is preserved in Skull A, and it is nearly identical to those in Skull B, apart from the greater preservation of the anterior-most portion of the vertical lamina (Fig. 2.5). The tip of the vertical lamina narrows by erosion of the dorsal edge, while maintaining the ventral edge at the same level ventrally as is present posteriorly.

The left nasal in Skull B is roughly in life position. The right nasal has been rotated such that the vertical lamina is now visible in dorsal view (Fig. 2.4e/f). The vertical lamina deepens anteriorly from a constriction in the posterior third of the element. It again deepens posterior to this constriction, terminating in a slightly bulbous ventral thickening that articulates with the anteroventral portion of the frontal (Fig. 2.5). The horizontal lamina reaches the middle point of the anterior edge of the frontal, meeting it in a transversely straight contact; the lamina gradually narrows anteriorly until it disappears near the anterior tip of the element (Fig. 2.4e/f).

**Prefrontal**—Both prefrontals are present and in near life position in both Skull A and Skull B. In Skull A, both prefrontals are slightly rotated dorsolaterally, disarticulating them from the respective maxillae (Fig. 2.3i/j). In Skull B, the right maxilla is slightly displaced dorsally and anteriorly (Fig. 2.4e/f). On both skulls, the prefrontals appear to be complete, yet there is a natural mould of what appears to be an apex extending approximately 50% farther rostrally in the left prefrontal of Skull B. This feature indicates less than perfect preservation of the prefrontals. The delicate anterior laminae are most likely incomplete, which is confirmed by the more complete prefrontal of the referred specimen, Skull D.

Of primary importance to note is the lack of an enclosed lacrimal foramen in the prefrontal, causing a broadly forked appearance where the prefrontal contacts the maxilla (Fig. 2.6f). The lateral fork (the lateral foot process) is very rounded, representing a continuation of the ventrolateral shelf of the prefrontal, which extends just lateral to the lateral foot process. The medial foot process extends ventrally from just below the level of the lateral foot process and makes up the ventral third of the dorsoventral extent of the prefrontal. Between the two foot processes, the bone is concave ventrolaterally, as viewed posteriorly, to allow for the passage of the lacrimal duct between this concavity and the maxilla.

In lateral view (Fig. 2.4a/b), the prefrontal is trilobed, the apex of the anterior lamina pointing rostrally, the medial foot process pointing posteroventrally, and a large, rounded dorsal lobe articulating with the frontal. The ventrolateral shelf makes only a slight contact with the maxilla along the lateral foot process and slightly anterior to this, and soon disappears entirely. Anterior to the maxillary contact, the anterior lamina rises at an approximately 45° angle towards the apex.

In dorsal view (Fig. 2.4e/f), the prefrontal is roughly triangular, though the damage to the anterior lamina precludes certainty of its shape. The dorsal lappet extends halfway across the anterior edge of the frontal, representing the most medial extent of the prefrontal. The posterior edge of the dorsal lappet joins the articular knob at a rounded right angle, creating an L-shaped articulation between the prefrontal and frontal in dorsal view. The articular knob, transitioning smoothly form a dorsal surface to a lateral surface, represents the inner orbital lobe; there is no notch between these features. This structure represents the most posterior extent of the prefrontal and articulates with the anterolateral corner of the frontal.

Ventral to the inner orbital lobe, the medial border of the prefrontal possesses a rectangular, medial extension, which undercuts and supports the frontal. Ventral to this structure, the bone narrows into a rod that forms the medial foot process. In lateral view, the prefrontal-frontal contact is concave anteriorly. The orbital surface of the prefrontal, which forms the anterior wall of the orbit, is slightly concave posteriorly. The medial foot process contacts the dorsal surface of the medial palatine process of the maxilla, just anterior to the contact with the palatine.

**Frontal**— The frontals are complete and present in their life positions in both Skull A and Skull B. In Skull A, a fracture runs obliquely through the entire specimen at the level of the frontals, and there is mild displacement along this fracture, yet all contacts are preserved (Fig. 2.3e/f).

The paired frontals are subrectangular in anterior view (Fig. 2.4i/j), and triangular with the medial side unenclosed in posterior view. The ventrolateral surface forms the majority of the median portion of the orbit. The dorsal surface is very rectangular except for the lateral-most corners, which are rounded for articulation with the prefrontal and parietal along the border of the orbit (Fig. 2.4e/f). An anteroposteriorly short and broad shelf of bone, the transverse frontal shelf, projects from just below the dorsal surface of the anterior edge of the frontal

(Fig. 2.4e/f). This is the medial continuation of the preorbital ridge of Frazzetta (1966), which, dorsally, receives the posterior lappet of the horizontal lamina of the nasal. The preorbital ridge supports the dorsal lappet of the prefrontal with an anterolateral expansion, which is in turn rooted to a depressed facet underlying the prefrontal that consumes the anterior third of the lateral border of the frontal. There is a notch between the preorbital expansion and the main body of the facet that is apparent in dorsal view. When viewed laterally, the prefrontal-frontal contact is concave anteriorly, and it is distinctly L-shaped, with the corner pointing anterolaterally, in dorsal view (Fig. 2.4e/f). The anterior surface of the frontal is pierced by the large, oblate foramen for the olfactory tract; there is no evidence of a suture on this surface, though the resolution of the scan may be insufficient for that level of detail. The anterior half of the ocular foramen is formed by the frontal (Fig. 2.3a/b).

The naso-frontal joint is transversely straight across both halves and the posterior edges of the horizontal nasal laminae broadly separate the prefrontals such that the nasals cover the middle third of the transverse extent of the frontals (Fig. 2.4e/f). The vertical laminae of the nasals do not contact the frontal along their entire posterior edge; instead, there is a ventral ramus on the lamina that expands posteriorly to make sturdy contact with the medioventral corner of the anterior surface of the frontal.

The fronto-parietal contact is once again transversely straight, turning slightly anteriorly at the lateral-most third, making way for the postorbital processes of the parietal (Fig. 2.4e/f). The suture is also straight in Tropidophiinae and *Charina*, but it is concave anteriorly in all other Booidea.

**Parietal**—The parietals of both specimens are nearly complete, though one or the other posterolateral corners have scaled off. In dorsal view, the contact between the frontals and the parietal is concave anteriorly, with a small laterally directed curve at the lateral-most fifths of the contact (Fig. 2.4e/f). There is a small lateral expansion at the anterolateral-most corners, with a longitudinal groove (Fig. 2.4a/b), representing the vestigial contact with the postorbital, much like in *Charina botta*e where the postorbital has been lost. Posterior to the postorbital process, there is a slight constriction, after which the parietal bells outward, giving the parietal a bulbous appearance in dorsal view (Fig. 2.4e/f). This is the widest part of the skull, expanding just past the width of the prefrontals. The bulbous nature of the parietal gives it a superficial similarity to Tropidophiinae, Ungaliophiinae, and *Charina;* although the parietal of *Eryx* is similarly bulbous, the pronounced features of the more lateral elements give *Eryx* a more boine appearance. Posterior to the bulbous section, the parietal constricts more severely towards the contact with the prootic. The lateral edges straighten longitudinally where the parietal extends posterior to the contact with the prootic, this portion making up a little more than a third of the dorsal length of the bone. The posterior border of the parietal is broadly concave posteriorly, the posterolateral corners approaching, but not making, contact with the exoccipitals (Fig. 2.3e/f), similar to the state found in *Charina* and unlike the state found in other Booidea, wherein a median point projects over the supraoccipitals. There is no sagittal crest in Skull A, but a sinusoidal, flat-topped rise is present in the middle fifth of the parietal along the portion of the parietal posterior to the contact with the prootic, similar again to *Charina*. Skull B does have a short sagittal crest in the same position, likely an ontogenetic difference (Fig. 2.4e/f).

In lateral view, the postorbital process extends from the anterodorsal corner of the parietal posteroventrally for nearly half of the depth of the anterior border of the parietal (Fig. 2.4a/b). At the ventral corner of the anterior border, the parietal encircles half of the foramen for the ocular nerve. Posterior to the foramen, the parietal deepens until just posterior to the widest point of the parietal, which represents the closest approach of the two sides of the parietal on the ventral side of the skull (Fig. 2.4g/h). Posterior to the deepest point, the ventral border of the parietal rises to meet the anteroventral corner of the prootic, and, with the most dorsal extent of the parabasisphenoid, forms the foramen for the CID nerve (*sensu* Rieppel, 1979). The lateral contact between the parietal and the prootic is oriented vertically, with the large opening for the maxillary branch ($V_2$) of cranial nerve five occurring just below the halfway point. The contact then continues horizontally at the dorsal border of the prootic; the corner of this L-shaped contact is rounded (Fig. 2.4a/b).

**Supraoccipital**—The supraoccipital is much wider than long, but the anterior third underlaps the parietal (Fig. 2.3e/f). The sagittal crest, particularly distinct in Skull B, continues on the supraoccipital until the posterior contact with the exoccipitals. A posteriorly concave, transverse ridge branches off from the medial point of the dorsal contact with the parietal. This ridge rises above the level of the posterior remainder of the supraoccipital, and is continued as a pair of lobes into the dorsolateral portion of the exoccipital (Fig. 2.3e/f). The ridge is quite distinct in both specimens, though narrower and somewhat taller in Skull B. The medioposterior contact with the exoccipital is sinusoidal: concave anteriorly to the same degree as the ridge, but curving laterally once it reaches the ridge to become nearly vertical on the lateral side until it contacts the supraoccipital (Fig. 2.3e/f).

**Exoccipital**— A large crystalline mass disrupts the left exoccipital in Skull A. The right is very well preserved (Fig. 2.6e), excepting a portion that is missing from the dorsomedial flange. In posterolateral view, the exoccipital is I-shaped, expanded above and below the fenestra ovalis. Ventrally, the exoccipital contributes to the dorsolateral portion of the occipital condyle. Moving anteriorly, the contact with the basioccipital rises dorsally to a point ventral to the fenestra rotunda, and then falls again for a short distance until the ventral contact with the prootic. The foramen magnum is bordered laterally by the narrow middle section of the exoccipital, and dorsally by a crescent-shaped shelf formed by the large dorsomedial flanges of the left and right exoccipitals (Fig. 2.3k/l). These flanges anteriorly contact the supraoccipital, anteroposteriorly thinning posterolaterally along the ridge that is continued from the supraoccipital, until just below the level of the dorsal border of the fenestra ovalis, where the flange abruptly terminates at a right angle to the posterior edge of the flange (Fig. 2.6e). This termination continues the line of the channel incised by the exiting jugular vein and vagus nerve (X), which emerges from a medium sized, posterodorsally directed foramen in the center of the lower half of the exoccipital (Fig. 2.6e). Along this channel there are two small foramina for the exit of the hypoglossal nerve (XII), one dorsal and one ventral across the channel. The channel itself is directed anteroventral-posterodorsally and broadens posteriorly. Within the foramen for the jugular vein and vagus nerve, there is a thin anterodorsal bridge of bone creating a much smaller auxiliary foramen within the larger foramen, likely functioning to divide one or the other of the glossopharyngeal (IX) or vagus (X) nerves from the jugular vein (Fig. 2.6e). The bridge of bone between the vagus/jugular foramen and the fenestra ovalis has only the slightest, posteriorly directed ridge, sinking it below the level of the rest of the crista circumfenestralis. The crista tuberalis has been reduced to a minor, nearly flat, ventral extension between the foramen and the fenestra rotunda (Fig. 2.6e). The fenestra rotunda is an elongate elliptical vacuity, separated from the fenestra ovalis by a thin portion of the crista interfenestralis that is depressed medial to the level of the rest of the crista circumfenestralis (Fig. 2.6e). The ventral end of this crista just excludes the basioccipital from the ventral-most point of the crista circumfenestralis and contacts the prootic anteriorly.

On the dorsal border of the fenestra ovalis, there is a broad, straight, rectangular shelf of the exoccipital that continues and exaggerates the line of the crista prootica. The shelf terminates abruptly, and the posterior border of the fenestra ovalis continues medial to the shelf.

**Prootic**—The prootic is a subrectangular element of high relief from the rest of the skull. The bone is anteroposteriorly elongate (Fig. 2.4a/b), making it unique among Booidea and possible sistergroups that have either a subsquare or anteroposteriorly shortened prootic. A large, rounded superior lobe makes up the anterodorsal fourth of the prootic and the most anterior extent of the bone. The lobe extends over a large, triangular foramen for the maxillary branch of the trigeminal nerve ($V_2$), approximately midway along the vertical contact between the prootic and the parietal and formed between the two. At the ventral end of this contact, along with the most dorsal extent of the parabasisphenoid, the three bones form a smaller foramen for the reentry of the CID-nerve. Moving along the ventral border of the prootic, the inferior anterior lobe overhangs the small laterosphenoid foramen for the exit of the CID-nerve (Fig. 2.3a/b). The prootic then angles ventrally, to meet the posterior opening of the vidian canal, which is primarily in the parabasisphenoid but a deep channel inscribes both the parabasisphenoid and the prootic leading to the opening (Fig. 2.5e). The prootic comprises the dorsal border of this channel; the channel rises at a low angle until it is entirely within the prootic. In this channel, directly under the center of the large foramen for the mandibular branch of the trigeminal ($V_3$), lies the small foramen for the palatine branch of the facial nerve (VII). The channel runs directly under the large, oval $V_3$ foramen, which plunges anteromedially into the prootic, creating an excavation posterior to the actual foramen (Fig. 2.5e). In the center of this depression lies the foramen for the hyomandibular branch of the facial nerve. There is a flattened lobe ventral to the exit of the vidian canal that represents the most posteroventral corner of the prootic and meets the crista interfenestralis at the ventral border of the fenestra ovalis. From this corner, the prootic rises at a sharper angle, forming the anterior border of the fenestra ovalis, until the rise flattens into a short, low crista prootica just above the level of the dorsal border of $V_2$ (Fig. 2.5e). At this most posterior point, the prootic meets the dorsal portion of the exoccipital, and the vertically inclined contact continues dorsally to meet with the supraoccipital. The parietal excludes the prootic from contact with the supraoccipital for the majority of the dorsal border of the prootic, excepting a short segment at the confluence of the exoccipital, the prootic, and the supraoccipital. The bulge of the prootic is very obvious in dorsal view, and continues posteriorly as a broad ridge into the exoccipital (Fig. 2.3e/f).

**Basioccipital**—Complete in both specimens, the basioccipital is a subcircular, shallow basin cupping the endocranial space. The contact with the parabasisphenoid is broad and transversely straight (Fig. 2.4g/h). Laterally, it rises dorsally in contact with the posterior third of the prootic, and at its highest point, is just excluded from the ventral border of the fenestra ovalis (crista circumfenestralis) (Fig. 2.4c/d). Posterior to this point, the basioccipital maintains contact with the exoccipital up to the base of the occipital condyle. The occipital condyle is formed by the basioccipital, with the exoccipital only slightly contributing at the dorsolateral-most corners, and the former forming the most posterior point of the basicranium (Fig. 2.4k/l). A wide fovea dentis in the basioccipital portion of the occipital condyle separates the ventral portions of the exoccipitals.

**Parabasisphenoid**—The parabasisphenoids of both skulls are present and well preserved, but the major transverse fracture in Skull A also affects the cultriform process in this specimen (Fig. 2.3g/h). The parabasisphenoid is an elongate element, extending from just below the anterior extent of the frontals to directly below the posterior border of the opening for $V_3$ (Fig. 2.4g/h). The half of the bone anterior to the anterior opening of the vidian canal is narrowed between the ventral wings of the parietal and slightly tapers anteriorly until a point one third along this portion, at which point it rapidly constricts at nearly right angles, forming the trabecular facet, into a narrow cultriform process that tapers slightly to its anterior tip. The cultriform process is dorsoventrally deeper than it is wide at any point, and a trabecular groove is present along its entire length, creating an hourglass-shaped cross section (Fig. 2.4c/d). The anterior openings of the vidian canals are shielded from the ventral aspect by a low-lying, smooth parasphenoid wing. The posterior half of the element, posterior to the anterior opening of the vidian canal, expands to the widest point of the bone, which contacts the parietal and prootic. From this widest point, the element more gradually narrows. The external surface is smooth, with two low relief mounds representing the vestiges of the basipterygoid processes (Fig. 2.4g/h). At the level of the posterior border of the laterosphenoid, the posterior opening of the vidian canal emerges, creating a small rise around the opening in the parabasisphenoid (Fig. 2.6e). This opening is on the contact between the prootic and the parabasisphenoid, and is slightly larger and more covered on the right side in both specimens. The contact between the basioccipital and the parabasisphenoid is transversely straight, creating a sharp L-shaped posterolateral corner in the parabasisphenoid (Fig. 2.4g/h).

The interior surface of the parabasisphenoid forms a deep, well-defined pituitary fossa (sella turcica), bordered posteriorly by a well developed crista sellaris, which slightly overhangs the sella turcica (not figured). The anterior surface of the crista sellaris is pierced on either side by the posterior foramen for the carotid artery (the carotis cerebralis of Rieppel 1979), which branched from the vidian canal just posterior to the lateral corners of the crista sellaris. The resolution is too low to precisely examine the opening for cranial nerve VI, but a possible candidate is located just posterior to the crista sellaris in a position more lateral than the opening for the carotid artery on the other side. The roof of the vidian canal posterior to the crista sellaris is absent, and anteriorly the canal inscribes a deep channel at the contact of the parabasisphenoid and the parietal, before plunging from view to its external anterior exit. The CID-nerve enters the braincase on the contact between the parabasisphenoid and the parietal, just anterior to the contact with the prootic.

**Supratemporal**—The only supratemporal preserved is the left one on Skull B. It is complete, but greatly displaced posteriorly, such that the anterior border is touching the left border of the foramen magnum, and is rotated such that the ventral surface is facing dorsally (not figured). The ventral surface is concave where it would be contacting the braincase. The anterior two thirds is blade-like, tapering anteriorly with a slight constriction posterior to the articulation with the quadrate. This portion is slightly thickened relative to the rest of the supratemporal blade; the posterior end is blunt and rounded.

**Quadrate**—The only quadrate present in either specimen is the left quadrate of Skull B (Fig. 2.4a/b). The element has been rotated so that the anterior side now faces laterally. The articulation with the supratemporal has been broken off, slightly truncating the length of the quadrate, though it appears rather short and oriented vertically. The stylohyal process for the stapes is present on the medial side of the quadrate, approximately two-thirds up the length of the quadrate. The dorsal portion of the bone is twisted nearly 90° from the line of the anteroposteriorly compressed distal condyles. These condyles are only vaguely divided, appearing nearly featureless but for a small depression at the center of the ventral surface.

**Compound**—The compound bone is preserved in both jaws of both specimens, though the posterior ends are missing from both sides in Skull A. The compound bone possesses a small retroarticular process (Fig. 2.4a/b). The lateral eminence of the compound bone rises considerably above the medial eminence, and is pierced on the anterolateral side by the anterior foramen for the mandibular branch of the trigeminal (or $V_3$ nerve) (Fig. 2.4a/b); overall it is very similar to *Ungaliophis continentalis*. The posterior opening for the CIII nerve is located in the center of the adductor fossa as a posteriorly directed foramen (Fig. 2.6c, arrow), far more posterior than is typical in ophidians, but similar to the position in *Eryx*, creating an elevated shelf forming the anterior half of the adductor fossa with the posterior half depressed to the level of the ventral border of the foramen. The most ventral point for the mandible is formed by the contact between the compound element and the posteroventral process of the dentary. From the lowest point, the ventral edge of the anterior process of the compound bone rises at approximately a 30° angle, to meet the horizontal dorsal edge (Fig. 2.4a/b). Here it forms a narrow v-shape that articulates with the posterior processes of the dentary. The dorsal edge of the process continues posteriorly until it meets the anterior foramen for the mandibular branch of the trigeminal nerve. Overall, there is a slight dorsal bowing of the entire element, from the retroarticular process to the most ventral point of the bone.

**Coronoid**—The coronoid bone appears to be absent in this taxon, a feature it shares with *Charina bottae*, Ungaliophiinae, Tropidophiinae, and Caenophidia.

**Angular**—There is only one identifiable angular on either specimen, and it is present in the left mandible of Skull B, although it is broken in half perpendicular to its length (Fig. 2.6d). The posterior half is nearly articulated with the compound bone, but the anterior element is displaced medially. There is a small constriction along the ventral border of the anterior piece. Overall, the angular is triangular in shape and extends along the ventral half of the medial side of the anterior third of the compound bone, and an equal distance anteriorly along the ventral shelf of the dentary.

**Splenial**—Both splenials are present in Skull A, the left in life position (Fig. 2.3a/b), but the right has been disarticulated and is now floating in the matrix between the anterior halves of the dentaries. The left splenial is present in Skull B, though displaced slightly medially (Fig. 2.4c/d). The posterior edge is vertical. The dorsal portion extends a quarter of the length of the ventral portion, and there is a slight notch between the two. The anterior mylohyoid foramen is present in the ventral flange at the same level as the anterior extent of the dorsal portion. The splenial reaches anteriorly along the ventral lamina of the Meckel's canal for approximately half of the length of the dentary.

**Dentary**—Both dentaries are preserved on Skull A, with 18 alveoli and nine teeth present on the right (Fig. 2.3a/b). The left dentary is assumed to have the same number of alveoli, but is missing a section of bone that is approximately two tooth positions long, thus there are nine teeth still preserved (Fig. 2.3c/d). The left dentary is completely preserved in Skull B, with a total of 17 alveoli, in which nine teeth are present (Fig. 2.4a/b). The right dentary is missing the entire portion anterior to the last four tooth positions. There is one mental foramen present in the anterior third of the dentary, below the fourth tooth position. A deep Meckel's canal persists to the anterior tip of the dentary along the ventral portion of the medial surface, which is just closed at the anterior tip (Fig. 2.6d). The posterior dorsal and ventral processes clasp the anterior third of the compound bone. The ventral posterior process contributes to the sheet of bone that becomes the ventral shelf of the Meckel's canal.

## Postcrania

**Trunk Vertebrae**— With the exception of caenophidian-specific features, the pattern of intracolumnar variation from cranial to caudal in *C. lego* follows the pattern of the caenophidians described by LaDuke (1991). The anterior vertebrae (Fig. 2.7a) are much taller than they are long, and sub-equal in width and height. They possess a large, posteriorly directed hypopophysis cranially, which gradually shortens until disappearing into the hemal keel after approximately 50 vertebrae. There are approximately 160 precloacal vertebrae belonging to the Skull B individual, the only individual that is represented by a nearly complete skeleton.

In dorsal view, the mid-trunk vertebrae are a bit wider than they are long, but they shorten anteriorly along the column and lengthen posteriorly (Fig. 2.7l). The zygophene broadens from its root on the neural arch anteriorly, then narrows again to the anterolateral tips. This lateral bulge becomes less apparent anteriorly and more apparent posteriorly, before being minimized in the caudal vertebrae along with the zygosphenes. The anterior edge is concave anteriorly with a small median bulge. This bulge gets larger posteriorly and disappears anteriorly along the column. Also, the width of the zygosphene broadens anteriorly and narrows posteriorly along the column, starting at more than a third of the width of the anterior face of the vertebrae to less than a third of the width, anteriorly to posteriorly along the column. The neural spine is approximately half the length of the neural arch and lengthens to just over half of the length of the vertebra posteriorly.  The spine always reaches a point just above the posterior notch between the postzygapophyses, which is relatively deep, and consistently so, throughout the trunk before flattening in the caudal vertebrae.  The posterior edges of the postzygapophyses are roughly transversely straight, creating a distinct angle between these edges and the median notch between them, which becomes less distinct in the caudal vertebrae.  The prezygapophyseal facets are subtriangular, transversely straight anteriorly, and increase in size posteriorly along the column until they are roughly equivalent with the postzygapophyses.  A much reduced prezygapophyseal process is visible in dorsal view only in the mid-trunk vertebrae (Fig. 2.7i).

In lateral view, the centrum is just longer than it is wide (Fig. 2.7j).  The synapophyses are not very well divided, although they become more so moving posteriorly along the column, with the parapophyseal portion reaching just below the ventral level of the centrum somewhere mid-trunk.  The postzygapophyseal portion of the neural arch is very upswept anteriorly and gradually levels out somewhere mid-trunk along the column.  The prezygagophyses are very slightly inclined superolaterally throughout the trunk.  After the hypopophyses have ceased to be present, the sharp, posteriorly rising hemal keel gradually flattens and reduces until it is absent in the posterior trunk vertebrae, defined only by the subcentral ridges, which remain flat throughout the column.  A small lateral ridge is found to be connecting the pre- and postzygapophyses, and is most prominent mid-trunk. The neural spine is a little less than two times as long as it is tall in the anterior trunk vertebrae, approaching more equal dimensions as less than two times as long as it is tall at mid-trunk, and once again a little less than two times as long as it is tall in the posterior trunk vertebrae. The neural spine is square in lateral view in most of the vertebral column except the caudal vertebrae, in which it appears to slightly trapezoidal.

In ventral view (Fig. 2.7k), the postzygapophyseal facet is shaped roughly like a right angle triangle. The subcentral grooves become more prominent as they progress posteriorly along the column, as do the subcentral ridges, but neither could be said to be extremely deep or pronounced, and there are subscentral foramina present. The hemal keel flattens and widens posteriorly and possesses a slight waist anteriorly that disappears posteriorly along the column.

In anterior view (Fig. 2.7g), the mid-trunk vertebrae are wider than they are tall, with a lower neural arch and neural spine that is approximately half the height of the neural canal. The vertebrae increase in height anteriorly and decrease in height posteriorly, but are roughly of equal dimensions in the caudal vertebrae. The cotyle is slightly depressed in the anterior and mid-trunk vertebrae, making it just shorter but wider than the neural canal; unfortunately anterior views are not available for the posterior trunk vertebrae, but the caudal vertebrae possess a round cotyle. The resolution of the CT-scans is too low to assess the presence of paracotylar foramina. The zygosphene is transversely straight and approximately as wide as the cotyle, with moderately sharply inclined facets. The prezygapophyseal facets are inclined at approximately 15° from horizontal. The neural canal is shaped like a loaf of sandwich bread, a sub-square ventral 2/3, but an expanded and half circle-shaped dorsal 1/3, in all vertebrae examined but is wider anteriorly and narrower posteriorly along the column.

**Cloacal Vertebrae**—Cloacal vertebrae are considered to be present in the column of Skull B individual because identifiable trunk and caudal vertebrae are present. Unfortunately, the cloacal vertebrae cannot themselves be identified as such because they were present in a heavily damaged section of the column. The resolution within Blocks 2 and 3 is too low to confidently identify any additional vertebrae of the posterior series from the other two individuals preserved, though there are some very small vertebrae that may be inferred to be caudal vertebrae emerging from the articulating surface of Block 2, though they are too indistinct to yield any morphological information.

**Caudal Vertebrae**—There are at least 30 post-cloacal vertebrae present in the Skull B individual, but the end of the caudal series is absent. The caudal vertebrae are much more elongate than their anterior counterparts and possess distinct, anterorlaterally directed and short pleurapophyses (Fig. 2.7w). Ventrally, there are very short hemapophyses present on at least the posterior vertebrae of the series (Fig. 2.6g), but the resolution from CT scan imaging is too low to identify these structures where the caudal series is still within the matrix (Fig. 2.7y). Dorsally, the caudal vertebrae possess a neural spine of low to median height, increasing in height posteriorly, that extends for approximately half of the length of the centrum, terminating over the posterior notch between the postzygapophyses (Fig. 2.7w and z). The zygosphenes are much narrower in dorsal view in the caudal vertebrae than in the trunk vertebrae, and seem almost to taper rather than expand anteriorly. The anterior border of the zygosphenal platform is slightly concave with a moderate median bulge. There are no accessory processes on the prezygapophyses, which are directed more anteriorly and are narrower and more pointed than those of the trunk vertebrae. The cotyle is very round (Fig. 2.7x); although it was not possible to directly view the condyle, a round cotyle generally means the condyle is expected also to be round. The prezygapophyses are not inclined in anterior view (Fig. 2.7x), but are slightly inclined in lateral view (Fig. 2.7w).

## PHYLOGENETIC ANALYSIS

## Dataset Selection

Two datasets were used to analyze the phylogenetic position of *Congerophis lego*. The first, from Palci et al. (2013), is a modified dataset based on Lee & Scanlon's (2002) phylogeny of snake relationships that used only osteological characters, and served to place the specimen in the broader context of Serpentes and narrow the choice of a more specific, second dataset. The second data set, from Kluge (1993), was chosen based on the results from Palci et al. (2013), for a higher resolution view of relationships between *C. lego* and the species usually included in the purported subfamily Erycinae.

## Analytical Methods

**Palci et al. (2013)**—The data matrix presented in this analysis includes *C. lego* as a single terminal taxon, scored using the unaltered character descriptions from Palci et al. (2013). Additionally, the taxon Erycinae s.l. is split into two clades: Erycinae sensu stricto, representing the old world genus *Eryx*, and *Charina* which consists of the new world genus, *Charina*. The purported erycine s.l. genus, the Calabar Python, *Calabaria* has been excluded from the analysis. In all analyses, Skull A and Skull B are initially scored separately, and then combined as a single terminal taxon. All taxonomic names for the terminal taxa follow Lee and Scanlon (2002).

All matrices were analyzed using the Heuristic Search algorithm in PAUP Version 4.0b10 (Swofford, 2002). All characters were unordered and equally weighted.

**Kluge (1993)**—The data matrix presented in this analysis includes *Congerophis lego* as a single terminal taxon, scored using a revised and expanded character list, modified from an analysis of the subfamily Erycinae at the specific level (Kluge, 1993). Character numbers have been changed to accommodate three new characters and the removal of one character; the original character numbers from Kluge (1993) appear in brackets immediately following the new numbers. In all analyses, Skull A and Skull B are initially scored separately, and then combined as a single terminal taxon. All taxonomic names for the terminal taxa follow Lee and Scanlon (2002).

**Character Descriptions**

**Palci et al. (2013)**—The dataset from Palci et al. (2013) was used unaltered (see Appendix A).

**Kluge (1993)**—57 of the following osteological characters have been selected for use in the fourth analysis conducted here. We have excluded the soft tissue characters from Kluge (1993) as they are inapplicable to the fossil taxa. The original character descriptions are modified for clarity where we thought necessary, and we have also added our own comments on the validity of certain characters. Three new characters have been added, 7, 18, and 43. Character 7 was added to aid in distinguishing new taxa that have been added to the matrix. Characters 18 and 43 have been listed as synapomorphies for fossil erycines s.l., and were added to test their validity as such. The additions and exclusions necessitated renumbering of the character list; the numbers from the original matrix of Kluge (1993) appear in brackets immediately following the new character numbers.

1. [1] Premaxilla: A conspicuously vertical anterior surface of the transverse process of the premaxilla is absent (0) or present (1) [mod].
2. [2] Premaxilla: The general outline of the anterior margin of the transverse process of the premaxilla is gently rounded (0) or more nearly straight to broadly concave (1). Though this character was originally constructed to describe the spatulate character of only toothless premaxillae, weapplied it to toothed outgroups with no modification.
3. [3] Premaxilla: The transverse process of the premaxilla is short (0) or long (1).
4. [4] Premaxilla: The internarial fenestra of the premaxilla or dorsal notch between the premaxilla and nasals is present (0) or absent (1) [mod]. This

character refers to the presence of a distinct fenestra formed anteriorly by the ascending and nasal processes of the premaxilla, and posteriorly by the anterior extent of the nasals, a common feature in boines. Also scored as (0) is the presence of a dorsal notch between the premaxilla-nasal contact, to agree with Kluge's (1993) scoring of *Charina trivirgata.*

5. [5] Premaxilla: The nasal process of the premaxilla is long (0), short (1), or absent (2). The long (0) state projects far under or between the nasals, while in the short (1) state, the nasal process is still present as a distinct, but small projection. In state (2), only a broad mound or narrow ridge is present.
6. [6] Premaxilla: The vomerine processes of the premaxilla are wider than they are long (0), slightly longer than they are wide (1), or much longer than they are wide (2) [mod].
7. [new] Premaxilla: Premaxillary teeth are present (0) or absent (1). This character is included to aid in defining the additional taxa beyond the Erycinae included in this analysis.
8. [7] Nasal: The anterior one-third to one-half of the vertical lamina of the nasal is nearly uniform in depth or increases anteriorly (0), or it decreases anteriorly and may be absent altogether (1) [mod].

9. [8] Nasal: The anterior end of the horizontal lamina of the nasal, as seen in dorsal view, gradually narrows (0) or slightly or markedly expands (1).
10. [9] Nasal: A slight notch is present (0) or absent (1) between the anterior ends of the horizontal laminae of the nasals. Can be scored in dorsal view.
11. [10] Nasal: The anterolateral edge of the horizontal lamina of the nasal, as seen in dorsal view, is concave (0) or bulges outward (1) [mod].
12. [11] Nasal: The lateroposterior margin of the horizontal lamina of the nasal, adjacent to the prefrontal, is nearly horizontal (0), or it is oriented vertically in the form of a small (1) or large (2) wall.
13. [12] Nasal: The posterior margin of the horizontal lamina of the nasal, adjacent to the midline, is straight (0) or forms a short to long posterior process (1).
14. [13] Maxilla: The modal, or median, number of adult maxillary teeth is 18 or more (0), 17-15 (1), 14-12 (2), or 11-9 (3). Tooth counts vary by one or two intraspecifically, as well as on opposite sides of the same individual; this character and those similar for the other dentigerous elements may be of little phylogenetic importance, but are included for consistency with Kluge (1993).
15. [14] Prefrontal: The anterolateral lamina of the prefrontal is large and in contact with the maxilla for most of the length of the lamina (0), of modest

size, creating a narrow gap between the maxilla and the length of the lamina as seen from lateral view (1), or small or nearly absent, creating a wide gap between the maxilla and the lamina as seen from lateral view (2) [mod].

16. [16] Prefrontal: The anterolateral and medial laminae of the prefrontal form a sharp, ≤ 90 angle (0), or gradually rounded (1) corner [mod].
17. [17] Prefrontal: The medial lamina of the prefrontal narrowly (0) or broadly (1) undercuts the frontal.
18. [new] Prefrontal: The lacrimal foramen is entirely surrounded by the prefrontal (0) or is not entirely surrounded by the prefrontal (1). This character was suggested by Rage (1984) as a synapomorphy for fossil erycines, and it is on this basis that it is included here.
19. [18] Frontal: the frontonasal facet, the place where the ventral lamina of the nasal contacts the frontal, is small and vertical and lies entirely between the olfactory canals (0), or the facet lies both between and below the olfactory canal and the horizontal-ventral portion of the facet is short (1) or long (2). *Ungaliophis* does not possess such a facet, and is therefore coded as inapplicable for this character.
20. [19] Frontal: The preorbital process of the frontal is in contact (0) or is not in contact (1) with the horizontal lamina of the nasal [mod].

21. [20] Frontal: In dorsal view of the disarticulated frontal, the preorbital process is entirely exposed, revealing a lateral notch between it and the body of the frontal (0), the preorbital process is slightly visible under the anterolateral corner of the dorsal surface of the frontal, with no lateral notch present (1), or the preorbital process is not visible and is entirely covered by the anterolateral corner of the dorsal surface of the frontal (2) [mod]. Not applicable in taxa that do not possess a preorbital process.
22. [21] Supraorbital: The supraorbital is present (0) or absent (1).
23. [22] Postorbital: The postorbital bone is long, enclosing at least 50% of the posterior orbital margin (0), short, barely projecting from the parietal, or absent (1) [mod].
24. [23] Optic Foramen: The ventral border (floor) of the optic foramen is formed by both the parietal and frontal (0) or by the parietal alone (1).
25. [24] Ectopterygoid: The lateral and medial heads on the anterior end of the ectopterygoid are present (0) or absent (1).
26. [25] Ectopterygoid: The anterior end of the ectopterygoid is wide and round (0) is narrow and pointed (1).
27. [26] Ectopterygoid: The posterior end of the ectopterygoid contacts the dorsal, dorsolateral, or lateral (0) or solely anterior (1) surface of the pterygoid [mod].

28. [27] Parietal: The bulbous middle-third of the parietal is narrower (0) or wider (1) than the distance between the lacrimal foramina [mod].

29. [28] Parietal: The postorbital process of the parietal is absent or small (0) or large (1).

30. [29] Parietal: A midsagittal crest is absent (0), or weakly (1) or markedly (2) developed in the anterior 1/3 to 1/2 of the parietal. The last two character states are subject to ontogenetic variation, and thus may be uninformative.

31. [30] Exoccipital: The exoccipitals are separated (0) or in contact (1) on the dorsal surface of the occipital condyle.

32. [31] Exoccipital: On the bridge of bone between the fenestra rotunda and the foramen for the jugular vein and vagus cranial nerve, there is a large ridge (0) or a small or no ridge, causing the bridge of bone to appear recessed medial to the level of the rest of the border of the tympanic opening (1) [mod]. State (1) is most pronounced in the members of the genus *Charina.*

33. [32] Vomer: The anterior bony margin of the external vomeronasal fenestra is uneven, due to small extensions of the vomer into the fenestra (0), or smooth, with no such extensions (1) [mod].

34. [33] Vomer: The caudal margin of the external vomeronasal fenestra is directed laterally (0), lateroposteriorly (1), or posteriorly (2).

35. [34] Vomer: The horizontal posterior lamina of the vomer is wide (0) or narrow (1).

36. [35] Septomaxilla: The septomaxilla is largely exposed (0) or hidden (1) beneath the nasal in dorsal view [mod].

37. [36] Septomaxilla: The dorsoposterior process of the septomaxilla is extremely long (0), short (1), or absent or nearly so (2).

38. [37] Palatine: The modal, or median, number of adult palatine teeth is approximately 6 or more (0), 5-3 (1), or 2-0 (2). See character 13 for comment on tooth counts; this may only be informative for *Calabaria reinhardtii* and *Charina bottae* as they do not have teeth on the palatine.

39. [38] Palatine: The choanal process of the palatine is large and continuous (0) or tiny and discontinuous (1).

40. [39] Palatine: The medioposterior corner of the palatine lies entirely laterally to or on a narrow ledge, appearing as a groove on the medial surface of the pterygoid (0) or wide ledge, appearing as a dorsally exposed projection from the medial surface of the pterygoid (1) [mod].

41. [40] Palatine: The maxillary process of the palatine is wide (0) or narrow (1).

42. [41] Palatine: The maxillary process of the palatine lies anterior to (0) or at (1) the level of the palatine-pterygoid joint.
43. [new] Palatine: The palatine is pierced by a foramen for the maxillary branch of the trigeminal nerve (0) or the palatine does not entirely surround this foramen (1). This character was suggested by Rage (1984) as a synapomorphy for fossil erycines, and it is on this basis that it is included here.
44. [42] Pterygoid: The modal, or median, number of adult pterygoid teeth is 12 or more (0), 11-9 (1), 8-6 (2), 5-3 (3), or 2-0 (4). See character 13 for comment on tooth counts; this may only be informative in the sense that *Calabaria reinhardtii* does not have pterygoid teeth.
45. [43] Pterygoid: The medioventral margin of the posterior one-third of the pterygoid is rounded (0) or folded into a shallow, dorsomedially exposed groove (1), or deep groove (2) [mod].
46. [44] Parabasisphenoid: The cultriform process of the parabasisphenoid is deep throughout its length, the trabecular groove is obvious along its entire length (0), shallow anteriorly and deep posteriorly, the groove is absent anteriorly and present posteriorly (1), or the parasphenoid is shallow throughout its length, the groove is absent (2) [mod].

47. [45] Parabasisphenoid: The interparietal area of the parabasisphenoid is narrow, sides parallel (0), of modest width, sides parallel (1), or very wide, with diverging sides (2).
48. [46] Parabasisphenoid: The parasphenoid wing of the parabasisphenoid, which flares over the anterior opening of the vidian canal, is present (0) or absent (1). Sometimes this structure elaborates ventrally into the basipterygoid process, but to be state 0, the structure does not have to project downward, but may be very flat and projecting anteriorly over the anterior opening of the vidian canal, obscuring it from a ventral aspect [mod].
49. [47] Parabasisphenoid: The right and left posterior vidian canals are approximately equal in size, or the left is larger than the right (0) or the right is larger than the left (1).
50. [48] Coronoid: The coronoid is present (0) or absent (1) on the prearticular portion of the compound bone.
51. [49] Coronoid: The coronoid contacts (0) or is separated from (1) the splenial. Taxa that do not have a coronoid are scored as (1).
52. [50] Dentary: The modal, or median, number of adult dentary teeth is 18 or more (0), 17-15 (1), 14-12 (2), or 11 or less (3). See character 13 for comments on tooth count characters.

53. [51] Caudal vertebrae: The dorsal surface of the neural spine of a posterior caudal vertebra is oval or flat (0) or grooved (1).
54. [52] Caudal vertebrae: An anteriorly projecting accessory process on the neural spine is absent (0) or present (1).
55. [53] Caudal vertebrae: The accessory process on the neural arch of a caudal vertebra is absent (0) or present (1).
56. [54] Caudal vertebrae: The distal tip of the posterior diapophysis of a caudal vertebrae is undifferentiated (0) or oriented nearly vertically into a thin, often convoluted, blade of bone (1).
57. [55] Caudal vertebrae: The distal tip of the anterior diapophyses of a caudal vertebra is undifferentiated (0) or elaborated into a horizontal blade that also originates from the centrum (1).
58. [56] Caudal vertebrae: The transverse process of a caudal vertebra is simple and tapers gradually or is bulbous (0) or a large and rounded anteroposteriorly oriented blade (1).
59. [57] Caudal vertebrae: A caudal hemapophysis projects ventrolaterally (0), is nearly vertical, rounded terminally, and lies close to its counterpart (1), or is curved towards its counterpart of the opposite side, flattened terminally, and widely separated from its counterpart (2).

## Results

**Analysis 1 (Palci et al., 2013)**—The first analysis involved the addition of *Congerophis lego* to the matrix of Palci et al. (2013; a modified version of the matrix by Lee & Scanlon, 2002), which included 27 terminal taxa and 212 characters. Skull A and Skull B of *C. lego* were added to this taxon-character matrix.

Two most parsimonious trees were recovered, with a total length of 639 steps (CI = 0.4632; RI = 0.7118; HI = 0.5368). The only polytomy in the strict consensus tree (Fig. 3.8a) includes the Bolyeriinae, Tropidophiinae, and (*Acrochordus*, Colubroidea), much like the original results of Lee and Scanlon (2002). Erycinae is sister to Skull A and Skull B, which are, in turn, sister to each other. One difference between these results and those of Lee and Scanlon (2002) is the movement of Ungaliophiinae to a sister group position with Booidea, a result also recovered in Palci et al. (2013).

The clade (Erycinae, (Skull A, Skull B)) is united by possessing (1) absent or inconsistent lateral maxillary foramina [also found in Tropidophiinae, *Acrochordus*, and (Typhlopidae, Anomalepididae)], (2) a nasal that extends anteriorly to almost reach the transverse process of the premaxilla [basal to Ophidia (fossil basal snakes, modern snakes), which had been reversed basal to core Macrostomata], (3) no lacrimal duct roof on the prefrontal [a unique reversal of the state in the ancestor of Macrostomata], (4) a lacrimal foramen located between the prefrontal and the maxilla [unique], (5) an incomplete posterior orbital margin [multistate in Erycinae; also found in *Varanus*, (Serpentes, *Najash*), (Bolyeriinae, Caenophidia); different from the core macrostomatan state], (6) a short main body of the parietal [also found in Typhlopidae, (*Cylindrophis*, *Anilius*), Mosasauroidea, *Pachyrhachis*, and Tropidophiinae; Skull B possesses the distinguishing length between the short and intermediate states] (7) an anteroposteriorly broad choanal process of the palatine [multistate in Erycinae; also found in Anilioidea, *Lanthanotus*, Mosasauroidea, all basal fossil snakes excluding *Eupodophis*, (Tropidophiinae, (Bolyeriinae, Caenophidia))], (8) a well developed, large, rectangular ectopterygoid process of the pterygoid [also found in Anilioidea and *Loxocemus,* and multistate in Erycinae], (9) a slightly curved lateral edge of the ectopterygoid [a unique reversal of the macrostomatan state], (10) no coronoid-angular contact [also found in Leptotyphlopidae, Uropeltidae, *Xenopeltis*, and all non-ophidians and fossil taxa excepting *Pachyrachis*], and (11) moderately (15°-30° from horizontal) inclined zygapophyses [a unique reversal of the core macrostomatan state, also found in all other Ophidia].

The autapomorphies of *Congerophis lego* are (1) nasal keel of premaxilla absent [possibly preservational artifact, also found in *Acrochordus* and outgroups], (2) palatine broadly enters the suborbital fenestra [a unique reversal of the state found in Booidea], (3) no postorbitofrontal ossifications [also found in *Najash*, Scolecophidia, and Anilioidea, and *Xenopeltis*] (4) no lateral crest on ventrolateral surface compound element [a unique reversal of the core macrostomatan state].

**Analysis 2: Palci et al. (2013), 'Erycinae' as Two Terminal Taxa**—The second analysis involved the addition of *C. lego* to a modified matrix of Palci et al. (2013), which included 29 terminal taxa and 212 characters.  Skull A and Skull B of *C. lego* were added to this taxon-character matrix, and the terminal taxon 'Erycinae' was divided into two terminal taxa, the Old World genus *Eryx* and the New World genus *Charina,* and rescored due to the high incidence of polymorphic characters in the original terminal taxon. Later, Skull A and Skull B were combined into a single terminal taxon.

Separating Skull A and Skull B into two terminal taxa, one most parsimonious tree was recovered (Fig. 2.9a), with a length of 654 steps (CI = 0.4526, RI = 0.7124, HI = 0.5474). Separating the terminal taxon 'Erycinae' into two terminal taxa seems to have resolved the polytomy present in the first analysis to (Tropidophiinae, (Bolyeriinae, Caenophidia)) and refining the position of *Anilius* into a position sister to *Cylindrophis.*

Condensing Skull A and Skull B into a single terminal taxon results in the recovery of one most parsimonious tree (Fig. 2.9b), with a total length of 653 steps (CI = 0.4533; RI = 0.7067; HI = 0.5467). *Eryx* is now sister to (Boinae, Pythoninae).

The autapomorphies of *Congerophis lego* are (1) the absence of a nasal keel on the premaxilla [likely a preservational artifact], (2) the absence of discrete postorbitofrontal ossifications [also found in *Najash*, Scolecophidia, and Anilioidea, and *Xenopeltis*], (3) the presence of two anteriorly projecting processes (alternatively the lateral and medial heads) on the ectopterygoid [also found in Scolecophidia, (Boinae, Pythoninae), and (Tropidophiinae, (Bolyeriinae, Caenophidia))], (4) the medial wall is lower than the lateral wall of the adductor fossa on the compound element [a unique reversal of the core macrostomatan state; common throughout lineage], (5) there is no lateral crest on ventrolateral surface compound element [a unique reversal of the core macrostomatan state], and (6) There are 9-11 pterygoid teeth present [also found in Madtsoiidae, Anilioidea, and (Boinae, Pythoninae)].

The clade (*Ungaliophis,* (*Charina, Congerophis lego*)(Eryx, (Boinae, Pythoninae)) is united by: (1) the vomerine process of the premaxilla and the vomer are not in contact [unique], (2) the maxilla-palatine articulation is located beneath the anterior half of the orbit [a reversal of the alethinophidians state, also found in *Anomochilus, Cylindrophis,* and some *Acrochordus*, but moved further back in both *Eryx* and *Charina*], (3) the choanal process of the palatine maintains a tiny point of contact with the vomer [a reversal of the macrostomatan state, that is once again reversed in (*Eryx,* (Boinae, Pythoninae); also found in Anomalepididae], (4) the maxillary process of the palatine is located at the posterior end of the main body of the palatine [unique in modern snakes, shared only with Pachyrhachis and Eupodophis], (5) a very deep groove is present along the ventromedial surface of the pterygoid quadrate ramus [unique; reversed in *Charina*], (6) the dorsal exposure of the supraoccipital is anteroposteriorly short [a reversal of the macrostomatan state, also found in all ophidians basal to Macrostomata; reversed in Boinae and *Charina*], (7) the dorsal and ventral posterior processes of the dentary are subequal in length [also found in Aniliodea], (8) the coronoid and angular are not in contact [not applicable to *Ungaliophis*], (9) the coronoid eminence is a well developed, distinct dorsal process [a reversal of the macrostomatan state; also found in *Acrochordus*], and (10) the anterior surangular foramen is situated anteriorly, between the apex and anterior limit of the coronoid process [also found in several non-ophidians, as well as *Anomochilus*, Uropeltidae, and Bolyeriinae].

The clade formed by *Charina* and *Congerophis lego* is united by (1) the absence of a lacrimal duct roof of the prefrontal [a unique reversal of the state in the ancestor of Macrostomata], (2) an incomplete posterior orbital margin [also found in *Varanus*, (Serpentes + *Najash*), (Bolyeriinae + Caenophidia); different from the core Macrostomatan state], (3) an anteroposteriorly broad plate of bone forming the choanal process of the palatine [also found in Anilioidea, *Lanthanotus*, Mosasauroidea, all basal fossil ophidians excluding *Eupodophis*, (Tropidophiinae  (Bolyeriinae, Caenophidia))], (4) a well developed, large, rectangular ectopterygoid process of the pterygoid [also found in Anilioidea and *Loxocemus*], (5) a slightly curved lateral edge of the ectopterygoid [a unique reversal of the macrostomatan state], (6) absence of splenial-coronoid contact [not applicable in *C. lego* or *Charina bottae* due to absence of coronoid, so invalid], (7) and moderately (15°-30° from horizontal) inclined zygapophyses [a unique reversal of the core macrostomatan state, also found in all other Ophidia].

The clade (*Eryx*, (Boinae, Pythoninae)) is supported by (1) the exclusion of the palatine from the suborbital fenestra [unique, but multistate in *Eryx*], (2) a W-shaped nasal-frontal boundary [reversed to convex posteriorly in pythonines; also found in *Haasiophis*, Anomalepididae], (3) a median projection of the posterior border of the parietal over the supraoccipital [also found in *Pachyrhachis*, *Dinilysia*, Cylindrophis, and Bolyeriinae], (4) a quadrate shaft that is more than 25% of the snout-occiput length [also found in *Pachyrhachis* and (Bolyeriinae, Caenophidia)], (5) a tiny point of contact between the vomer and the choanal process of the palatine [also found in *Xenopeltis, Loxocemus,* and (Bolyeriinae, Caenophidia)], (6) no separation of the vomers by the choanal process of the palatine [also found in non-alethinophidians, and (Tropidophiinae, (Bolyeriinae, Caenophidia))], (7) a simple contact between the ectopterygoid and the lateral edge of the pterygoid [unique], (8) a prominent basipterygoid process [also found in taxa basal to (*Najash*, Modern Snakes)], (9) a deeply notched dorsal margin of the splenial [also found in *Varanus* and Uropeltidae], (10) a large, distinct coronoid bone [a reversal of the core macrostomatan state also found in Bolyeriinae], and (11) the equal height of the lateral and medial walls of the abductor fossa of the compound bone [a reversal of the core macrostomatan state also found in Bolyeriinae].

### Analysis 3 (Kluge, 1993)

The third analysis involved the addition of *Congerophis lego* to the matrix of Kluge (1993), modified to include only osteological characters, which included 14 terminal taxa and 57 characters. Skull A and Skull B of *C. lego* were added to this taxon-character matrix. Later, the characters concerning the postcrania (51-57 in the original matrix) were excluded and the analysis was rerun. To maintain direct comparison to Kluge (1993), the hypothetical outgroup "Ancestor" of Kluge

(1993) was retained. The character numbers used in this section are the numbers of the original analysis (in brackets in the character descriptions, above).

The analysis of Kluge's (1993) unaltered matrix resulted in a total of 13 most parsimonious trees, with a length of 107 steps (excluding the two uninformative characters, CI = 0.7238, RI = 0.8513, HI = 0.2762). Two characters were found to be uninformative in Kluge's (1993) original analysis: number 21 (original), the presence or absence of the supraorbital bone, only present in *Calabaria*; and number 47 (original), the right posterior opening of the vidian canal is larger than the left or they are equal in size/the reverse, which is supposedly a synapomorphy for the entire clade that was the focus of the analysis. We have retained them in the data matrix to remain consistent with Kluge (1993), but as uninformative characters they do not affect the analysis. In the strict consensus tree (Fig. 3.10a) excluding all soft tissue characters resulted in a large polytomy between *Eryx elegans*, *E. miliaris, E. somalicus, E. tataricus*, and (*E. jaculus*, *E. johnii*), as well as a polytomy between that clade and *E. colubrinus, E. muelleri,* and *E. conicus.* More importantly, *Congerophis lego* is represented by the sister relationship of Skull A and Skull B, and is sister to the clade formed by all species of *Charina* and *Eryx*.

It is important to note that, of the 10 characters recovered for *Congerophis lego*, three [27(1), 32(1), and 34(1)] are also found in the (*Charina, Calabaria*) clade, and two [40(1), 43(2)] are also found in the *Eryx* clade. An additional three [22(1), 31(1), 48(1)] are also found in *Charina* alone. The two apomorphies of *Congerophis lego* are 43(2) the medioventral margin of the posterior one-third of the pterygoid is folded into a deep groove [which is, in fact, not unique, being shared by all species of *Eryx* except for *E. jaculus* and *E. johnii*, and 57(0) the hemopophysis of the caudal vertebrae projects ventrolaterally [also found in *E. jayakari*].

The characters that unite (*Eryx*(*Calabaria, Charina*)) are 5(1), 24(1), 35(1), 36(1), 39(1), 41(1), 51(1), and 53(1), two of which (5 and 36) change state leading to the *Eryx* clade.

When the postcranial characters were removed from the analysis a total of 39 most parsimonious trees were found, with a length of 96 steps (excluding the two uninformative characters, CI = 0.7234, RI = 0.8539, HI = 0.2766). In the strict consensus tree (Fig. 2.10c) resulted in the same polytomies within the *Eryx* clade as the unaltered matrix, but *Congerophis lego* has move into a sister group position to the (*Calabaria*, *Charina*) clade, with a polytomy failing to resolve whether Skull A or Skull B is closer to this clade. Collapsing Skull A and Skull B into a single terminal taxon clearly resolves this polytomy.

The 11 synapomorphies of the clade (*Congerophis lego*, (*Calabaria*, *Charina*)) are as follows: 5(1) the nasal process of the premaxilla is short [an artifact, considering the state is unknown in *Congerophis lego*], 14(1) the anterolateral lamina of the prefrontal is of modest size, 22(1) the postorbital bone is short, barely projecting from the parietal, or absent [reversed in *Calabaria*], 27(1) the bulbous middle-third of the parietal is wider than the distance between the lacrimal foramina, 31(1) on the bridge of bone between the fenestra rotunda and the foramen for the jugular vein and vagus cranial nerve, a small or no ridge [reversed in *Calabaria*], 32(1) the anterior bony margin of the external vomeronasal fenestra is smooth, 33(1) the caudal margin of the external vomeronasal fenestra is directed lateroposteriorly [transformed into the third seemingly transformational character state, a posteriorly directed margin, in *Charina*], 34(1) the horizontal posterior lamina of the vomer is narrow, 36(1) the dorsoposterior process of the septomaxilla is short, 48(1) The parasphenoid wing of the parabasisphenoid is absent [reversed in *Calabaria*], and 49(1) the coronoid is separated from the splenial [the original scoring of Kluge (1993) was not altered in this analysis, although, based on our own observations, the coronoid of *Calabaria* is in point contact with the splenial].

The 24 synapomorphies of the clade for the genus *Eryx* are: 3(1), 4(1), 5(2), 6(2), 7(1), 8(1), 10(1), 11(2), 12(1), 14(2), 15(1), 16(1), 18(2), 19(1), 23(1), 24(1), 28(1), 29(2), 35(1), 36(2), 38(1), 41(1), 44(1), and 45(1). These will be expanded upon in the results of the fourth analysis.

### Analysis 4 (Kluge, 1993) Expanded Matrix including fossil taxa

The fourth analysis involved the addition of *Congerophis lego* to a matrix modified from Kluge (1993), including only osteological characters from the original matrix, in addition to three new characters pertaining to the additional taxa, for a total of 59 characters. One character, character 15 in the original matrix, was removed because the states were identical in all taxa. Five additional taxa were added to the analysis to replace Kluge's (1993) hypothetical outgroup taxon "Ancestor". We used the following taxa to test the ingroup relationships: *Python molurus, Boa constrictor, Tropidophis haetianus, Ungaliophis continentalis,* and *Anilius scytale* as the outgroup taxon. Furthermore, the putative python *Calabaria reinhardtii* was removed, because the original analysis by Kluge (1993) was heavily biased towards an ingroup relationship with this taxon and the dubious Erycinae s.l. These changes brought the total number of terminal taxa to 17. Skull A and Skull B of *Congerophis lego* were added to this taxon-character matrix. Later, Skull A and Skull B were combined into a single terminal taxon, *C. lego*, and subject to the same method. The character numbers in these results refer to my modified character list, not the original list from Kluge (1993).

Separating Skull A and B into separate terminal taxa, resulted in 4 most parsimonious trees, with a length of 130 steps (CI = 0.5969, RI = 0.8237, HI =

0.4031). The removal of character 15 reduced the number of most parsimonious trees from 27 to 4 and shortened the trees by 12 steps, but it also reduced resolution in the *Eryx* clade. All species in the clade formed by the genus *Eryx*, apart from *E. jaculus* and *E. johnii*, which are sister to each other, form polytomy in the strict consensus tree (Fig. 3.11a). *Boa constrictor* is sister to this polytomy. The other major branch, sister to (*Boa constrictor*, *Eryx*) is the clade (*Ungliophis continentalis*, (*Tropidophis* haetianus, (*C. lego*, *Charina*))). *Python molurus* is in the sister group position to these two major clades, and *Anilius scytale* roots the tree in the outgroup position. All characters are now informative, unlike in the original analysis by Kluge (1993).

The two major clades, (*Boa constrictor*, *Eryx*) and (*Ungliophis continentalis*, (*Tropidophis* haetianus, (*Congerophis lego*, *Charina*))) are united by five synapomorphies: 5(1) a short nasal process of the premaxilla [which has been reversed in *Tropidophis haetianus* and further reduced in the *Eryx* clade], 7(1) no premaxillary teeth [unique in this matrix], 18(1) a lacrimal foramen that is not entirely surrounded by the prefrontal [unique in this matrix], 41(1) a narrow maxillary process of the palatine [reversed in *Ungaliophis continentalis* and the genus *Charina*, and 44(1) 11-9 pterygoid teeth [a state that only *Congerophis lego*, *Boa constrictor*, *E. muelleri*, and *E. jayakari* do not alter].

The clade formed by *Boa constrictor* and *Eryx* is united by 13 synapomorphies: 3(1) long transverse processes of the premaxilla [also found in Tropidophis haetianus], 6(2) vomerine processes on the premaxilla that are much longer than wide [reversed in *E. muelleri*], 10(1) a slight notch between the anterior ends of the nasals [reversed in *E. colubrinus, E. conicus, E. jayakari,* and *E. muelleri*], 12(1) a small wall present on the lateroposterior edge of the horizontal lamina of the nasal [elaborated further into a large wall in *Eryx*], 13(1) the posterior margin of the horizontal lamina of the nasal forming a posterior process [not applicable in *Boa constrictor*], 14(0) 18 or more maxillary teeth [changed to smaller numbers in all *Eryx*], 20(1) a preorbital process of the frontal that is not in contact with the nasal [not applicable in *Boa constrictor*], 29(1) a large postorbital process of the parietal [also found in *Tropidophis haetianus*], 31(1) exoccipitals that are in contact on the dorsal surface of the occipital condyle [reversed in *E. colubrinus, E. conicus, E. muelleri,* and *E. elegans*], 38(1) 5-3 palatine teeth [reversed in *E. conica*; also found in *Charina trivirgata*], 42(1) a maxillary process of the palatine lying at the level of the palatine-pterygoid joint [also found in *Congerophis lego*], 45(2) a deep groove present along the medioventral margin of the posterior third of the pterygoid [also found in *Congerophis lego* and *Python molurus*; reversed in *E. johnii* and *E. jaculus*], and

49(1) the right posterior vidian canal is larger than the left [also found in the clade (*C. lego*, *Charina*).

*Ungaliophis continentalis* is united with (*Tropidophis haetianus*, (*Congerophis lego*, *Charina*)) by 30(0) the absence of a midsagittal crest on the parietal [also found in *E. elegans*], 50(1) the absence of the coronoid bone [unique in this analysis], and 51(1) in line with the previous, no contact between the coronoid and the splenial.

The clade (*Tropidophis haetianus,* (*Congerophis lego*, *Charina*)) is supported by five synapomorphies 4(0) the presence of an internarial fenestra or dorsal notch [also found in *Boa constrictor*], 25(1) the loss of the lateral and medial heads of the ectopterygoid [also found in all *Eryx* and reversed in *Congerophis lego*], 28(1) a middle third of the parietal that is wider than the distance between the lacrimal foramina [unique in this analysis], 33(1) a smooth anterior bony margin of the vomeronasal fenestra [unique in this analysis], and 44(0) 12 or more pterygoid teeth [reduced in number in *C. lego* and *Charina bottae*].

Combining Skulls A and B into a single terminal resulted in the recovery of 4 most parsimonious trees, with a length of 130 steps (CI = 0.5969, RI = 0.8237, HI = 0.4031). *Congerophis lego* and *Charina* are united by seven synapomorphies, including 14(2) the possession of 14-12 maxillary teeth [more are present in

*Charina trivirgata*], 23(1) a short or absent postorbital bone [shared only with the outgroup taxon in this analysis], 32(1) the absence of a ridge on the bridge of bone between the fenestra rotunda and the opening for the jugular vein and vagus nerve [unique], 34(2) a posteriorly directed caudal margin of the vomeronasal fenestra [an artifact, considering the state is unknown in *Congerophis lego*], 35(1) a wide horizontal posterior lamina of the vomer [unique in this analysis], 37(1) a short dorsoposterior process of the septomaxilla [an artifact, considering the state is unknown in *C. lego,* but likely the same state], and 49(1) the right posterior vidian canal is larger than the left [also found in all *Eryx*].

*Charina bottae* and *C. trivirgata* show strong affinities and are united by nine synapomorphies: 1(1) a conspicuously vertical anterior surface of the transverse process of the premaxilla [unique in this analysis], 17(0) a medial lamina of the prefrontal that narrowly undercuts the frontal [also found in *Ungaliophis*], 26(1) a narrow and pointed anterior end of the ectopterygoid [also found in the outgroup], 27(1) the posterior end contacting solely the anterior surface of the pterygoid [unique in this analysis], 38(1) 5-3 palatine teeth [no palatine teeth present in *Charina bottae,* showing a reduction of the state found in the rest of the clade; this character is present in the majority of *Eryx* species as well, interpreted as homoplasy], 41(0) a wide maxillary process of the palatine [also found in *Anilius, Ungaliophis* and *Python*], 42(1) the same maxillary process lies at the level of the palatine-pterygoid joint [also found in all *Eryx* species and *Boa*], 53(1) dorsally grooved caudal neural spines [also found in all *Eryx* species], 55(1) an accessory process on the neural arch of a caudal vertebra [also found in all *Eryx* species].

Species of the genus *Eryx* are united by 25 synapomorphies: 5(2) the nasal process of the premaxilla is absent [unique in this analysis], 8(1) the anterior one third of the vertical lamina of the nasal decreases depth anteriorly [unique in this analysis], 9(1) and anterior end of the horizontal lamina of the nasal slightly or markedly expands [unique in this analysis], 11(1) the anterolateral edge of the horizontal lamina of the nasal bulges outward [unique in this analysis], 12(2) a large, vertical wall is present on the lateroposterior margin of the horizontal lamina of the nasal [unique in this analysis], 14(3) there are 11-9 teeth present on the maxilla [more in *E. conicus* and *E. colubrinus*], 15(2) the anterolateral lamina of the prefrontal is small or nearly absent [unique in this analysis], 16(1) the anterolateral and medial laminae of the prefrontal form a gradually rounded corner [potentially also present in *Congerophis lego*, but because of taphonomic deformation, cannot be confirmed], 19(2) the frontonasal facet is long and lies between and below the olfactory canal [unique in this analysis], 25(1) the lateral and medial heads of the ectopterygoid have been lost [also found in *Charina*], 36(1) the septomaxilla is hidden beneath the nasal in dorsal view [unique in this analysis], 37(2) the dorsoposterior process of the septomaxilla is absent or nearly so [unique in this analysis], 39(1) the choanal process of the palatine is tiny and discontinuous [unique in this analysis], 44(3) there are 5-3 teeth on the pterygoid [more are present in *E. colubrinus, E. conicus, E. jayakari,* and *E. muelleri*], 46(1) the cultriform process of the parabasisphenoid is shallow anteriorly and deep posteriorly [*E. johnii* and *E. jaculus* possess a more reduced state], 47(1) the interparietal area of the parabasisphenoid is of modest width with parallel sides [*E. jaculus, E. jayakari* and *E. johnii* possess diverging sides], 48(1) the parasphenoid wing of the parabasisphenoid is absent [also found in *Ungaliophis continentalis*], 52(2) there are 14-12 teeth on the dentary [highly variable, changed in five of the 11 species of *Eryx*], 53(1) the dorsal surface of the posterior caudal vertebrae are grooved [also found in *Charina*], 54(1) there is an anteriorly projecting accessory process on the neural spine of the caudal vertebrae [unique], 55(1) there is an accessory process on the neural arch of the caudal vertebrae [also found in *Charina*], 56(1) the distal tip of the posterior diapophysis of a caudal vertebra is oriented nearly vertically into a thin blade of bone [unique], 57(1) the distal tip of the anterior diapophysis of a caudal vertebra is elaborated into a horizontal blade that also originates from the centrum [also found in *Charina trivirgata*], 58(1) the transverse process of a caudal vertebra is a large and rounded anteroposteriorly oriented blade [unique], and 59(2) a caudal hemopophysis is curved towards its counterpart, flattened terminally, and widely separated from its counterpart [unique].

## DISCUSSION AND CONCLUSIONS

### The phylogenetic position of *Congerophis lego*

In all analyses performed, *Congerophis lego* is in a well-supported sistergroup relationship with the New World genus *Charina.* This clade is supported by the following synapomorphies: the absence of a lacrimal duct roof of the prefrontal, the incomplete posterior orbital margin of the orbit, and the slightly curved lateral edge of the ectopterygoid, all of which represent reversals of the macrostomatan state while the anteroposteriorly broad plate of bone forming the choanal process of the palatine, the well developed, large, rectangular ectopterygoid process of the pterygoid, and the moderately (15°-30° from horizontal) inclined zygapophyses, though often also found in basal snakes or select highly derived macrostomatans, appear to be uniquely derived in this clade.

The same conclusion was reached in analyses three and four, although the bias towards a monophyletic Erycinae s.l in the matrix of Kluge (1993) and the over emphasis of the caudal characters, initially placed *Congerophis lego* outside the erycine s.l. clade. The removal of the caudal characters in the third analysis again moved *C. lego* into the sister position to *Charina* (demonstrating the plausible homoplasy of the additional process on the neural arch of a caudal vertebra in both *Eryx* and *Charina*). Three unique features distinguish the clade (*Congerophis, Charina)*: the short or absent postorbital bone, the absence of a ridge on the bridge of bone between the fenestra rotunda and the opening for the jugular vein and vagus nerve, and a wide horizontal posterior lamina of the vomer. These results suggest a strong relationship with the New World genus *Charina*, which is not surprising considering their geographic restriction to the New World.

### Relationships of *Tropidophis* to *Congerophis lego* and *Charina*

In the fourth analysis, *Tropidophis* is nested between *Ungaliophis* and the clade (*Charina, Congerophis lego*). Since there are no other studies that corroborate this relationship, and the synapomorphies uniting these taxa place an overemphasis on characters describing tooth counts and the overall shape of the skull (which is very similar), this result is considered unreliable. Of the three unique synapomorphies (out of five) of this clade, the bulbous parietal, the pterygoid tooth count (the number of which are reduced in the sister taxa), and the smooth anterior margin of the vomeronasal foramen, only the last describes non-ontogenetic, potentially valid variation.

## Phylogenetic position of the Ungaliophiinae

Perhaps one of the most intriguing sister group relationships arising from these results is the position of Ungaliophiinae in both analyses. The two analyses using the matrix of Kluge (1993) recovered *Ungaliophis* as sister to (*Tropidophis* and (*C. lego, Charina*), but united only by the absence of a midsagittal crest on the parietal, a character affected by ontogeny and independently evolved in many lineages, and the loss of the coronoid bone, a typically caenophidian feature that may well have evolved more than once.

A close relationship between *Charina* and the Ungaliophiinae has been recovered in every molecular analysis where both taxa were included (Vidal and Hedges, 2002; Slowinski and Lawson, 2002; Noonan and Chippendale, 2006; Weins, et al., 2012; Pyron, Burbrink, and Weins, 2013); Pyron, Burbrink, and Wiens (2013) went so far as reassigning the New World genus to Ungaliophiinae in their analysis.

This seems to be a point of disagreement between the morphological and molecular approaches. In Gauthier et al (2012), Ungaliophiinae was recovered at the base of the Booidea, in a similar arrangement to that found in Analyses 1 and 2 above. Still, this may support a closer morphological relationship between members of the Booidea and Ungaliophiinae. The combined morphological and molecular analysis of Lee et al. (2007), although they chose to use the combined

‘Erycinae’, also reconstructed Ungaliophiinae at the base of a Booidea that does not include Pythoninae. The synapomorphies supporting the position of the Ungaliophiinae are: the maxillary process of the palatine is located at the posterior end of the main body of the palatine; a very deep groove is present along the ventromedial surface of the pterygoid quadrate ramus (which is reversed in *Charina*); a distinct coronoid eminence of the compound bone; and the dorsal and ventral posterior processes of the dentary are subequal in length.

This study is not the first to suggest the close affinities of Ungaliophiinae and a supposed fossil North American erycine s.l.; *Calamagras weigeli*, was recently reassigned to the ungaliophines by Smith (2012) which has unpaired hemapophyses in the caudal vertebral, a feature not found in *Congerophis lego* (Fig. 2.6h). Though this reassignment was based partially on vertebral proportions, which, as argued here, are of dubious value as characters supporting taxa and clades, it stands to reason that the vertebrae of the Ungaliophiinae and North American taxa should look similar as they are closely related to each other as recovered by this analysis.

## Relationships of Boinae and *Eryx*

The results of this study indicate a close relationship between the Boinae and the Old World genus *Eryx*. The sister relationship of these two taxa was recovered in both analyses with strong character support including: a small wall present on the lateroposterior edge of the horizontal lamina of the nasal, a W-shaped nasal-frontal boundary, a maxillary process of the palatine lying at the level of the palatine-pterygoid joint, a deep groove present along the medioventral margin of the posterior third of the pterygoid, a prominent basipterygoid process, the equal height of the lateral and medial walls of the abductor fossa of the compound bone, and a large coronoid bone. In Analysis 2, Pythoninae was recovered in the sister group position to Boinae, a clade that was sister to *Eryx*. Though the Booidea is traditionally viewed as these three taxa, this arrangement requires either the reversal of two solid pythonine characters (the presence of premaxillary teeth and the supraorbital ossification), or the independent loss of those two characters in the four terminal taxa that are basal to the Pythoninae in Analysis 2, neither of which are the most parsimonious solutions to the question. Though there is little agreement between the four analyses conducted here, the Boinae and *Eryx* are commonly grouped together in other analyses.

Morphological analyses consistently group the Boinae with the undifferentiated 'Erycinae' (Cundall, 1993; Gauthier et al., 2012), and the erycines s.l. are typically referred to as "erycine boas", so this result is not a new one. Interestingly, and despite their inherent non-comparability with morphological analyses, the results of recent molecular analyses corroborate this same relationship (Vidal and

Hedges, 2002; Slowinski and Lawson, 2002; Noonan and Chippendale, 2006; Weins, et al., 2012; Pyron, Burbrink, and Weins, 2013).

## A polyphyletic Erycinae?

The separation of 'Erycinae' into its generic and geographic constituents, *Eryx* and *Charina*, caused each to significantly change position with regard to the closely related taxa. In the second analysis, *Charina* occupies the basal position of Booidea, while *Eryx* formed a sister relationship with (Boinae, Pythoninae), effectively making the subfamily Erycinae s.l. paraphyletic. In the fourth analysis, several of the additional taxa were recovered within the ingroup clade, which, in the original Kluge (1993) analysis were separated into the genera *Charina* and *Eryx*. The Erycinae s.l., in all recent studies, have been a rather poorly supported clade of snakes regardless of the use of morphological data sets (Gauthier et al., 2012) or molecular (Vidal and Hedges, 2002; Slowinski and Lawson, 2002; Noonan and Chippendale, 2006; Weins, et al., 2012; Pyron, Burbrink, and Weins, 2013).

## The problem of the tail

The classical uniting feature of the Erycinae s.l. has long been the fused, club-like tail with additional apophyses on the neural arch (Hoffstetter, 1962), a dorsally grooved and expanded neural spine, and expansions of the distal portions of all processes. Here it is argued that this feature may have independently evolved in both New World and Old World taxa. The results of the phylogenetic analyses clearly support the polyphyly of the Erycinae s.l. with primarily cranial evidence, though it is clear that the caudal characters gave the strongest signal for historical notions of the monophyly of the erycines s.l. The removal of the caudal characters in Analysis 3 and subsequent recovery of *Congerophis lego* as sister to *Charina*, rather than basal to all erycines s.l. demonstrates the plausible homoplasy of the additional apophyses on the caudal vertebrae in both *Eryx* and *Charina*.

Additionally, Greene (1973) suggested that if the skeletal peculiarities are adaptations for defensive tail display, they might represent convergence in response to similar predation pressures. Both are semifossorial snakes and plausibly subject to similar adaptive pressures. The function of the erycine s.l. club tail, as well as the results of this phylogenetic analyses, suggest this character is homoplastic.

## What is an 'erycine'?

Breithaupt and Duvall (1986) speculated that the fossils on UW11120 belonged to the fossil vertebral form genera *Ogmophis* and *Calamagras*, the putative North American erycines s.l. This "received wisdom", so to speak, required the detailed analysis of the subfamily Erycinae s.l.. Because of the presumed monophyletic status of the Erycinae s.l., no morphological study could be complete without a discussion of the synapomorphies supporting that concept of monophyly. The original works of Hoffstetter (1962) and Hoffstetter and Rage (1972), where the latter authors published a list of the shared affinities of the New and Old World genera, culminated in the Handbuch der Palaeoherpetologie by Rage (1984), in which he named six diagnostic characters uniting fossil and modern Erycinae s.l. All of these features are vertebral, not surprisingly, but unfortunately, many of them are not specific to erycines s.l. but are shared by many of the Booidea and select additional subfamilies. We present here a review of the 6 characters listed by Rage (1984), with a critique of their value, diagnostic strength, and applicability.

**1) (shared) The lacrimal foramen is not entirely surrounded by the prefrontal**– *Congerophis lego* shares this feature with the Erycinae s.l., as does Tropidophiinae, Ungaliophiinae, Boinae, and some pythonines. Because of the broad distribution of this character, we consider the many instances as potentially homoplastic, and thus unfit to define any of these groups.

**2) (shared) The palatine foramen is not entirely surrounded by the palatine**–*Congerophis lego* shares this feature with the Erycinae s.l., as does Tropidophiinae, Ungaliophiinae, Boinae, and some pythonines. Because of the broad distribution of this character, it is similarly homoplastic following the rationale for Character 1 above.

**3) (shared) The neural arch is flattened**–the neural arch in *C. lego* and Erycinae s.l. is only slightly flatter than the typical terrestrial *Boa* condition observed in the majority of taxa, as is typical with any semifossorial or fossorial taxon. This feature alone can be typical of snakes that are clearly not erycines s.l., such as *Rottophis,* tropidophines, and *Loxocemus* (Szyndlar and Bohme, 1996). This character is highly affected by life habit, and the difference is hardly discrete, making for a poor diagnostic character. Additionally, the height varies throughout the column of any individual snake, thus it is recommended that proportional vertebral characters should not be used to diagnose any but the broadest taxonomic categories (i.e., "boid-like", colubroid), especially when only isolated vertebrae are available.

**4) (shared) The neural spines of the trunk vertebrae are usually low**–the neural spine in *C. lego* and the Erycinae s.l. is indeed lower than the typical terrestrial snake condition, and is rejected here for the same reasons given above for Character 3.

**5) (shared) The prezygapophyseal process is very reduced but not absent**–the prezygapophyseal process is typified by the pronounced state in Colubroidea, but varies with no observable consistency amongst modern snakes. They are indeed present in all erycines s.l. examined, though they vary in form from a small blade or mound not visible in dorsal view, to a distinct process emerging from beneath the prezygapophyseal facet that is clearly visible in dorsal view. *Congerophis lego* possesses a small ventrolateral mound that extends past the border of the prezygapophyseal facet in dorsal view, in common with the New World genus *Charina*. From the exaggerated state in colubrids to the absence of the structure in basal snakes, the intermediate states may be of dubious utility unless they are consistent. It is also possible that polyphyly of the Erycinae s.l. is contributing to the inconsistency of this character within the supposed clade.

**6) (not shared) The neural spines of the caudal vertebrae are swollen**–there is no specialization of the caudal vertebrae of *Congerophis lego*. *Loxocemus* does have swollen caudal neural spines (personal observation), and *Tropidophis* possesses swollen neural spines along much of the trunk, but the extent to which the erycines s.l. are swollen is not readily comparable to any other taxon. The fused and elaborated tail is seemingly the most definitive characteristic of the Erycinae s.l., although it could have evolved in response to a similar predation strategy in both burrowing genera (Greene, 1973; see discussion).

Following Rage (1984), Kluge (1993) outlined six definitive erycine s.l. synapomorphies, which we here critique in the same manner as the criticisms given above of the Rage (1984) character list:

**1)(not shared) The loss of the lateral and medial heads on the anterior end of the ectopterygoid**–*Congerophis lego* displays a pointed, narrow anterior tip of the ectopterygoid, and if it weren't for the detailed resolution of reconstructive software, it would appear single-headed, the left and right moieties possess only a slight concavity between them. There seems to be a trend towards non-differentiation of the anterior heads of the ectopterygoid in several groups. Tropidophiinae display the single-headed state, while Ungaliophiinae possess a state very similar to *C. lego*. Alhough the ectopterygoid is more robust in boines, they seem to be trending towards the loss of the medial head, the lateral projecting farther anteriorly and dominating the anterior tip of the element. This feature may indicate progressive loss of the medial and lateral heads in numerous taxa, or perhaps the affinity of these taxa, but it certainly does not, by itself, define the Erycinae s.l..

**2) (shared) The palatine contacting a wide ledge of bone projecting medially from the pterygoid**–in *C. lego*, the medial pterygoid process of the palatine fits into a groove with a small ledge projecting medially from the pterygoid, expanding slightly anteriorly. This is the same arrangement as in *Charina*, but this ledge is nowhere near as wide as it is in *Eryx*. This extremely broad ledge also projects and expands more anteromedially in all boines observed, but is perhaps more similar to the state in some pythonines (all species of *Aspidites, Python, Morelia* examined, but not in *Liasis*), in which the shelf expands in width posteriorly rather than anteriorly. This groove is present to some degree in *Loxocemus* and *Tropidophis*. The broad distribution within Booidea suggests this character does not tightly define the erycines.

**3) (not shared, equivocal)The maxillary process of the palatine lying posteriorly, at the level of the palatine-pterygoid contact**–Although *Congerophis lego* possesses a maxillary process that is anterior to the most anterior portion of the palatine-pterygoid contact, it is not far anterior relative to the rest of the skull.

This character is inconsistent within the Erycinae s.l., with *Charina trivirgata* displaying a state similar to that in *Congerophis lego,* which is arguably hard to define as a discrete process in *Charina bottae.* Additionally, the position of this process is not unique among the Booidea, and is similar in all Boinae examined. Considering the distribution of this character, it seems to unite the Old World *Eryx* and the Boinae more than the erycines s.l., and is therefore insufficient to define the group.

**4) (shared, nonhomologous?) The right posterior opening for the vidian canal being larger than the left**–While this is true for all erycines s.l. and for *Congerophis lego*, this feature varies wildly from individual to individual and across modern snake species. Bolyeriinae and all Boinae excepting *Candoia* also share this character (Underwood, 1967), and Pythoninae display the opposite condition. Contrary to Kluge (1993), the openings are equal in size in all *Calabaria* examined, as well as those examined by other authors (e.g., Underwood, 1967). The character seems to have only broad-level observable consistency, and thus should not be used to define the Erycinae s.l. only.

**5) (not shared) Caudal neural spines that are grooved dorsally**–There are no specializations of the caudal vertebrae of *Congerophis lego*. *Loxocemus* does have swollen, dorsally grooved neural spines (personal observation), but the extent to which the erycines s.l. neural spines are swollen is not similar to any other taxa. The fused and elaborated tail is seemingly the most definitive characteristic of the Erycinae s.l., though it could have evolved in response to similar predatory pressures in both burrowing genera (Greene, 1973; see discussion).

**6) (not shared) An accessory process on the neural arch of a caudal vertebra**– There are no specializations of the caudal vertebrae of *C. lego*. Both Old and New World erycine s.l. taxa possess at least a small accessory process erupting from either sided of the neural arch of the caudal vertebrae that expand posteriorly along the column and contribute to the overall fusion of the caudal series in these taxa. These accessory processes seem to be the only consistent, unique character that unites the erycines s.l., but this may provide a convergent defensive function rather than representing a true homology between the Old and New World taxa (Greene, 1973).

And finally, Gauthier et al. (2012) named one unreversed and unique synapomorphy for erycines s.l. that we will review here and critique. The brevity of their erycine s.l. synapomorphy list is likely attributed to their inclusion of *Calabaria* in the erycine s.l. subfamily:

**1) (not shared) The presence of pterapophyses** (the accessory process of Kluge, 1993) **on the neural arch of the caudal vertebrae**–There are no caudal specializations in *Congerophis lego*. Calling the elaborations of the caudal vertebrae ‘pterapophyses’ creates a problem with terminological consistency; pterapophyses are exemplified by the extreme, wing-like elaborations of the neural spine of some modern colubroids and the Palaeophiinae (Rage 1984), and they are very likely nonhomologous with those of the Erycinae s.l.. Regardless of the terminology debate, these accessory processes on the caudal vertebrae seem to be the only consistent, unique character that unites the erycines s.l., but this may provide a convergent defensive function rather than representing a true homology between the Old and New World taxa (Greene, 1973).

In concluding this study, it is clear that a new taxonomy needs to be proposed in support of the new grouping of *Charina* with *Congerophis*, and to rediagnose the Erycinae as distinct within Boidae. We provide here revised taxonomy for these snake clades.

REPTILIA Linnaeus, 1758

SQUAMATA Oppel, 1811

## OPHIDIA Brongniart, 1800

### CHARININAE new subfamily

**Etymology**– From the type genus, *Charina*.

**Type genus**—*Charina*, Gray, 1849

**Type species**— *Charina trivirgata* (Cope, 1861; = *Lichanura trivirgata*)

**Included taxa**—*Charina trivirgata, Charina bottae, Congerophis lego* (fossil)

**Diagnosis**—Apomorphies of the taxon: Distinct, subtriangular ectopterygoid process of the pterygoid that protrudes anterolaterally from the main body of the pterygoid; basipterygoid processes reduced to gradual mounds; broad plate of bone forming the choanal process of the palatine, with a dorsal finger of bone extending anteriorly towards the vomer; extreme reduction or loss of the coronoid bone; extremely reduced or lost postorbital ossification; a posteriorly concave posterior border of the parietal with the sagittal crest continued by the supraoccipital; a bulbous parietal, wider than distance between lacrimal foramina; ventral expansion of vertical lamina of nasal where contacts frontal; an additional, smaller foramen dividing the foramen for the jugular vein, and cranial nerves IX and X nerves; a distinct rectangular shelf of the exoccipital, forming the dorsal border of the fenestra ovalis; a long and narrow posterior process of the vomer; a long, narrow, and anteriorly tapering cultriform process of the parabasisphenoid with a trabecular groove; a preorbital process of the frontal that does not contact the nasal.  Differing from Erycinae in having: a laterosphenoid that is always present and robust; a maxilla that heightens anteriorly; an incomplete postorbital margin; no median projection of parietal over supraoccipials; a long dorsoposterior process of the septomaxilla; a present and broad choanal process; anteriorly tapering horizontal lamina of the nasals; a distinct ectopterygoid process of the pterygoid; a posterolaterally directed crista circumfenestralis; no sagittal crest on the anterior half of the parietal; a preorbital process of the frontal that does not contact the nasal; very reduced to absent parasphenoid wings of the parabasisphenoid.  Differing from Ungaliophiinae in having: a snout that tapers to much narrower than parietal; a much more rod-like maxilla and dentary; a horizontal lamina of the nasal that extends more than half the length of the nasal; a smooth ventral surface of the pterygoid; a much more elongate supratemporal; only point contact occurring between the main body of the maxilla and the prefrontal, at the lateral foot process; a more distinct, protruding ectopterygoid process of the pterygoid; hemapophyses present in the caudal vertebrae.  Differing from Tropidophiinae in having: a very slender palatine process of the vomer; an incomplete postorbital margin; no median ridge on the posterior parabasisphenoid; contact between the supratemporal and the parietal; a prootic with no dorsal excursion; a parietal that is much longer than it is wide; a dorsal point of contact between the nasal and frontal in addition to a ventral contact;

posterior processes of the dentary that are subequal in length. Differing from Boinae in having: the posterior 50% of the skull is wider than the anterior 50%; prefrontals that are widely separated on the dorsal surface of the skull; no lateral vertical wall of the nasal; no ventrolateral ledge on the compound bone; an incomplete postorbital margin; indistinct or absent basipterygoid processes of the parabasisphenoid; a large choanal process of the palatine.

## ERYCINAE Hoffstetter, 1962

**Etymology**–From the type genus, *Eryx.*

**Type genus**—*Eryx,* Daudin, 1803

**Type species**— *Eryx jaculus* (Olivier, 1801; = *Boa turcica*)

**Included taxa**—*Eryx colubrinus, E. conicus, E. elegans, E. jaculus, E. jayakari, E. johnii, E. miliaris, E. muelleri, E. somalicus, E. tataricus*

**Diagnosis**—Apomorphies of the taxon: the nasal process of the premaxilla is absent; the anterior one third of the vertical lamina of the nasal decreases depth anteriorly; and anterior end of the horizontal lamina of the nasal slightly or markedly expands; a large, vertical wall is present on the lateroposterior margin of the horizontal lamina of the nasal; the septomaxilla is hidden beneath the nasal in dorsal view and the dorsoposterior process is absent or nearly so; the choanal process of the palatine is tiny and discontinuous; there is an anteriorly projecting accessory process on the neural spines of the caudal vertebrae; the distal tip of the posterior diapophysis of a caudal vertebra is oriented nearly vertically into a thin blade of bone; the transverse process of a caudal vertebra is a large and rounded anteroposteriorly oriented blade; a caudal hemopophysis is curved towards its counterpart, flattened terminally, and widely separated from its counterpart. Differing from Charininae in having: no choanal process of the palatine; a median projection of the parietal over the supraoccipitals; a saggittal crest along the length of the parietal; a smooth, rounded lateral edge of the pterygoid where it articulates with the ectopterygoid; a posteriorly directed crista circumfenestralis; robust parasphenoid wings of the parabasisphenoid; a maxilla of uniform height throughout its length; a large postorbital bone enclosing or nearly enclosing the posterior border of the orbit. Differing from Boinae in having: a parietal that is wider than the combined frontals; a prefrontal with no dorsal excursion; no internarial fenestra; no ventrolateral ledge on the compound bone; premaxilla and nasals contacting to form a sharp anterior border to the snout; no nasal or ascending processes of the premaxilla; additional apophyses on the neural arch of the caudal vertebrae; a dorsal groove and expansion of the neural spine in the caudal vertebrae.

FIGURE 2-1. Overview of the articulated Blocks 2 and 3 and Skulls A and B, representing the entire preserved type specimen of *Congerophis lego* gen. et sp. nov., UW 11120. **A.** picture. **B.** diagram. Scale bar equals 5 cm.

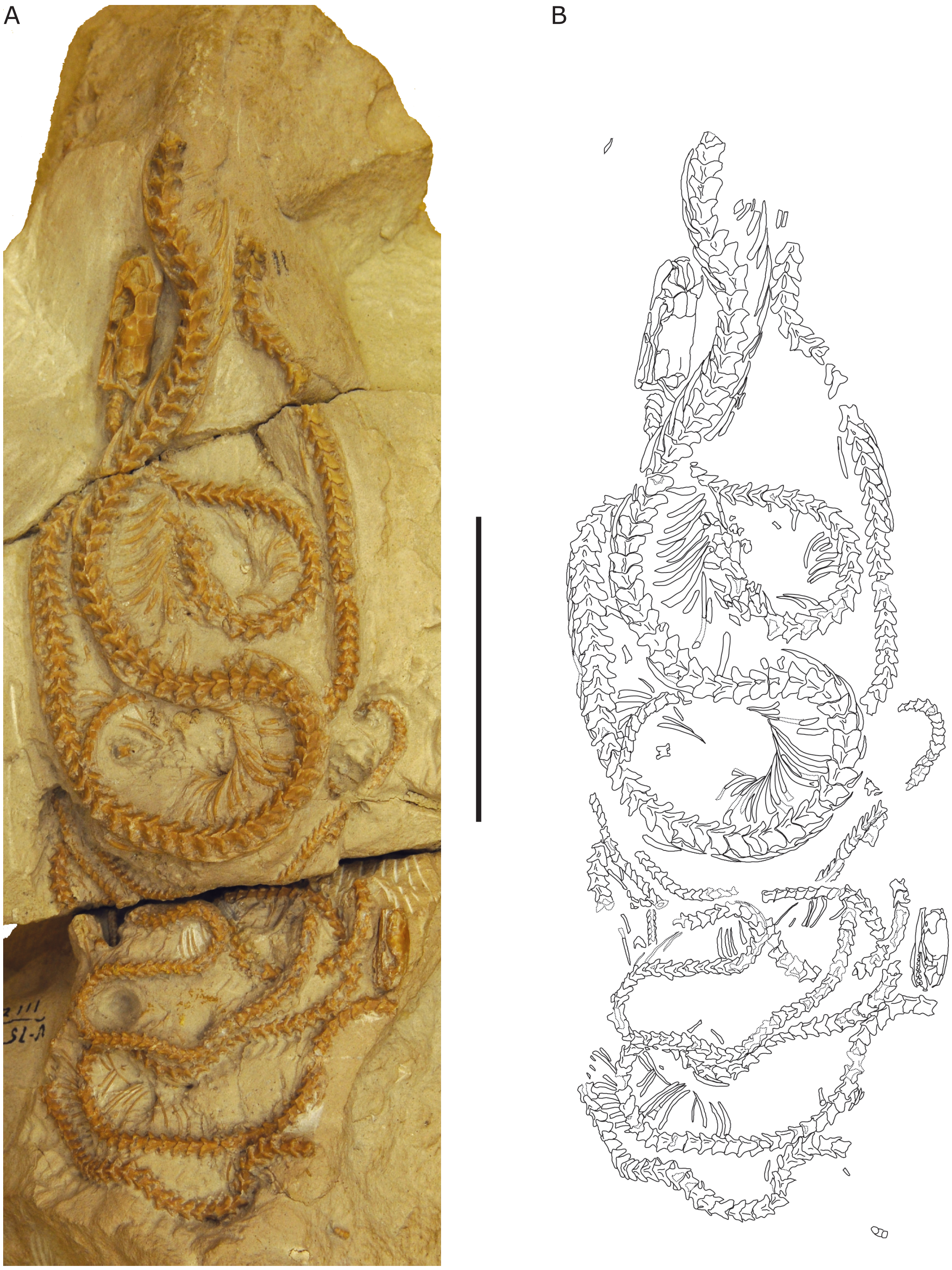
A
B

FIGURE 2-2. Overview of Block 1 and Skull D, representing the referred specimen of *Congerophis lego* gen. et sp. nov., UW 11120. **A.** picture. **B.** diagram. Scale bar equals 5 cm.

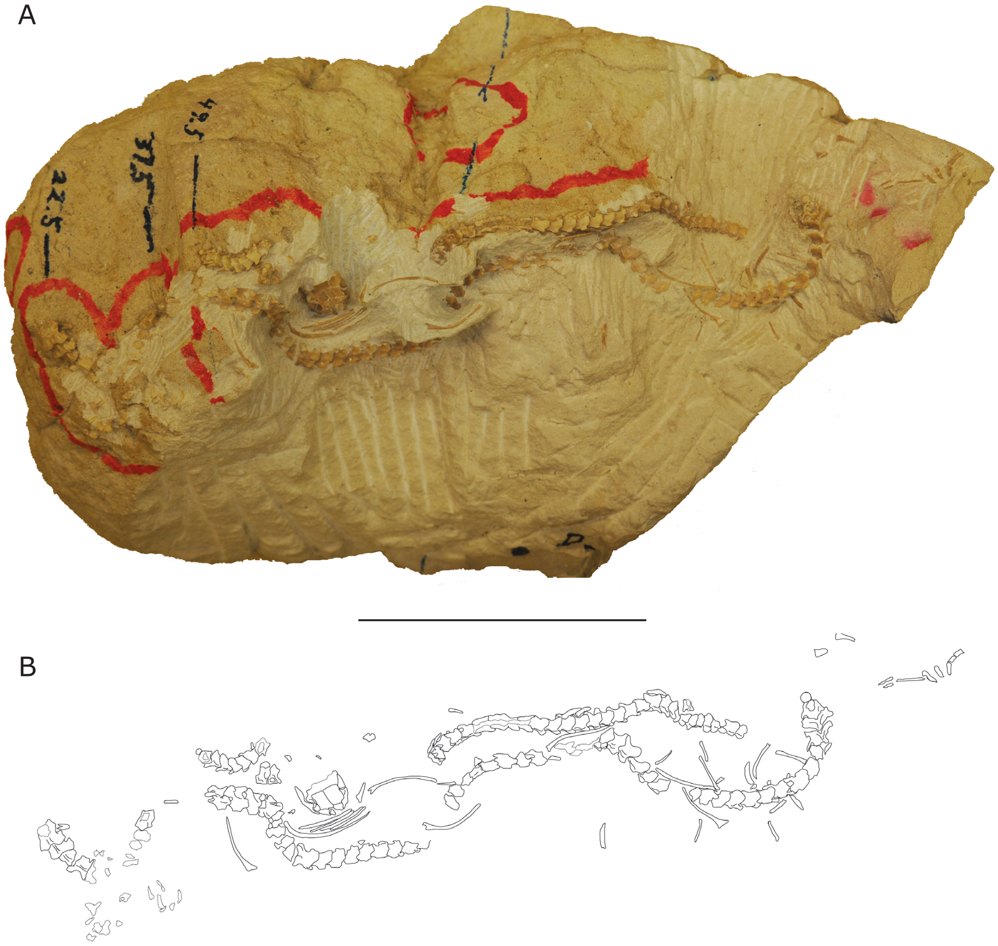
A
22.5
37.5
49.5
B

FIGURE 2-3. Skull of *Congerophis lego* gen. et sp. nov., Skull A. **A.** rendering, right lateral view. **B.** diagram, right lateral view. **C.** rendering, left lateral view. **D.** diagram, left lateral view. **E.** rendering, dorsal view. **F.** diagram, dorsal view. **G.** rendering, ventral view, with mandibles removed. **H.** diagram, ventral view, with mandibles removed. **I.** rendering, anterior view. **J.** diagram, anterior view. **K.** rendering, posterior view. **L.** diagram, posterior view. Scale bars equal 2 mm. Abbreviations: Ar-Articular, BO-Basioccipital, C-Compound element (r-right, l-left), cm-crystalline mass, D-Dentary (r-right, l-left), EO-Exoccipital, EPt-Ectopterygoid, F-Frontal, fT-foramina for the Trigeminal Nerve, M-Maxilla, N-Nasal, P-Parietal, Pa-Palatine, Pb-Parabasisphenoid, Pf-Prefrontal, Pr-Prootic, Pt-Pterygoid, S-Splenial(r-right, l-left), SM-Septomaxilla, SO-Supraoccipital, V-Vomer, Vc-Vidian canal.

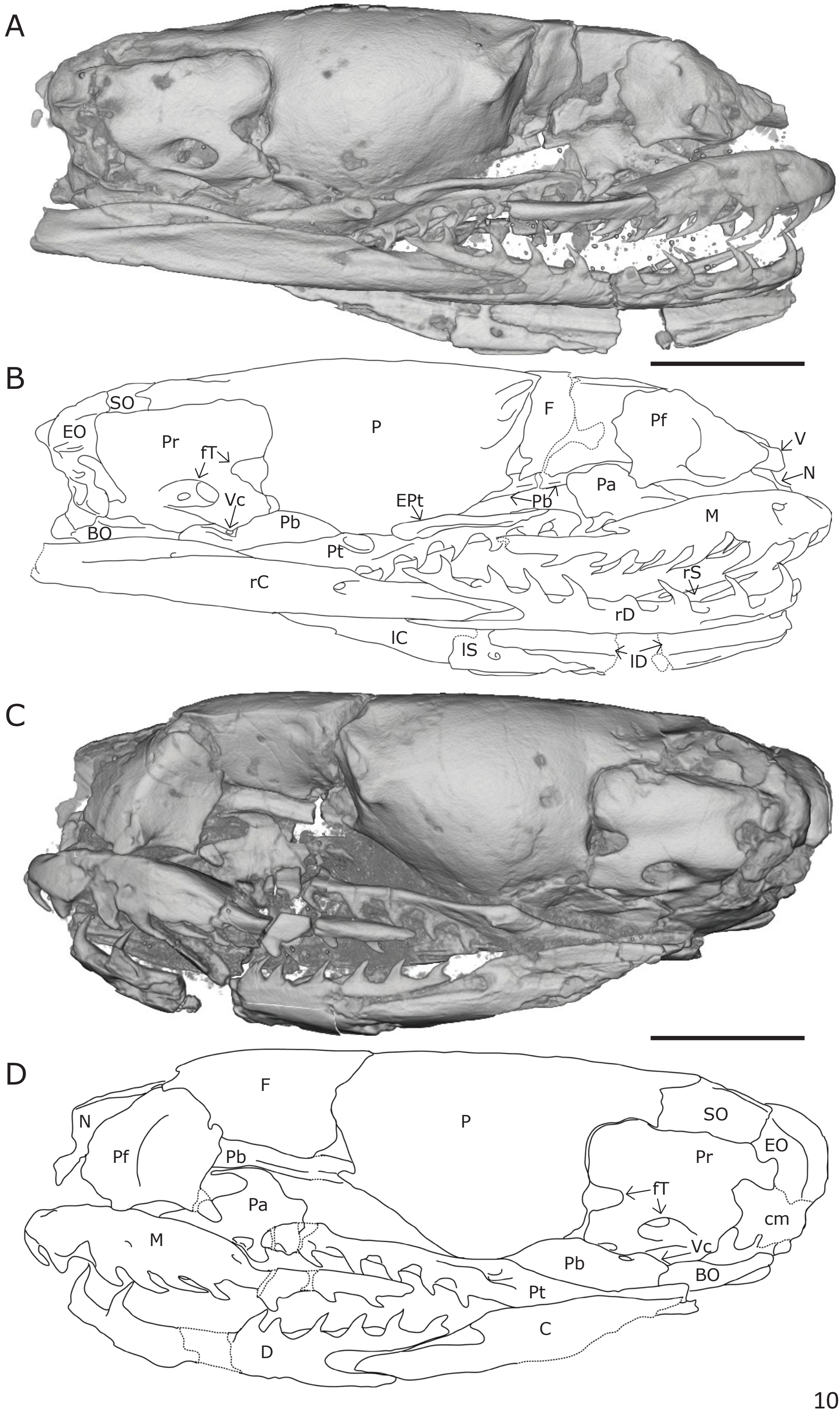
A
B
SO
EO
Pr
fT
Vc
BO
P
Pb
Pt
EPt
F
Pf
V
N
Pa
M
rC
rS
rD
lC
lS
lD
C
D
F
P
N
Pf
Pb
Pa
M
SO
Pr
EO
fT
Vc
cm
Pb
BO
Pt
C
D

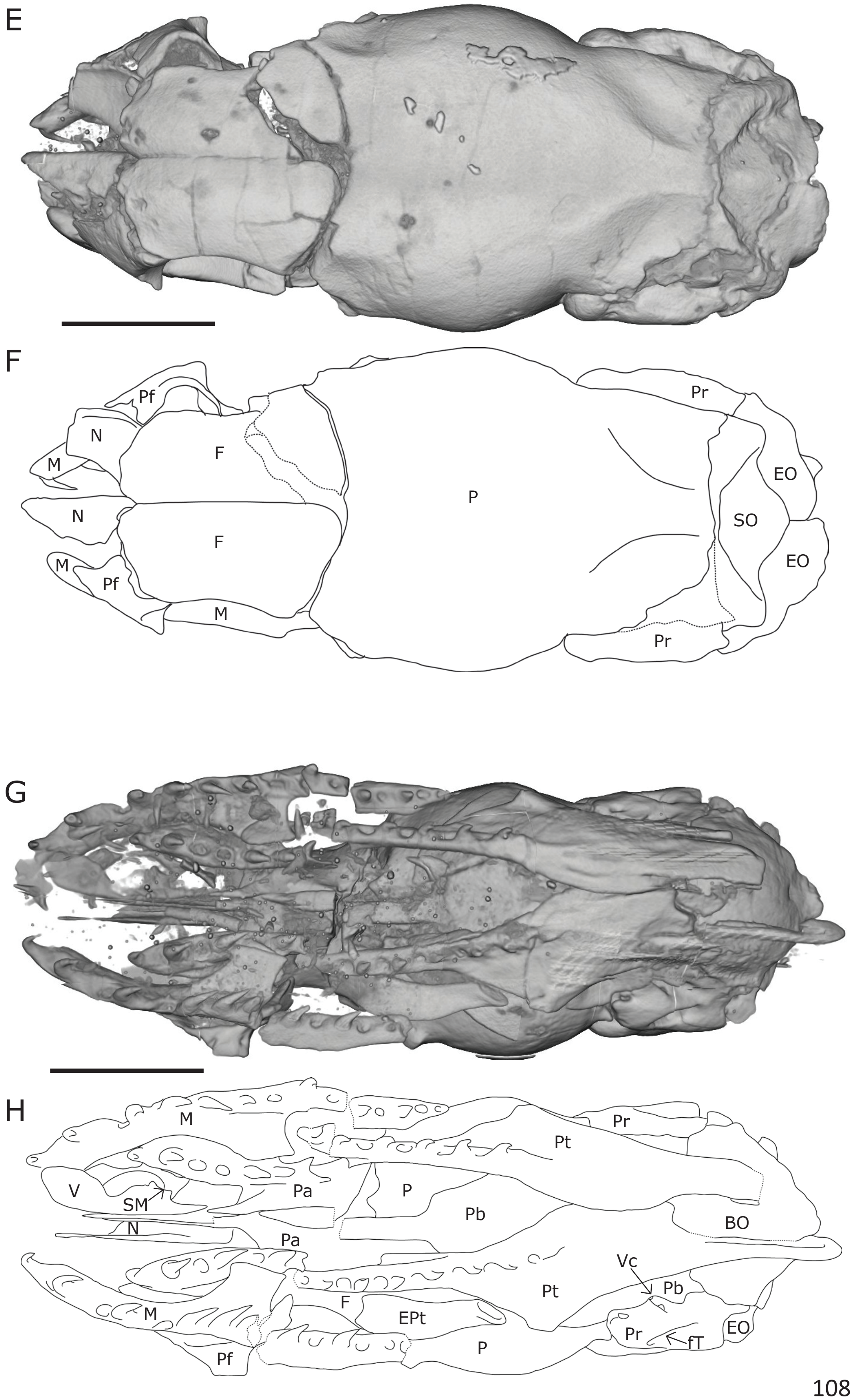
E
F
Pf
N
M
F
P
Pr
EO
SO
N
F
EO
M
Pf
M
Pr
G
H
M
Pr
Pt
V
SM
Pa
P
Pb
BO
N
Pa
Vc
Pt
Pb
F
EPt
M
Pr
fT
EO
Pf
P

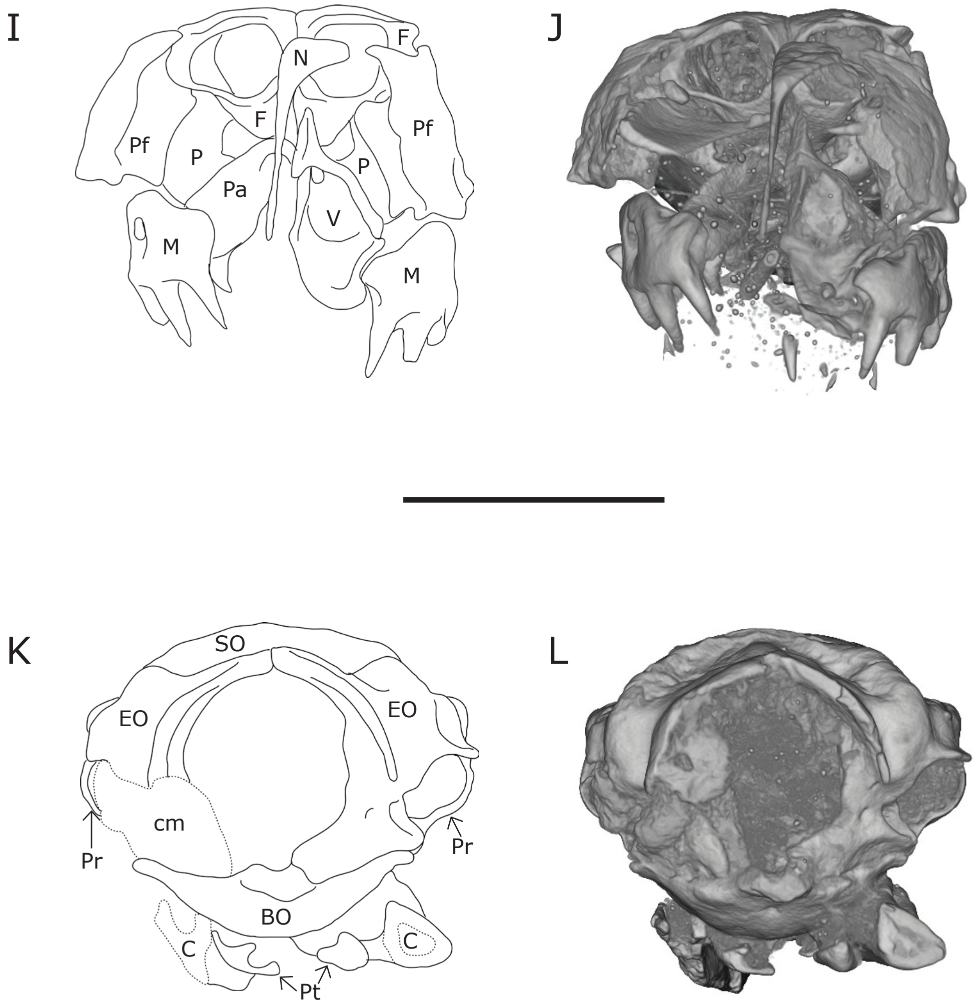
I
N
F
F
Pf
P
Pa
P
Pf
V
M
M
J
K
SO
EO
EO
cm
Pr
Pr
BO
C
C
Pt
L

FIGURE 2-4. Skull of *Congerophis lego* gen. et sp. nov., Skull B. **A.** rendering, dorsal view. **B.** diagram, dorsal view. **C.** rendering, ventral view, with mandible and right palate removed. **D.** diagram, ventral view, with left (only) mandible and right palate removed. **E.** rendering, left lateral view. **F.** diagram, left lateral view. **G.** rendering, right lateral view, with the remains of the right mandible removed, the right maxilla was not preserved. **H.** diagram, right lateral view, with the remains of the right mandible removed, the right maxilla was not preserved. **I.** rendering, anterior view, right snout elements removed. **J.** diagram, anterior view, right snout elements removed. **K.** rendering, posterior view. **L.** diagram, posterior view. Scale bars equal 2 mm. Abbreviations: Ar-Articular, BO-Basioccipital, C-Compound element, D-Dentary, EO-Exoccipital, EPt-Ectopterygoid, F-Frontal, fT-foramina for the Trigeminal Nerve, M-Maxilla, N-Nasal, P-Parietal, Pa-Palatine, Pb-Parabasisphenoid, Pf-Prefrontal, Pr-Prootic, Pt-Pterygoid, Q-Quadrate, S-Splenial, SM-Septomaxilla, SO-Supraoccipital, V-Vomer, Vc-Vidian canal.

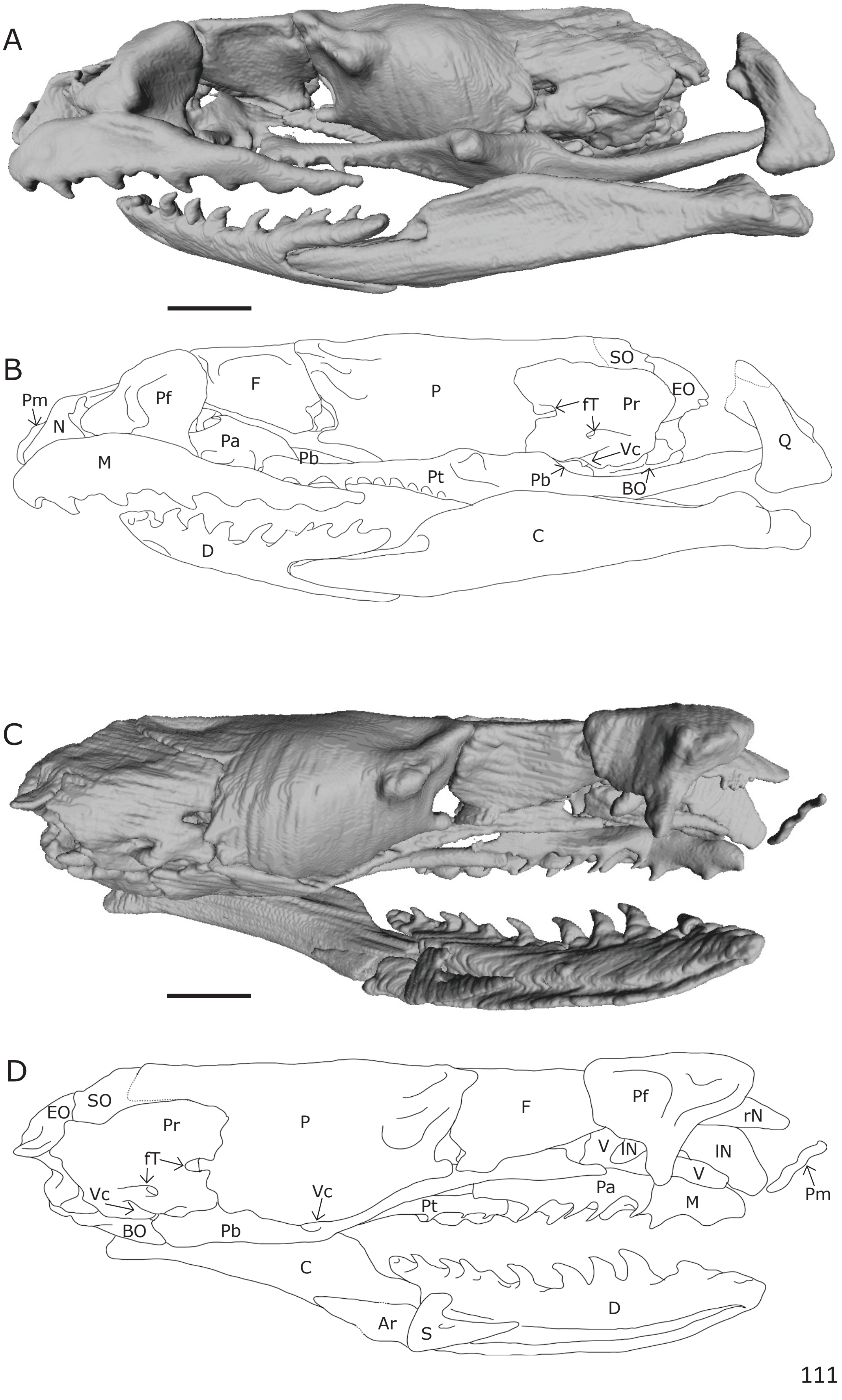
A
B
Pm
N
Pf
F
P
SO
EO
fT
Pr
Pa
M
Pb
Pt
Vc
Pb
BO
Q
D
C
C
D
EO
SO
Pr
P
F
Pf
rN
V
lN
lN
V
fT
Vc
Vc
Pa
Pt
M
Pm
BO
Pb
C
D
Ar
S

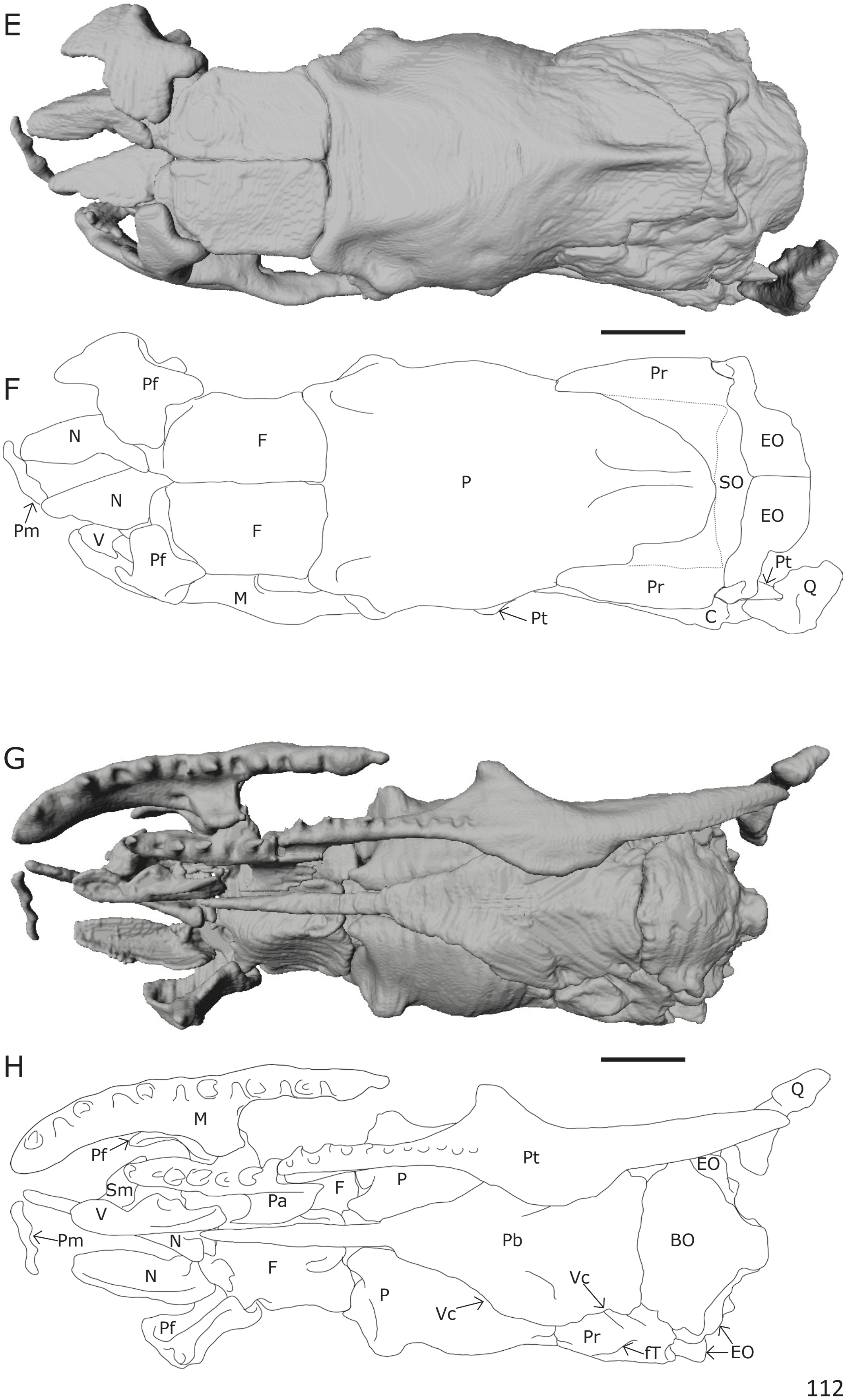
E
F
Pf
Pr
N
F
EO
P
SO
N
Pm
EO
V
F
Pf
Pt
Pr
Q
M
Pt
C
G
H
Q
M
Pt
Pf
EO
Sm
P
F
Pa
V
Pm
Pb
BO
N
N
F
P
Vc
Vc
Pf
Pr
fT
EO

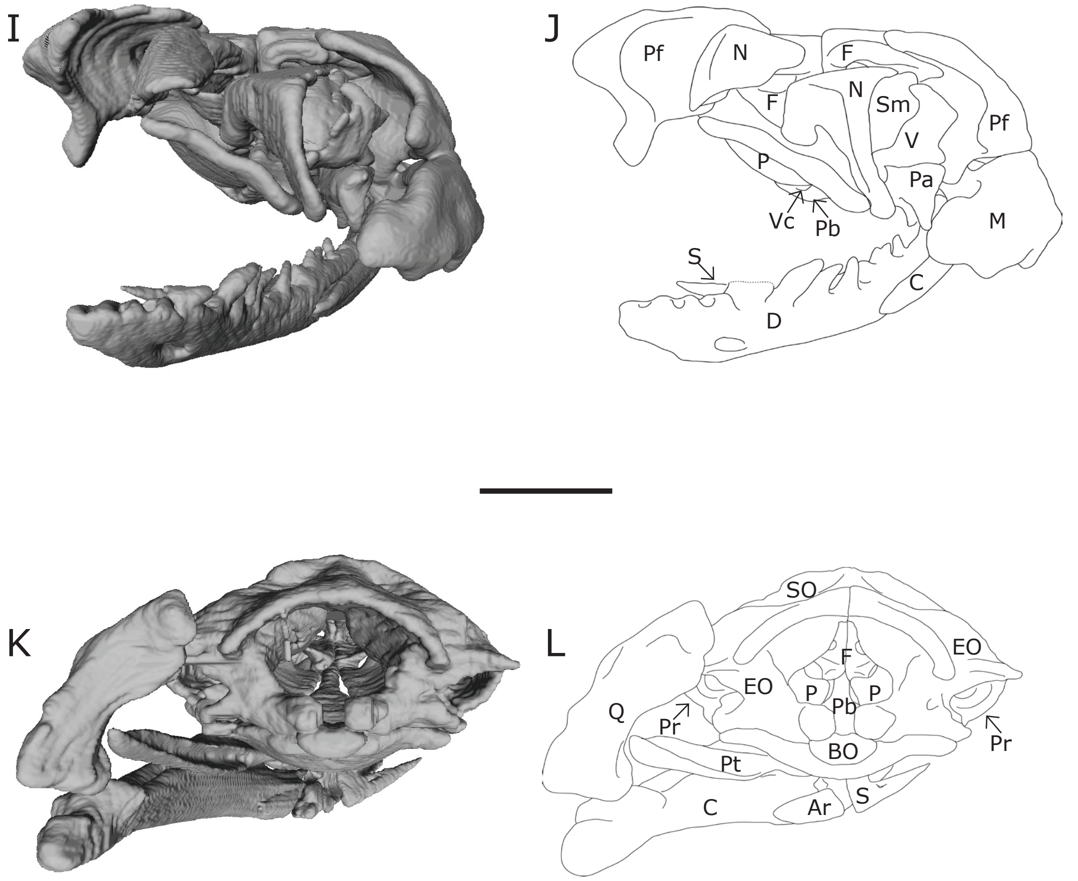
I
J
Pf
N
F
F
N
Sm
V
Pf
P
Pa
Vc
Pb
M
S
C
D
K
L
SO
EO
F
EO
P
P
Pb
Q
Pr
Pr
BO
Pt
S
C
Ar

FIGURE 2-5. Sagittal view of *Congerophis lego* gen. et sp. nov., Skull A.. Scale bar equals 1 mm.

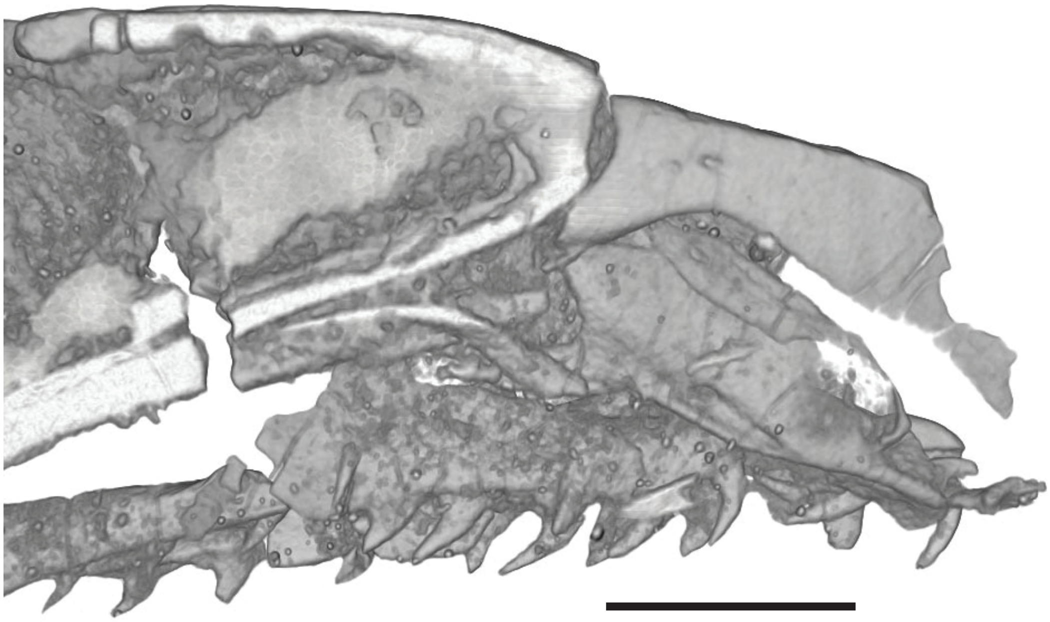

FIGURE 2-6. Important structures of *Congerophis lego* gen. et sp. nov.. **A.** Left palatine and pterygoid of Skull B, lateral view. **B.** Left palatine and pterygoid of Skull B, dorsal view. **C.** Left mandible of Skull B, dorsal view. **D.** Left mandible of Skull B, medial view. **E.** Right crista circumfenestralis of Skull A, posterolateral view. **F.** Left orbit of Skull B, dorsoposterior view. **G.** Hemapophyses on the caudal vertebrae belonging to Skull B, ventral view. **H.** Right ectopterygoid of Skull A, dorsal view. Abbreviations: ant: Anterior, cr: Crista tuberalis, fT: Foramena for the trigeminal branches $V_2$ and $V_3$, hm: Hemapophyses, jv: Foramen for the jugular vein, $V_3$: Entrance foramen for the mandibular branch of trigeminal. Vc: Posterior opening of vidian canal. Scale bars equal 1 cm.

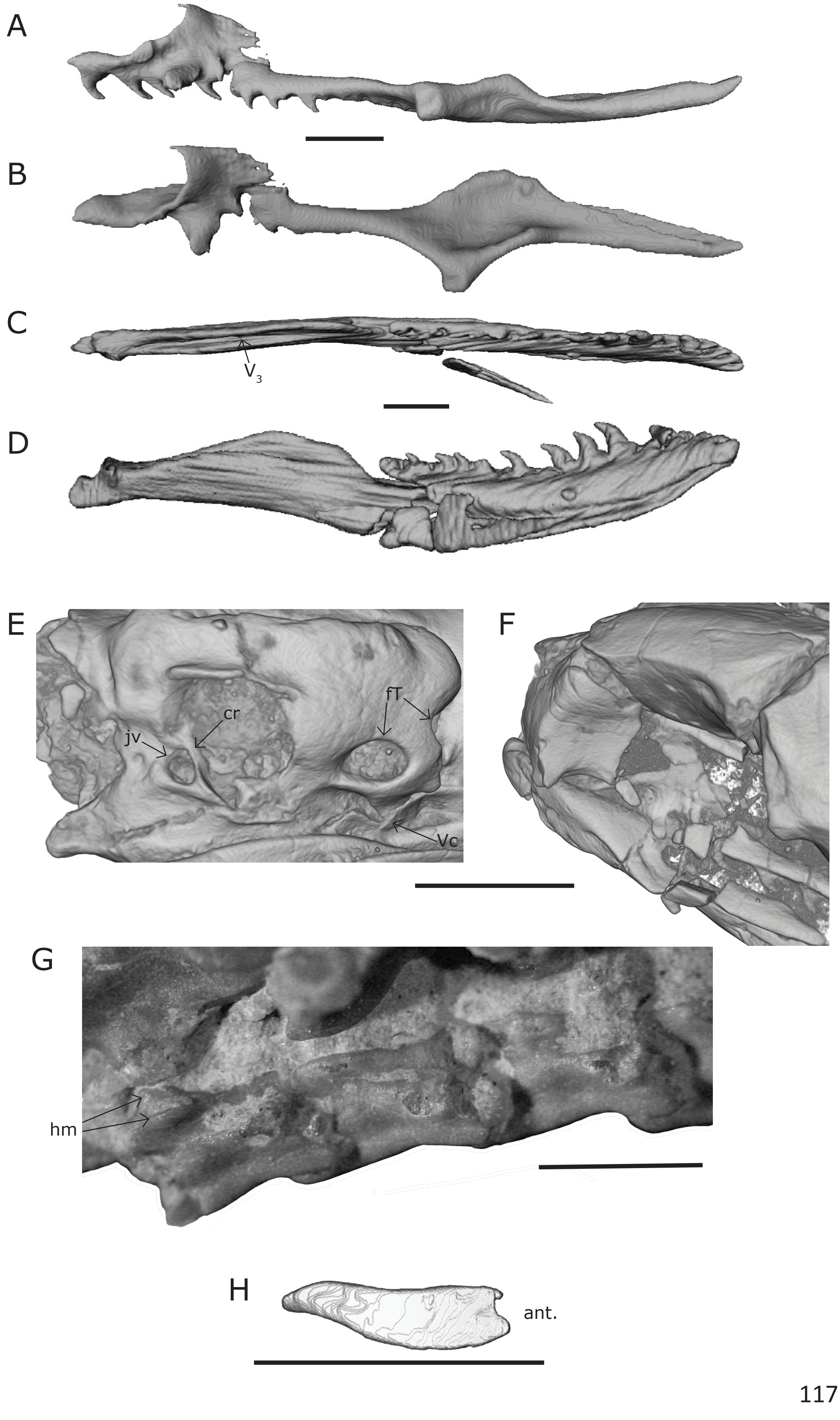
A
B
C
$V_3$
D
E
fT
cr
jv
Vc
F
G
hm
H
ant.

FIGURE 2-7. The various vertebrae found in *Congerophis lego* gen. et sp. nov.. **A-C.** views of the anterior cervical vertebrae of the Skull B individual in Block 3. **D-H.** views of the anterior trunk vertebrae of the Skull D individual in Block 1. **I-L.** views of the mid-trunk vertebrae of the Skull D individual in Block 1. **M-O.** views of the posterior trunk vertebrae of the Skull D individual in Block 1. **P-S.** views of the caudal vertebrae of the Skull D individual in Block 1. Lateral views: **A, D, I, M, P.** Anterior views: **E, J, Q.** Ventral views: **B, E, K, N, R.** Posterior views: **G.** Dorsal views: **C, H, L, O, S.** Scale bars equal 2 mm.

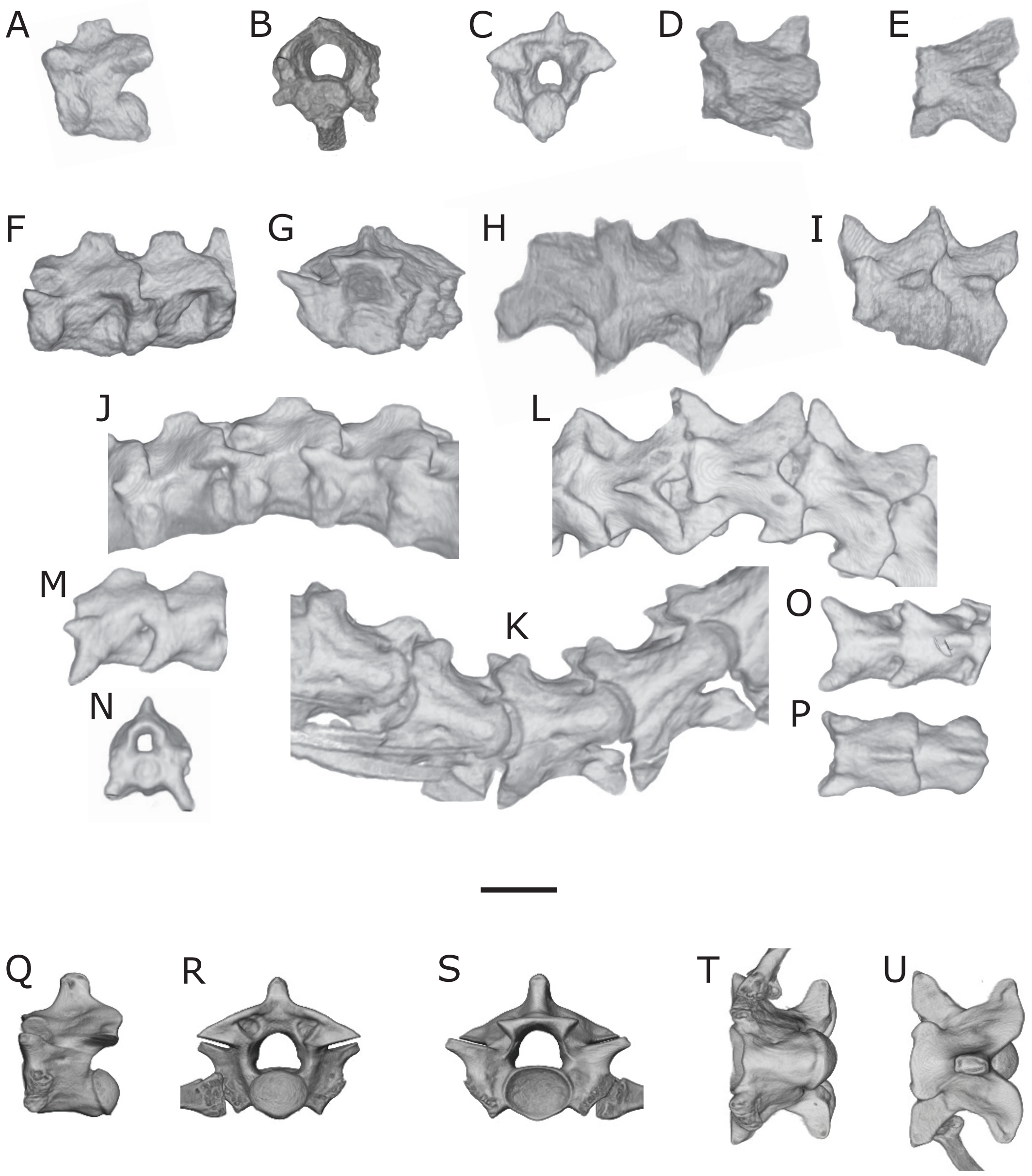
A
B
C
D
E
F
G
H
I
J
L
M
K
O
N
P
Q
R
S
T
U

FIGURE 2-8. Strict consensus tree of two most parsimonious trees from Analysis 1 in which Skulls A and B were scored separately and added to the unaltered matrix of Palci et al. (2013)

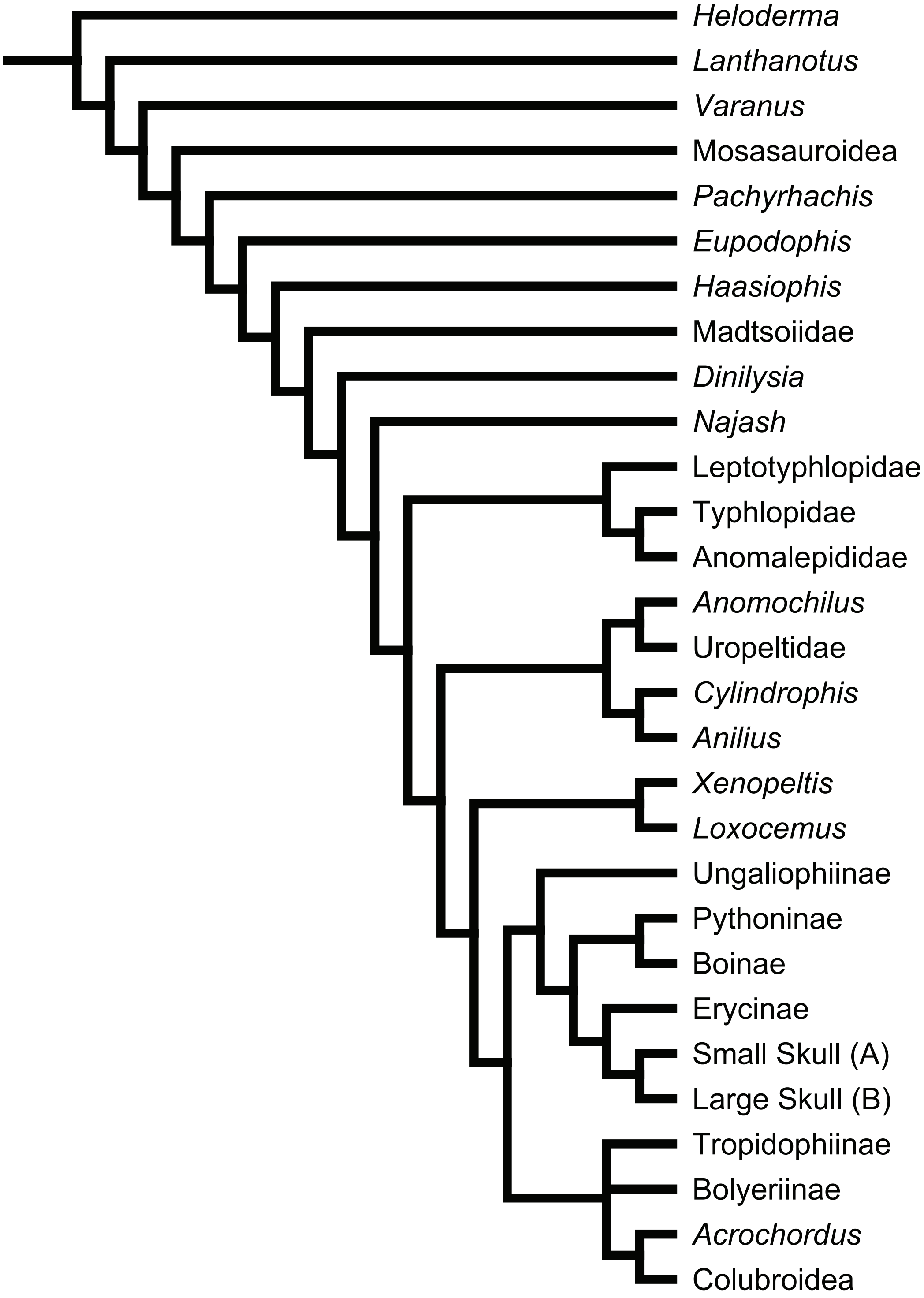
*Heloderma*
*Lanthanotus*
*Varanus*
Mosasauroidea
*Pachyrhachis*
*Eupodophis*
*Haasiophis*
Madtsoiidae
*Dinilysia*
*Najash*
Leptotyphlopidae
Typhlopidae
Anomalepididae
*Anomochilus*
Uropeltidae
*Cylindrophis*
*Anilius*
*Xenopeltis*
*Loxocemus*
Ungaliophiinae
Pythoninae
Boinae
Erycinae
Small Skull (A)
Large Skull (B)
Tropidophiinae
Bolyeriinae
*Acrochordus*
Colubroidea

FIGURE 2-9. The results of Analysis 2, in which *Charina* and *Eryx* were scored separately. **A.** The single most parsimonious tree showing the sister relationship of the separately scored Skulls A and B. **B.** The single most parsimonious tree with Skulls A and B combined into a single terminal taxon.

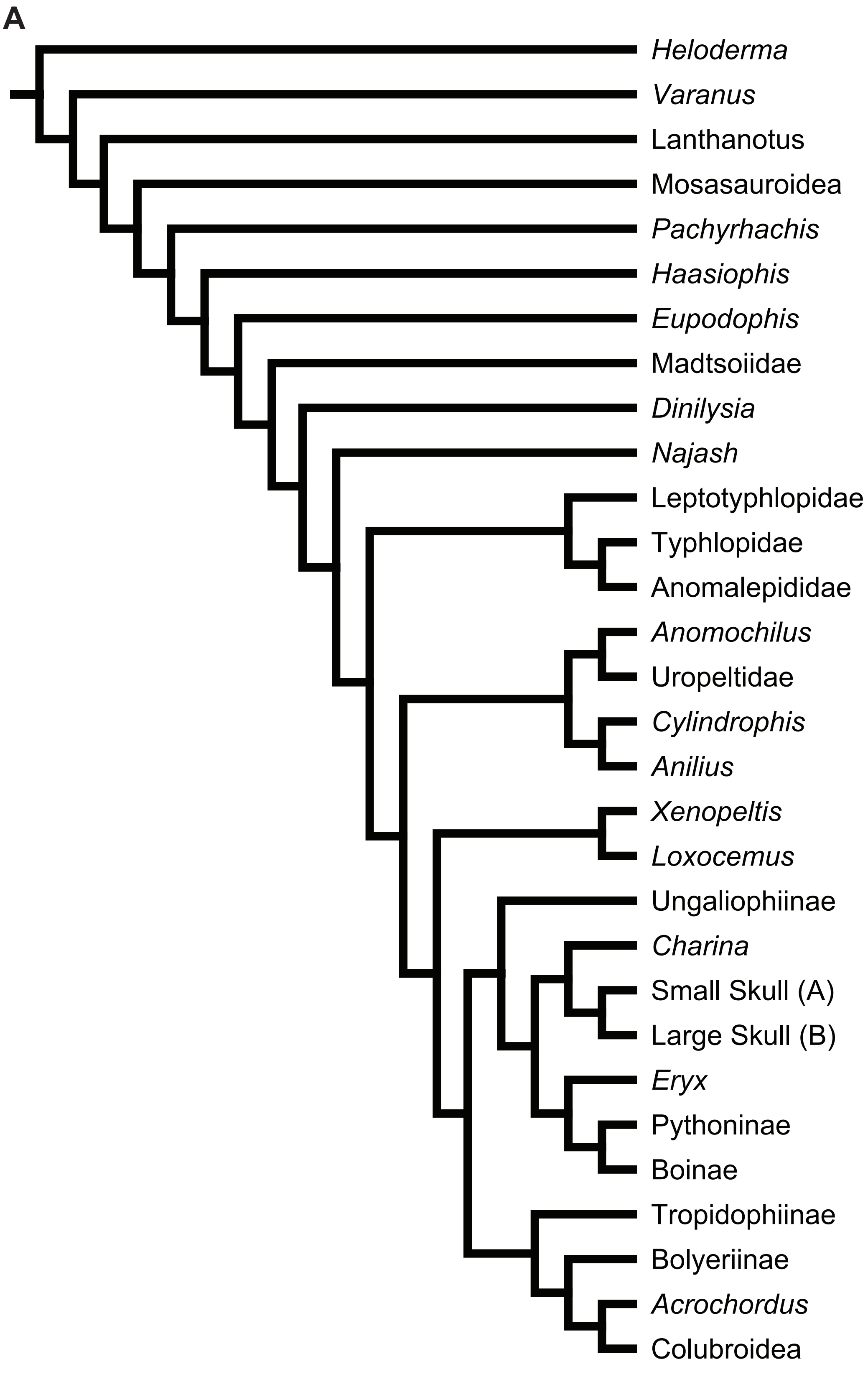
A
*Heloderma*
*Varanus*
Lanthanotus
Mosasauroidea
*Pachyrhachis*
*Haasiophis*
*Eupodophis*
Madtsoiidae
*Dinilysia*
*Najash*
Leptotyphlopidae
Typhlopidae
Anomalepididae
*Anomochilus*
Uropeltidae
*Cylindrophis*
*Anilius*
*Xenopeltis*
*Loxocemus*
Ungaliophiinae
*Charina*
Small Skull (A)
Large Skull (B)
*Eryx*
Pythoninae
Boinae
Tropidophiinae
Bolyeriinae
*Acrochordus*
Colubroidea

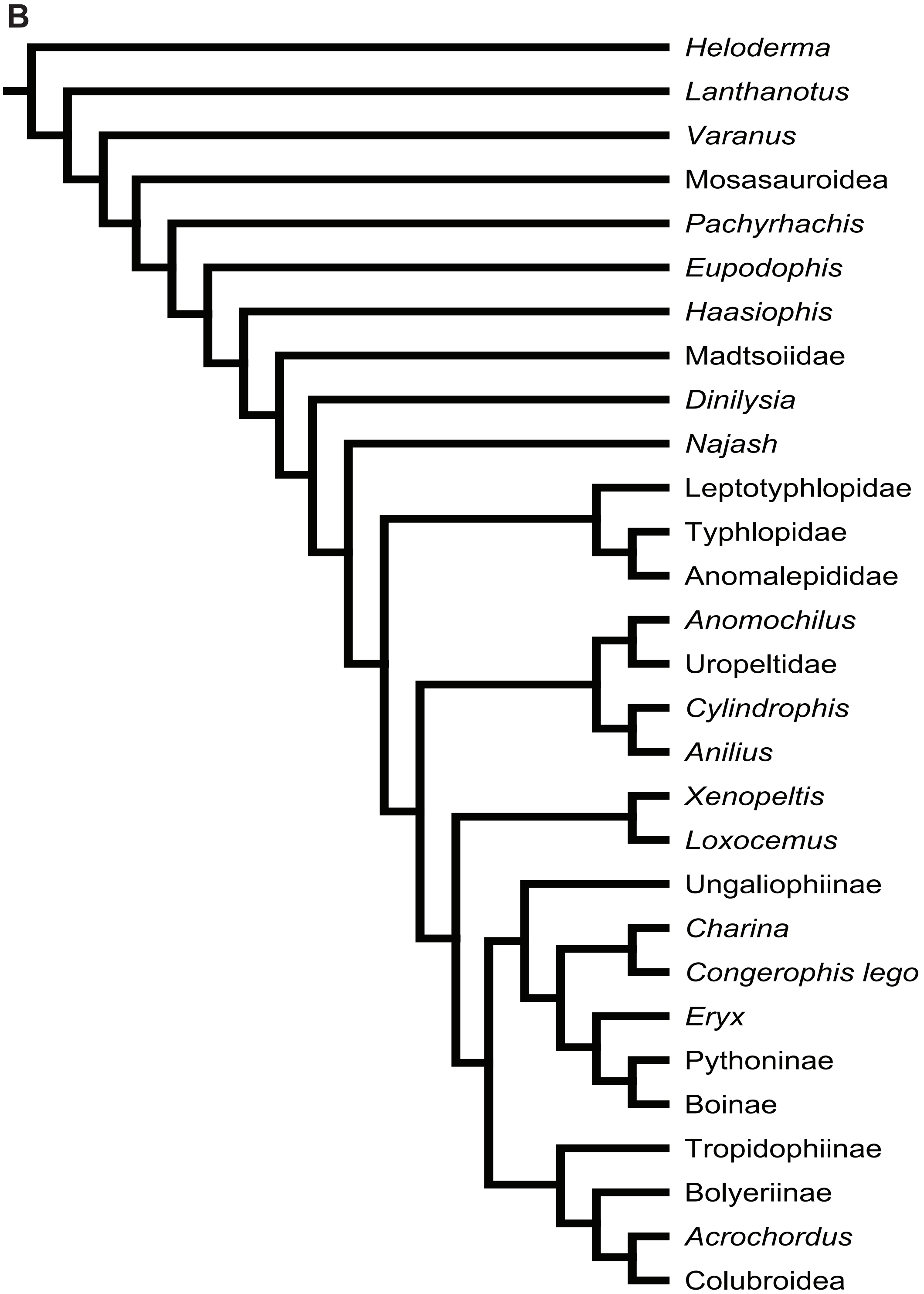
B
*Heloderma*
*Lanthanotus*
*Varanus*
Mosasauroidea
*Pachyrhachis*
*Eupodophis*
*Haasiophis*
Madtsoiidae
*Dinilysia*
*Najash*
Leptotyphlopidae
Typhlopidae
Anomalepididae
*Anomochilus*
Uropeltidae
*Cylindrophis*
*Anilius*
*Xenopeltis*
*Loxocemus*
Ungaliophiinae
*Charina*
*Congerophis lego*
*Eryx*
Pythoninae
Boinae
Tropidophiinae
Bolyeriinae
*Acrochordus*
Colubroidea

FIGURE 2-10. The results of Analysis 3, in which *Congerophis lego* gen. et sp. nov. was added to the unaltered matrix of Kluge (1993). **A.** The strict consensus of the 13 most parsimonious trees showing the sister relationship of the separately scored Skulls A and B, with caudal characters retained. **B.** The 50% majority rule of the 13 most parsimonious trees showing the sister relationship of the separately scored Skulls A and B, with caudal characters retained, percent majority values indicated along branches. **C.** The strict consensus of the 39 most parsimonious trees with Skulls A and B scored separately and caudal characters removed. **D.** The 50% majority rule of the 39 most parsimonious trees with Skulls A and B scored separately and caudal characters removed, percent majority values indicated along branches.

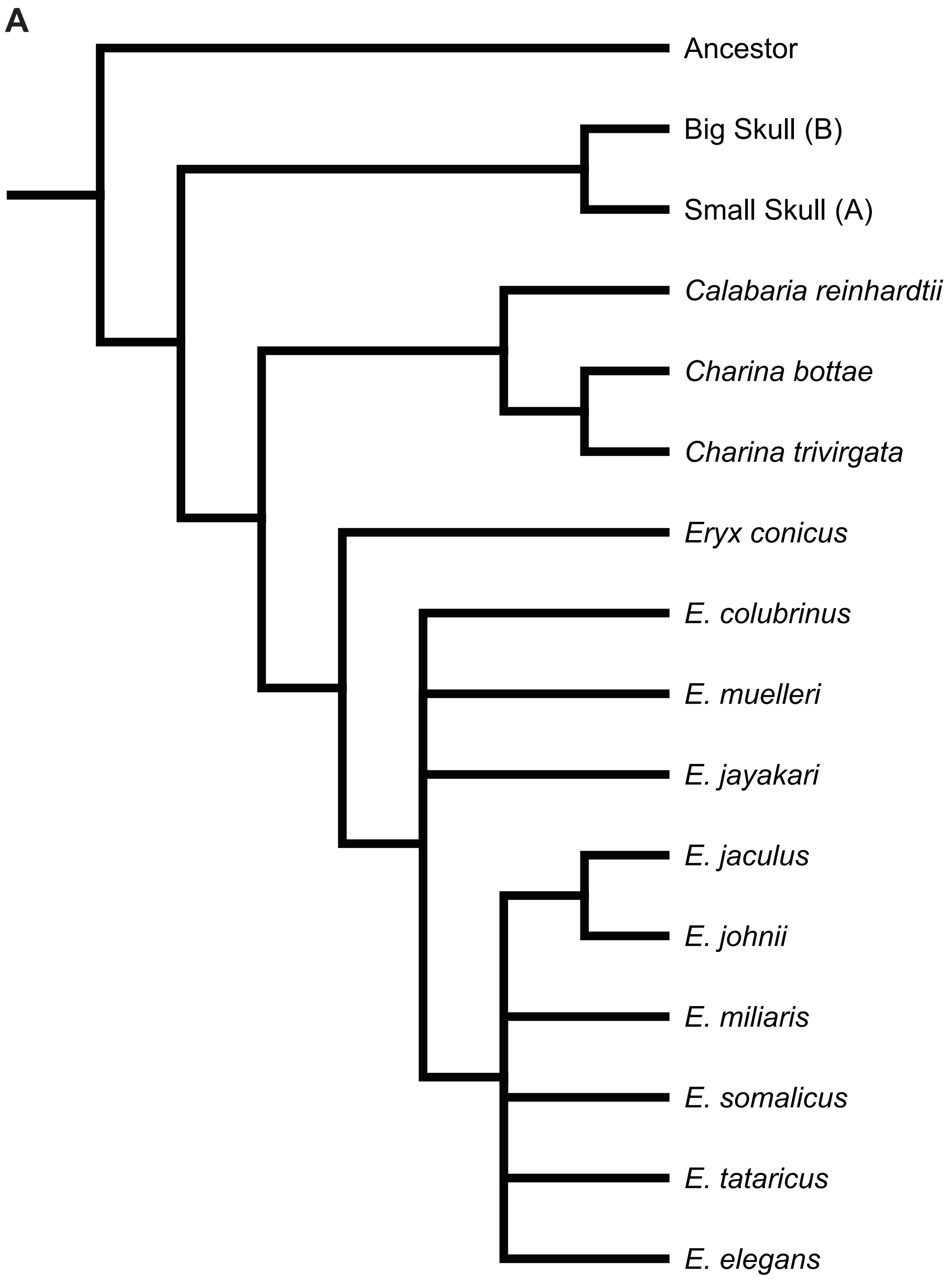
A
Ancestor
Big Skull (B)
Small Skull (A)
*Calabaria reinhardtii*
*Charina bottae*
*Charina trivirgata*
*Eryx conicus*
*E. colubrinus*
*E. muelleri*
*E. jayakari*
*E. jaculus*
*E. johnii*
*E. miliaris*
*E. somalicus*
*E. tataricus*
*E. elegans*

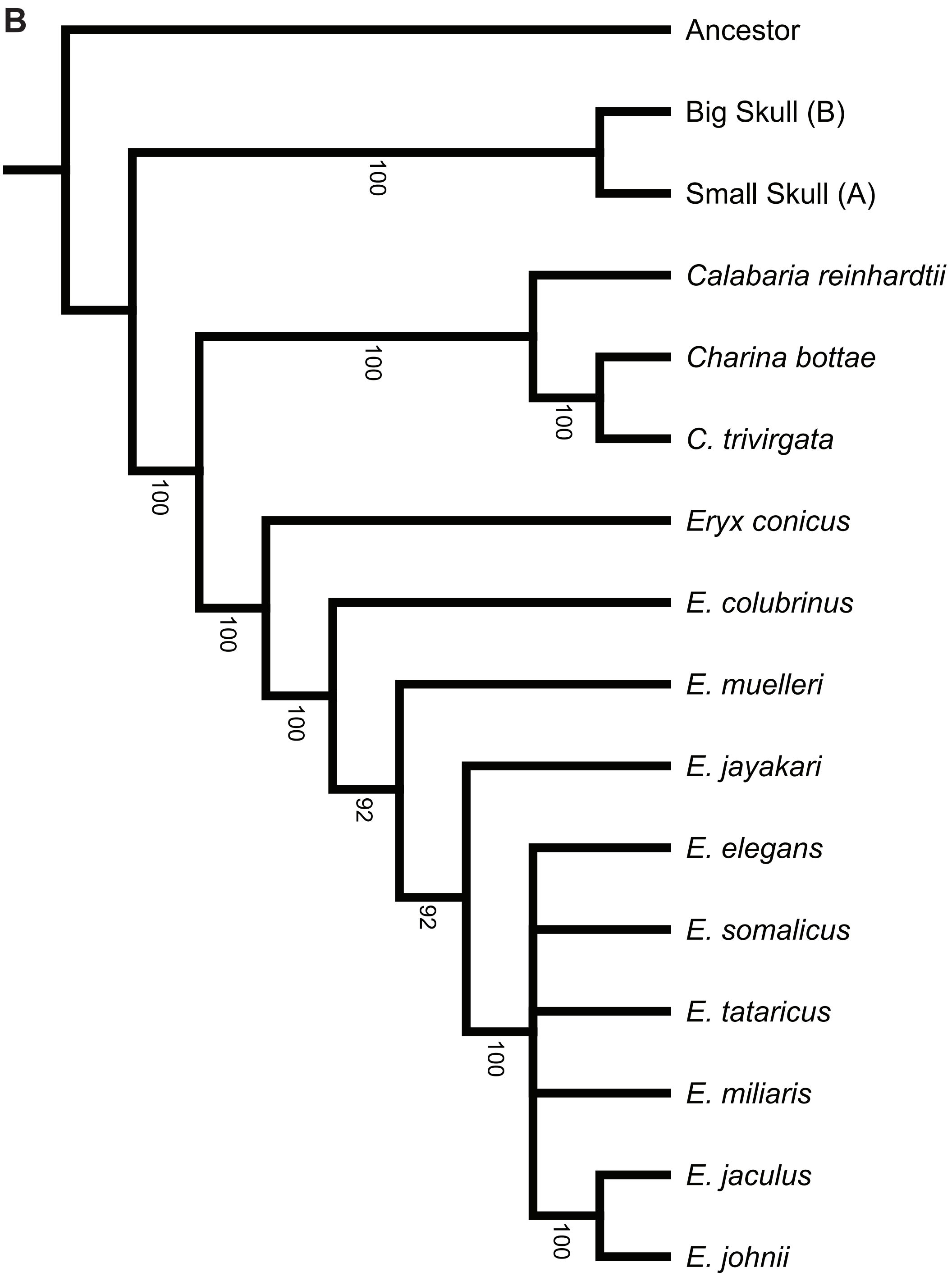
B
Ancestor
Big Skull (B)
Small Skull (A)
*Calabaria reinhardtii*
*Charina bottae*
*C. trivirgata*
*Eryx conicus*
*E. colubrinus*
*E. muelleri*
*E. jayakari*
*E. elegans*
*E. somalicus*
*E. tataricus*
*E. miliaris*
*E. jaculus*
*E. johnii*
100
100
100
100
100
100
92
92
100
100

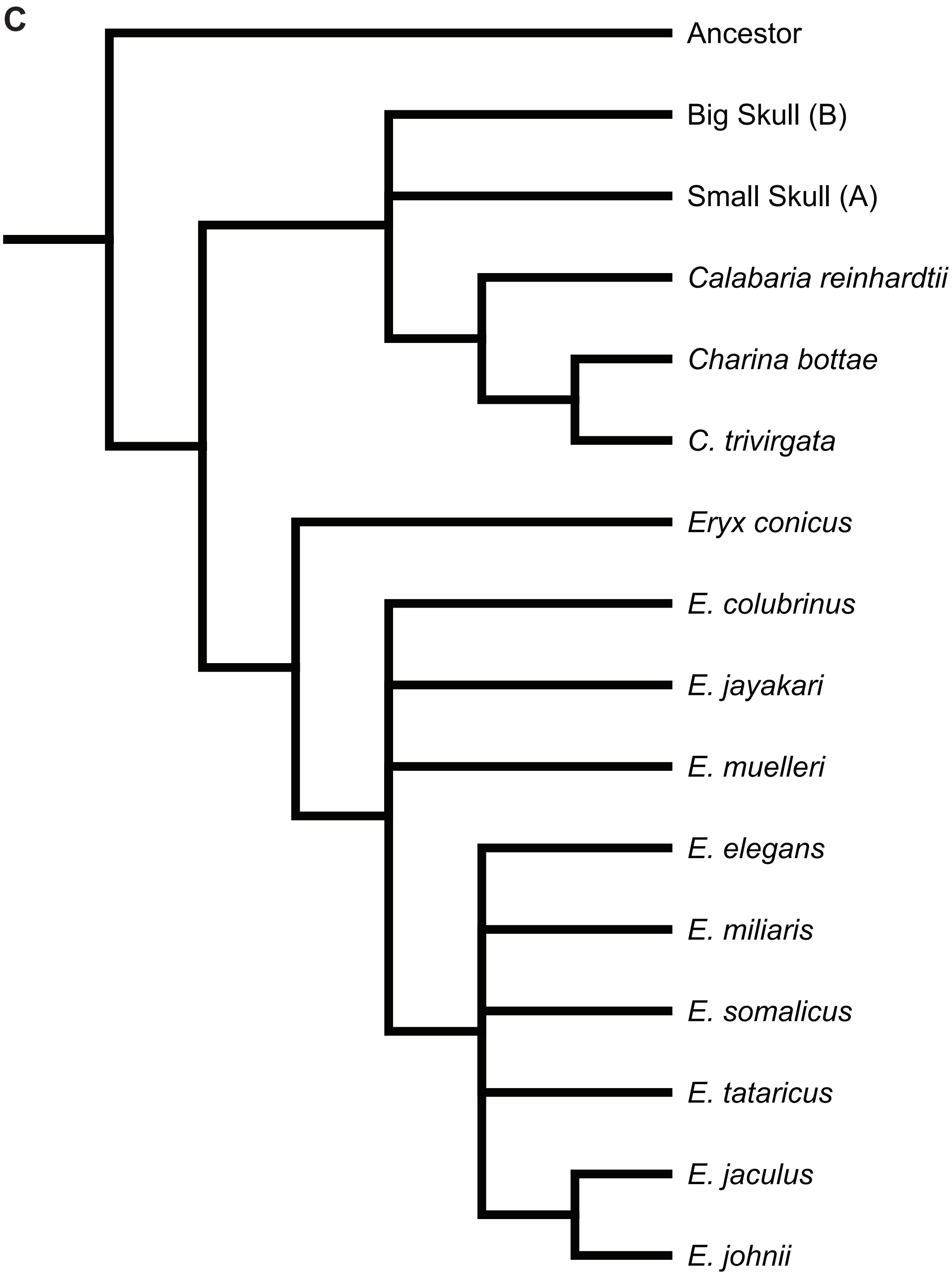
C
Ancestor
Big Skull (B)
Small Skull (A)
*Calabaria reinhardtii*
*Charina bottae*
*C. trivirgata*
*Eryx conicus*
*E. colubrinus*
*E. jayakari*
*E. muelleri*
*E. elegans*
*E. miliaris*
*E. somalicus*
*E. tataricus*
*E. jaculus*
*E. johnii*

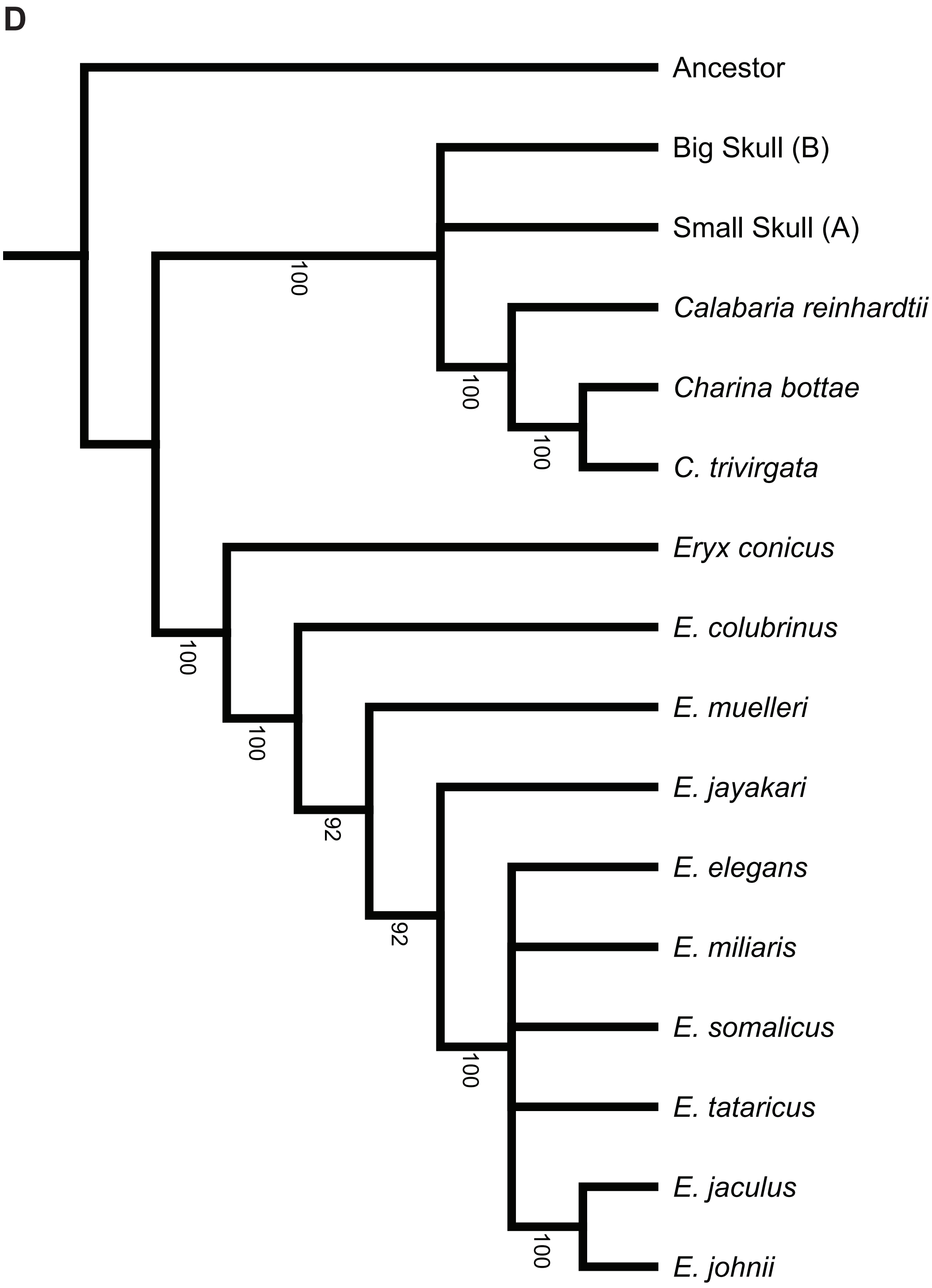D
Ancestor
Big Skull (B)
Small Skull (A)
*Calabaria reinhardtii*
*Charina bottae*
*C. trivirgata*
*Eryx conicus*
*E. colubrinus*
*E. muelleri*
*E. jayakari*
*E. elegans*
*E. miliaris*
*E. somalicus*
*E. tataricus*
*E. jaculus*
*E. johnii*
100
100
100
100
100
92
92
100
100

FIGURE 2-11. The results of Analysis 4, in which the hypothetical "Ancestor" taxon was replaced with *Anilius scytale*, *Calabaria reinhardtii* was removed, additional comparative taxa were added, and character 15 was removed. **A.** The strict consensus of the four most parsimonious trees demonstrating the sister relationship of Skulls A and B. **B.** The strict consensus of the four most parsimonious trees with Skulls A and B combined into a single terminal taxon, *Congerophis lego* gen. et sp. nov. **C.** The 50% majority rule of the four most parsimonious trees with Skulls A and B combined into a single terminal taxon, *Congerophis lego*, gen. et sp. nov. with percent majority values indicated along branches.

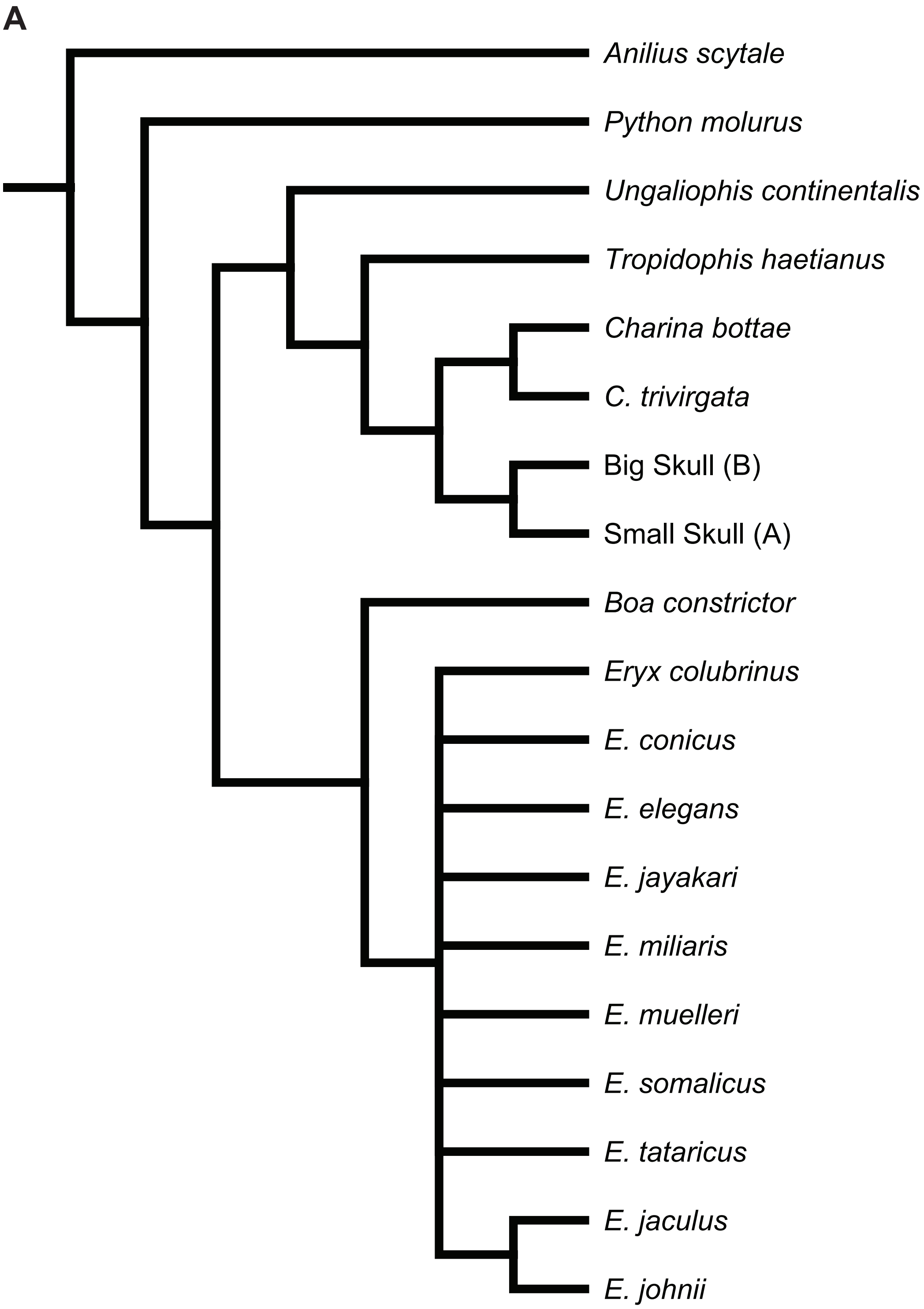
A
*Anilius scytale*
*Python molurus*
*Ungaliophis continentalis*
*Tropidophis haetianus*
*Charina bottae*
*C. trivirgata*
Big Skull (B)
Small Skull (A)
*Boa constrictor*
*Eryx colubrinus*
*E. conicus*
*E. elegans*
*E. jayakari*
*E. miliaris*
*E. muelleri*
*E. somalicus*
*E. tataricus*
*E. jaculus*
*E. johnii*

**B**

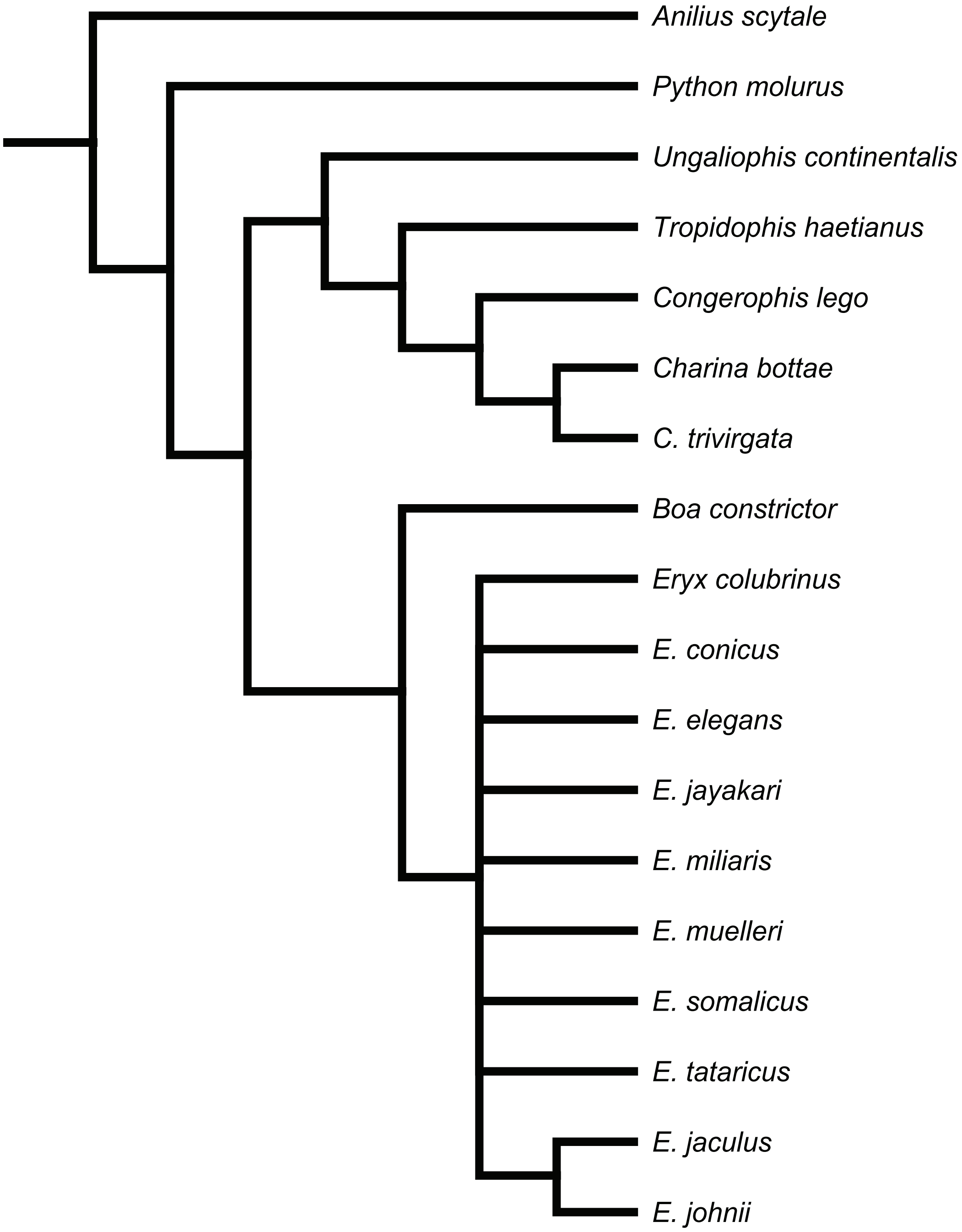
*Anilius scytale*
*Python molurus*
*Ungaliophis continentalis*
*Tropidophis haetianus*
*Congerophis lego*
*Charina bottae*
*C. trivirgata*
*Boa constrictor*
*Eryx colubrinus*
*E. conicus*
*E. elegans*
*E. jayakari*
*E. miliaris*
*E. muelleri*
*E. somalicus*
*E. tataricus*
*E. jaculus*
*E. johnii*

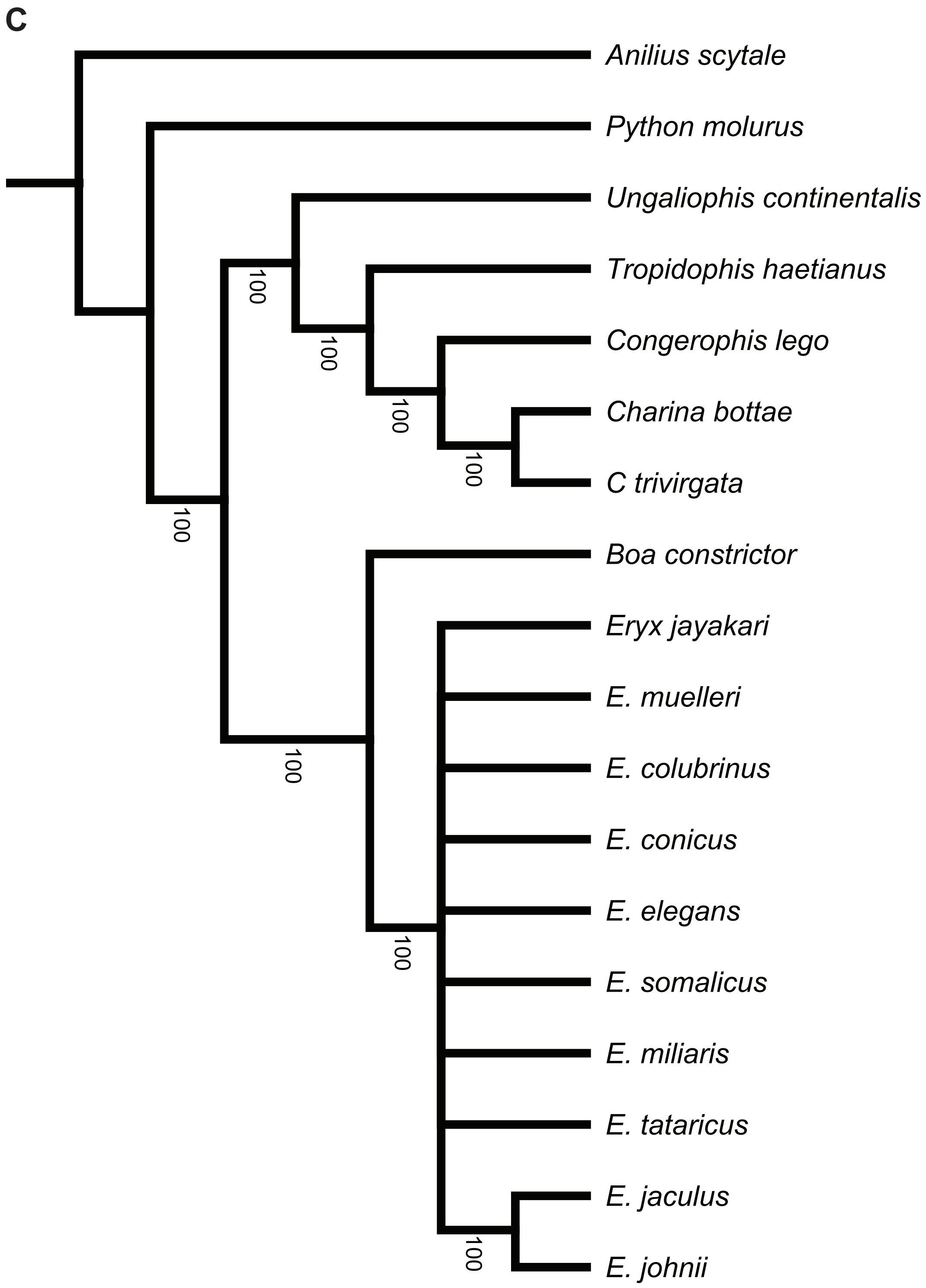
C
Anilius scytale
Python molurus
Ungaliophis continentalis
Tropidophis haetianus
Congerophis lego
Charina bottae
C trivirgata
Boa constrictor
Eryx jayakari
E. muelleri
E. colubrinus
E. conicus
E. elegans
E. somalicus
E. miliaris
E. tataricus
E. jaculus
E. johnii
100
100
100
100
100
100
100
100

# LITERATURE CITED

Bonaparte, C.L. 1831. Saggio di una distribuzione metodica degli animali vertebrati. Rome, 86 pp.

Breithaupt, B.H., and D. Duvall, 1986. The oldest record of serpent aggregation. Lethaia 19:181-185.

Brongniart, A. 1800. Essai d'une classification naturelle des reptiles. 1ère partie. Establissement des Orders. Bulletin des Sciences, par la Societé Philomatique, Paris 11:81-82.

Cope, E.D., 1861. Contributions to the ophidiology of Lower California, Mexico and Central America. Proceedings of the Academy of Natural Sciences of Philadelphia 13:292–306.

Cope, E.D., 1873. Synopsis of new vertebra from the Tertiary of Colorado, obtained during the summer of 1873. Washington, D.C. U.S. Government Printing Office 1-19.

Cope, E.D., 1883. The Vertebrata of the Tertiary formations of the West. Book I. Reports of the United States Geological Survey of the Territories, F. V. Hayden, United States Geologist-in-Charge 3:1-1002.

Cundall, D., V. Wallach, and D.A. Rossman. 1993. The systematic relationships of the snake genus *Anomochilus.* Zoological Journal of the Linnean Society, 109(3):275-299.

Gauthier, J.A., M. Kearney, J.A. Maisano, O. Rieppel, and A.D.B. Behlke. 2012. Assembling the squamate tree of life: Perspectives from the phenotype and the fossil record. Bulletin of the Peabody Museum of Natural History 53(1):3–308.

Greene, H.W. 1973. Defensive tail display by snakes and amphisbaenians. Journal of Herpetology 7(3):143-161.

Hoffstetter, R., 1962. Revue des recéntes acquisitions concernant l'histoire et la systématique des Squamates. Colloques Internationaux du Centre National de la Recherche Scientifique 104:243-278.

Hoffstetter, R., J.-C. Rage. 1972. .Les Erycinae fossiles de France (Serpentes, Boidae): compréhension et histoire de la sous-famille. Annales de Paléontologie (Vértebrés) 58:82–124.

Kluge, A.G. 1993. *Calabaria* and the phylogeny of erycine snakes. Zoological Journal of the Linnean Society 107:293-351.

LaDuke, T.C. 1991. The fossil snakes of Pit 91, Rancho LaBrea, California. Contributions in Science 424:1-28.

Lawson, R., J.B. Slowinski, and F.T. Burbrink. 2004. A molecular approach to discerning the phylogenetic placement of the enigmatic snake *Xenophidion schaeferi* among the Alethinophidia. Journal of the Zoological Society of London 263:285-294.

Lee, M.S.Y., A.F. Hugall, R. Lawson, and J.D. Scanlon. 2007. Phylogeny of snakes (Serpentes): Combining morphological and molecular data in likelihood, Bayesian and parsimony analyses. Systematics and Biodiversity 5(4):371-389.

Lee, M.S.Y., and J.D. Scanlon. 2002. Snake phylogeny based on osteology, soft anatomy and ecology. Biological Reviews 77:333-401.

Linneus, C. 1758. Systema Naturae, Edition X, vol. 1 (Systema naturae per regna tria naturae, secundum classes, ordines, genera, species, cum characteribus, differentiis, synonymis, locis. Tomus I. Editio decimal, reformata.) Holmiae Salvii, 824 pp.

Longrich, N.R., B.-A. S. Bhullar, and J.A. Gauthier. 2012. A transitional snake from the Late Cretaceous period of North America. Nature 488:205-208.

McDowell, S.B. 2001. Systematics. In: Seigle, R. A., J. T. Collins, and S. S. Novak, Snakes: Ecology and Evolutionary Biology. The Blackburn Press, New Jersey, p. 3-50.

Noonan, B.P., and P.T. Chippendale. 2006. Dispersal and vicariance: The complex evolutionary history of boid snakes. Molecular Phylogenetics and Evolution 40:347-358.

Oppel, M. 1811. Die Ordungen Familien, und Gattungen der Reptilien als Prodrom einer Naturgeschichte derselben. J. Lindauer, München, 86 pp.

Palci, A., M.W. Caldwell, and R.L. Nydam. 2013. Reevaluation of the anatomy of the Cenomanian (Upper Cretaceous) hind-limbed marine fossil snakes *Pachyrhachis*, *Haasiophis* and *Eupodophis*. Journal of Vertebrate Paleontology, 33:1328-1342.

Pyron, R.A., F.T. Burbrink, and J.J. Wiens. 2013. A phylogeny and revised classification of Squamata, including 4161 species of lizards and snakes. BMC Evolutionary Biology 13(93):1-77.

Rage, J.-C. 1984. Serpentes (Handbuch der Paläoherpetologie, v. 11), Gustav Fischer Verlag, Stuttgart, 80pp.

Rieppel, O., 1978. A functional and phylogenetic interpretation of the skull of the Erycinae (Reptilia, Serpentes). Journal of Zoology 186(2):185-208.

Slowinsky, J.B., and R. Lawson. 2002. Snake phylogeny: Evidence from nuclear and mitochondrial genes. Molecular Phylogenetics and Evolution 24(2):194-202.

Swofford, D.L. 2002. PAUP*. Phylogenetic" Analysis Using Parsimony (*and Other Methods). Version 4. Sinauer Associates, Sunderland, Massachusetts.

Tchernov, E., O. Rieppel, H. Zaher, M.J. Polcyn, and L.L. Jacobs. 2000. A fossil snake with limbs. Science, 287(5460):2010-2012.

Underwood, G. 1967. A contribution to the classification of snakes. British Museum of Natural History, London. 179pp.

Vidal, N., and S.B. Hedges. 2002. Higher-level relationships of snakes inferred from four nuclear and mitochondrial genes. Comptes Rendus Biologies 325(9):977-985.

Weins, J.J., C.R. Hutter, D.G. Mulcahy, B.P. Noonan, T.M. Townsend, J.W. Sites Jr., and T.W. Reeder, 2012. Resolving the phylogeny of lizards and snakes (Squamata) with extensive sampling of genes and species. Biology Letters Published Online, doi:10.1098/rsbl.2012.0703.

Zaher, H., and C.A. Scanferla. 2012. The skull of the Upper Cretaceous snake *Dinilysia patagonica* Smith-Woodward, 1901, and its phylogenetic position revisited. Zoological Journal of the Linnean Society, 164:194-238.

# CHAPTER 3

# *OGMOPHIS* COPE, 1884, *CALAMAGRAS* COPE, 1874, AND UTILITY AND TAXONOMIC PROBLEMS OF SNAKE VERTEBRAL FORM TAXA

Manuscript to be submitted to Journal of Vertebrate Paleontology as: Croghan, J., Caldwell, M.W., Breithaupt, B.B., & Bamforth, E., "*Ogmophis* Cope, 1884, *Calamagras Cope 1874,* and utility and taxonomic problems of snake vertebral form taxa"

# INTRODUCTION

Most of the known fossil snake taxa are understood from assemblages of isolated vertebrae, or short strings of articulated vertebrae (Rage, 1984; Holman, 2000). Snake vertebrae vary considerably in living taxa both within the column of a single individual, among individuals of the same species, and among closely related taxa. From amongst the possible vertebral zones in a snake, mid-trunk vertebrae are used where possible for making comparisons between fossil and modern snakes. For example, two clearly monophyletic, closely related taxa of modern boiine snakes, *Casarea* and *Bolyeria*, demonstrate quite divergent mid-trunk vertebral morphologies (Hecht and LaDuke, 1988), while the majority of caenophidian snakes are difficult to distinguish at any level other than familial (and sometimes not even at that level) without access to the full column and modern comparative material (LaDuke, 1991). *Rottophis* (Szyndlar and Boehme, 1996) is an example of a boid that, until caudal vertebrae were described, was thought to be related to the modern *Eryx;* this illustrates the difficulty of assigning vertebrae to families or subfamilies, especially within the Booidea. The majority of fossil snakes species, especially North American erycine s.l. taxa, are distinguished not on the basis of novel or extreme morphologies, but on a locality assemblage, or the minutiae of proportional differences that are easily within the realm of variation for a single vertebral column (Rage, 1984; Szyndlar and Rage, 2003).

The many erycine s.l. fossils from North America are particularly over-diagnosed with regard to these fine scale proportional differences. Erycines s.l. seem to dominate much of the snake fauna of the Cenozoic in North America in terms of number of species present. This likely does not represent the actual diversity or dominance of these snakes at the time, but rather the taxon splitting that has occurred with regards to the naming of purported erycine s.l. vertebrae on a locality-by-locality, or find-by-find basis.

Although there is no strict definition, a booid-like vertebra is considered to be anteroposteriorly short (as wide as or wider than it is long) and generally heavily built with no well-developed prezygapophyseal processes (Gasc, 1974; Szyndlar, 1984). The erycine s.l. variation on this general form includes a low vault of the neural arch and a low neural spine (as defined by Holman, 2000, though several forms in Holman's work seem to possess a relatively vaulted neural arch and a neural spine that approaches "normal" height, an inconsistency that has apparently gone unnoticed), which seems to be rooted in the semi-fossorial Old World *Eryx*. This is not an apomorphy of modern erycines s.l., which are defined on the basis of the entire snake, but is used extensively with North American fossil snakes to identify a relatively common find. The group has become somewhat of a wastebasket with little morphological support, and this is not the first analysis to mention the need for reanalysis of the North American fossil erycines as a whole (e.g., Smith, 2012; Szyndlar and Rage, 2003; Holman, 2000; Rage 1984; Gilmore, 1938).

Of the many genera considered to be potentially erycine s.l. by Holman (2000), two contain the majority of the species. Long before the New World genus *Charina* was considered part of the alleged subfamily Erycinae s.l., Cope (1873), in the same work in which the taxon was named, hypothesized that *Calamagras* was related to the relatively recently described *Charina trivirgata.* Since this initial association, the relationship has gone uncontested, despite the lack of more modern erycine s.l. features in the fossil taxa. Szyndlar and Rage (2003) stated that the only diagnostic features of erycine s.l. vertebrae are the additional apophyses on the caudal vertebrae, and no confirmed caudal vertebrae associated with *Calamagras* or *Ogmophis* have been found (Smith, 2012; Szyndlar and Rage 2003). Holman (1977) had mentioned a fused section of tail vertebrae of cf. *Calamagras angulatus* (UCM 30959), but this assignment was made with no discussion or figures. Holman (1979) also mentioned a section of fused vertebrae apparently referred to *Ogmophis voorhiesii* (CM 35005), again, with no discussion or figures. All snakes display fusion of the posterior-most vertebrae, yet the presence of additional apophyses on the neural arch contributing to this fusion cannot be assessed at this time. The holotype of *Ogmophis* has since been lost, although the majority of authors have maintained that it has simply been "misplaced" (Holman, 2000). Gilmore (1938) was the first author to notice it missing, stating that the type appeared to be lost; only a figure of very poor quality from Cope, reproduced by Gilmore (1938), exists to represent the specimen.

It is fair to state that the diversity of fossil erycines s.l. has been overestimated. The understudied area of intracolumnar variability, the locality-driven process of naming new species in North American paleoherpetology, and the fundamental confusion as to what features constitute an erycine s.l. have all contributed to the disorganization of the North American fossil Erycinae s.l.. All of the above matters may have their root in misplaced confidence in the authority of Cope and his classical erycine s.l. genera, *Ogmophis* and *Calamagras*. In light of two spectacularly preserved specimens, representing four individuals with nearly complete cranial material of the newly described *Congerophis lego*, we argue here that the material serving as types for the genera *Ogmophis* (Cope, 1884) and *Calamagras* (Cope, 1873) is insufficient to define these taxa at the generic level or lower. Furthermore, all contemporaneous species of these taxa are here reassigned to *Congerophis lego* on the basis of their similar morphology and the observed intracolumnar variation of the four nearly complete individuals presently described.

## INSTITUTIONAL ABBREVIATONS

American Museum of Natural History, New York, NY (AMNH); Carnegie Museum of Natural History (CM); Saskatchewan Museum of Natural History, Regina, SK, Canada (SMNH); University of Alberta Museum of Zoology, Edmonton, AB, Canada (UAMZ); University of Colorado Museum, Boulder, Colorado (UCM); Florida Museum of Natural History, Gainesville, FL (UF); University of Wyoming, Laramie, WY (UW).

## MATERIALS AND METHODS

For comparison, seven fossil taxa and one modern taxon were selected on the basis of their overall similarity to *Congerophis* and figured, including four species of *Calamagras*, three species of *Ogmophis,* and the modern North American booid *Charina (Lichanura) trivirgata.* All available views in the literature of the vertebrae of each taxon were included in Figure 3.2, along with all possible views of the vertebrae at five points along the vertebral column associated with Skull D in Block 3 of UW11120, a referred specimen of *Congerophis lego.*

One specimen of *Charina trivirgata* (UAMZ 3819) was CT-scanned using a Skyscan 1174. The type and referred specimens of *Congerophis lego*, UW11120, were CT-scanned at the High-Resolution X-Ray Computed Tomography Facility at The University of Texas at Austin using an ACTIS ultra-high-resolution subsystem source. Scanning parameters were individually optimized and thus varied across specimens. The datasets were rendered in three dimensions using Avizo 7.1 (Visualization Sciences Group). The CT data and detailed scan parameters will be made available from the Digital Morphology database.

Fossil specimens examined in this study include: *Calamagras angulatus* AMNH 1654; *Calamagras floridanus* UF 6150; *Calamagras murivorus* AMNH 1630; *Calamagras primus* AMNH 3828 (mistakenly listed by Holman [2000] as AMNH 3829); *Congerophis lego* UW11120; *Charina trivirgata* UAZM 3819; *Ogmophis arenarum* CM 744; *Ogmophis compactus* SMNH 1433; *Ogmophis oregonensis* AMNH, lost. Modern specimens examined in this study include: *Charina bottae* AMNH 64945; *Ungaliophis panamensis* AMNH 76305.

## TAXONOMIC PROBLEMS AND REVISIONS OF THE GENERA *CALAMAGRAS* AND *OGMOPHIS* AND THEIR CONSTITUENTS

### The genera *Calamagras* and *Ogmophis* as *nomina dubia*:

*Ogmophis*, as defined by Holman (2000), is the larger taxon with a neural spine that occupies more than one half of the length of the neural arch, prominent subcentral ridges, and a flattened hemal keel. *Calamagras*, is the smaller taxon and possesses a neural spine that occupies less than one half of the length of the neural arch, a hemal keel that is present, and a deeper interzygapophyseal constriction typically anterior to the mid-length point on the centrum. Additional features were given in the diagnoses in Holman (2000), though it is unclear whether or not these were the personal observations of Holman. The majority of the diagnostic features of both genera can be effectively attributed to the intracolumnar variation seen along the vertebral column of *Congerophis lego*: the subcentral ridges become more prominent posteriorly, and the hemal keel that is present anteriorly and at midtrunk, flattens and widens posteriorly (Fig. 3.2). The interzygapophyseal constriction anterior to mid-length is not consistent among all species of *Calamagras* or *Ogmophis* (Fig. 3.2), and also decreases slightly in depth and moves from anterior to mid-length to more posterior to mid-length, cranio-caudally, in *Congerophis lego.* Rage (1984), referencing the original descriptions, noted that the length of the neural spine is the sole distinguishing character between these two taxa. The length of the neural spine relative to the neural arch does increase slightly posteriorly along the vertebral column of *C. lego*, though there is yet to be a study describing variation of the neural spine length/neural arch length ratio for confirmation of this observation. Overall, the length of the neural spine in *C. lego* averages approximately 50% of the length of the neural arch, disallowing the assignment of *C. lego* to either of the genera in question. Thus, there are no characters that can reliably distinguish

*Ogmophis* from *Calamagras*, or place either outside of the intracolumnar variation for *Congerophis,* and they should now be considered *nomina dubia.*

<u>The taxonomy of select species of *Calamagras* and *Ogmophis:*</u>

*Ogmophis* and *Calamagras* have a broad temporal distribution, from the mid-Eocene Bridgerian North American land mammal age to the mid-Miocene Barstovian (Fig 3.1). *Congerophis lego* is an Oligocene snake from early Orellan (33.9-33.3 MYA) sediments of the White River Formation in Wyoming, which has been radiometrically dated elsewhere in the formation to a minimum age of 32 million years before present (Breithaupt and Duvall, 1986).

For comparative purposes, we selected and figured all species of *Ogmophis* and *Calamagras* that were similar to *Congerophis lego*, with no regard for temporal or spatial distribution (Fig. 3.2). Of all of the extremely similar species of *Ogmophis* and *Calamagras,* the Oligocene distribution of *O. oregonensis, O. compactus, C. murivorus,* and *C. angulatus* make these species likely candidates for synonymization with *Congerophis lego*, though the practice of diagnosing species on the basis of isolated or short strings of vertebrae discourages the retention of their species names.

Recently, there have been some higher-level reassignments of purportedly erycine sensu lato extinct taxa, demonstrating the ease with which mid-trunk vertebrae of one family or subfamily can be mistaken for another. *Helagras* *priciformis,* an additional erycine s.l. genus not discussed in this study, was recently placed in the Madtsoiidae (Head and Holroyd, 2008). Smith (2012), upon the discovery of additional material of both *Calamagras weigeli* and *Ogmophis compactus*, made two conservative, but somewhat confusing, familial reassignments of the two species: he placed the former into Ungaliophiinae and the latter into Loxocemidae with no further comment on the relationships of these species with their respective genera. While this assignment makes sense based on morphology, it is recognized that the trunk vertebrae belonging to Ungaliophiinae, in particular, are difficult to differentiate from those belonging to any erycine s.l. or *Congerophis lego.* Indeed, Smith (2012) used slight measurements of overall proportions of the vertebrae, as well as yet another caudal character, that hemopophyses are apparently absent in the caudal vertebrae, to make the assignment to Ungaliophiinae. The loxocemid assignment is restricted to the posterior trunk vertebrae, which demonstrate the apparent triangular pattern of pronounced subcentral ridges and deep subcentral grooves. *C. lego* carries less pronounced versions of these structures in the posterior trunk vertebrae (Fig. 3.2ii), but also carries a shorter neural spine than that of *O. compactus,* a character that has also been shown to vary within the vertebral column in colubrids (LaDuke, 1991).

*Ogmophis oregonensis* as a *nomen dubium*:

The type specimen of *Ogmophis oregonensis* is lost, and figures (see Holman, 2000, for the most recent reproduction) are of extremely poor quality; no other records of the species are known. Because of this, we recommend that the species be regarded a *nomen dubium.* This is also the type species of the genus, which we choose not to maintain, in favor of the synonymization of *Ogmophis* with *Congerophis*, on the basis of the completeness of the latter, and the similarity of other material in the poorly defined genus *Ogmophis.*

*Calamagras murivorous* as *Congerophis murivorous,* comb. nov.:

*Calamagras murivorous*, the type species of the genus, is diagnosed as for the genus, which has now been synonymized with *Congerophis*, and is therefore not retained. The species is well represented in the Oligocene deposits of Colorado, though, and as such, demands closer examination. The synapophyses of *C. murivorous* are more distinct from the ventral aspect of the centrum and seem more massive altogether than those of *Congerophis lego*. Arguably, this observation is not part of the diagnosis for the taxon (Holman, 2000), but is worth noting. Otherwise, *Calamagras murivorous* bears a striking resemblance to *Congerophis lego.* Currently, we recommend reassignment of *Calamagras murivorous* to *Congerophis.*

*Calamagras angulatus* as *Congerophis angulatus*, comb. nov.:

*Calamagras angulatus* (Cope, 1873), again from the Oligocene of Colorado, bears the strongest resemblance to the anterior mid-trunk vertebrae of *Congerophis lego* (see Fig. 3.2), in that it is anteroposteriorly shortened, with upswept postzygapophyses. The hypapophyses in *C. lego* are present until approximately the 50th vertebra, at which point the hemal keel bears a small point posteriorly; the keel gradually flattens and widens posteriorly along the column. The diagnosis for *Calamagras angulatus* in Holman (2000) matches these details. *C. angulatus* differs from *Congerophis lego* only in the relatively low profile of the synapophyses, contributing to dorsoventrally narrow prezygapophyseal processes which conspicuously resemble the extant *Ungaliophis panamensis.* Recent molecular analyses have demonstrated that modern Ungaliophiinae and *Charina* are closely related (Pyron, Burbrink, and Weins, 2013), which may explain the similarity of these fossil snakes. Indeed, the relations of *Calamagras angulatus* may prove to be similar to those of *C. weigeli* (as *C. weigeli* was recently assigned to the Ungaliophiinae, Smith, 2012), but until more complete specimens of the species are found, *C. angulatus* is tentatively referred to *Congerophis*. *Calamagras angulatus* is found at the same locality as *C. murivorous.* These specimens are sufficiently different to retain distinction in the literature, and the simplest course is to retain *C. murivorous* and *C. angulatus* as species, although we believe the diagnosis of vertebrae to the species level to be suspect.

*Calamagras floridanus* as cf. *Congerophis lego:*

*Calamagras floridanus* (Auffenberg, 1963) is from the early Miocene of Florida, and regardless of the difference in geographical and temporal distribution, is the most similar to *Congerophis lego.* Holman (2000) revised the diagnosis of the species, placing emphasis on the short, thick, truncated neural spine that the type specimen bears. The neural spine appears to expand a small amount dorsally as it is figured, a feature that it does not share with *C. lego*, though the two taxa seem indistinguishable in every other view. Unfortunately, the zygosphene on the only published or numbered specimen of this species is broken. It would seem reasonable to recommend complete synonymization of this species with *C. lego* if not for the minimum 12 million year gap between their known occurrences. Because of this, *Calamagras floridanus* is referred to cf. *Congerophis lego* until the duration and range of the latter species may be assessed.

*Calamagras primas* as cf. *Congerophis lego:*

*Calamagras primas* (Hecht, 1959), from the Eocene deposits of Wyoming, is also extremely similar to *Congerophis lego*, but was diagnosed to have a thin and reduced neural spine and a zygosphene that is convex anteriorly. The relative crenulation of the anterior border of the zygosphene has been demonstrated to change along the column of caenophidians (LaDuke, 1991), and is clearly variable in *C. lego* (Fig. 3.2). The lower hemal keel described in the holotype of *Calamagras primas* parallels the greater development of the crenulations of the anterior border of the zygosphene, as is seen in the posterior trunk vertebrae of *Congerophis lego* (Fig. 2.2ii, tt). It appears that *Calamagras primas* could represent a posterior vertebra of *Congerophis lego*, but once again, the minimum 18 million year difference in time of occurrence between these two taxa is cause for hesitation. *Calamagras primas, Congerophis lego,* and *Calamagras floridanus* may represent an anagenic lineage, but until the duration of these taxa can be assessed we recommend reassignment of *C. primas* to cf. *Congerophis lego.*

*Ogmophis arenarum* as *Congerophis arenarum*, comb. nov.:

*Ogmophis arenarum,* found in Miocene deposits in Montana, is generally very similar to *C. lego,* yet differs in several distinct characters that have not been shown to vary intracolumnarly. The parapophyses extend below the level of the centrum in anterior view, and the cotyle is more oblate than any of the taxa compared in Figure 3.2. Additionally, the channel between the borders of the cotyle and the prezygapophyses is deeply inscribed, so much so that in ventral view the channel forms distinct notches between these structures (Fig. 3.2 mm). Although this channel has been shown to increase in depth slightly along the length of a caenophidian column (LaDuke, 1991), the degree to which *O. arenarum* differs from the posterior trunk vertebrae of *C. lego*, in addition to the intracolumnarly invariant characters, justifies the retention of its taxonomic distinctness, but with generic reassignment to *Congerophis*.

## CONCLUSION

The genera *Ogmophis* and *Calamagras* cannot be distinguished from each other, and several species of both are recognized as conspecific with the recently described *Congerophis lego*. The species of either genus that have not been reassigned to *C. lego* should be considered *nomina dubia* until a more detail review of these specimens can be conducted. The taxic assignments of *Calamagras weigeli* and *Ogmophis compactus* remain open questions because the familial reassignment of these taxa in Smith (2012) to the Loxocemidae and the Ungaliophiinae are inconsistent with the higher level assignment of *Congerophis lego* to the Charininae. Isolated “mid-trunk” fossil snake vertebrae, in the absence of unique and novel elaborations, are not suitable to diagnose taxa at or below the level of the genus, and indeed, neither, in many cases, at the level of the subfamily or family.

A suggested taxonomy is as follows: *Ogmophis* and *Calamagras*, are *nomina dubia ; Calamagras murivorous, Calamagras angulatus,* and *Ogmophis arenarum* are transferred to *Congerophis murivorous,* comb. nov., *Congerophis angulatus,* comb. nov, and *Congerophis arenarum,* comb. nov.; *Calamagras primas* and *Calamagras floridanus* will become cf. *Congerophis lego* until the range of the latter is revealed or additional material of the former are discovered. *Ogmophis oregonensis* is regarded as a *nomen dubium,* as are all species of *Calamagras* and *Ogmophis* that have not been reassigned to other genera.

FIGURE 3-1. Temporal distribution of *Calamagras* and *Ogmophis* species in North America as listed in Holman (2000).

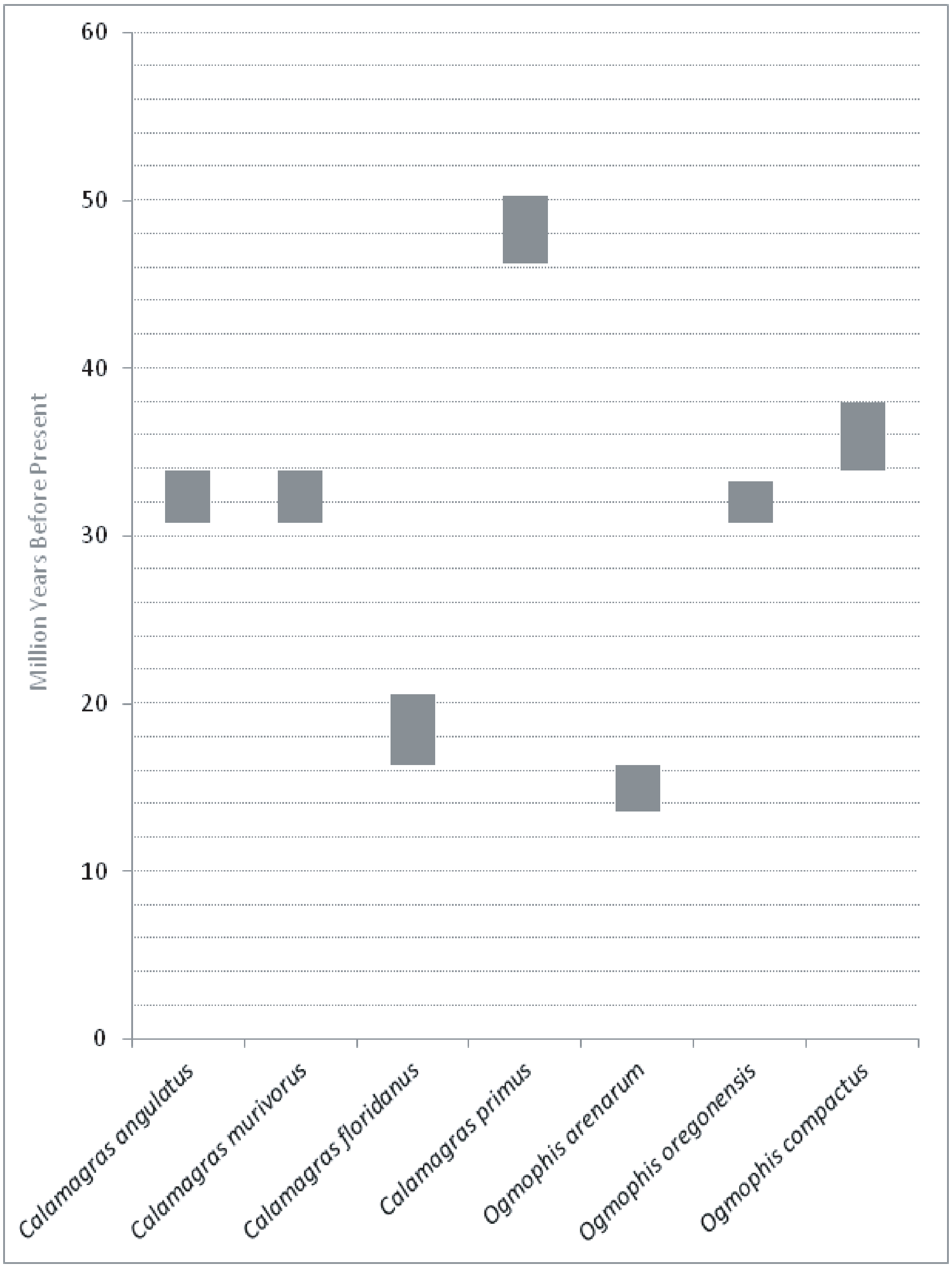
60
50
40
30
20
10
0
Million Years Before Present
Calamagras angulatus
Calamagras murivorus
Calamagras floridanus
Calamagras primus
Ogmophis arenarum
Ogmophis oregonensis
Ogmophis compactus

FIGURE 3-2. Comparative views of fossil and modern snake vertebrae of interest. Not to scale. Lateral views: A-M. Anterior views: N-Y. Posterior views: Z-FF. Ventral views: GG-QQ. Dorsal views: RR-AAA. *Congerophis lego*, UW11210: A-D, N-P, Z, GG-JJ, and RR-UU; anterior trunk vertebra: A, N, Z, GG, RR; mid-trunk vertebra: B, O, HH, SS; posterior trunk vertebra: C, II, TT; caudal vertebra: D, P, JJ, UU. *Calamagras angulatus*, AMNH 1654, reprinted from Gilmore (1938): E, Q, AA, KK. *Calamagras primus*, reprinted from Hecht (1959): F, R, BB, LL, VV. *Calamagras murivorous*, AMNH 1630: GG, OO, WW; AMNH 1598, reprinted from Gilmore (1938): S, CC. *Calamagras floridanus,* UF 6150, reprinted from Holman (2000): H, T, XX. *Ogmophis arenarum,* CM744, reprinted from Gilmore (1938): I, U, DD, MM. *Ogmophis compactus*, SMNH 1433, reprinted from Gilmore (1938): J, V, EE, NN. *Charina trivirgata*, UAZM 3819: K, W, FF, PP, YY. *Charina bottae*, AMNH 64945, reprinted from Bogert (1968): L, X, ZZ. *Ungaliophis panamensis,* AMNH 76305, reprinted from Bogert (1968): M, Y, QQ, AAA.

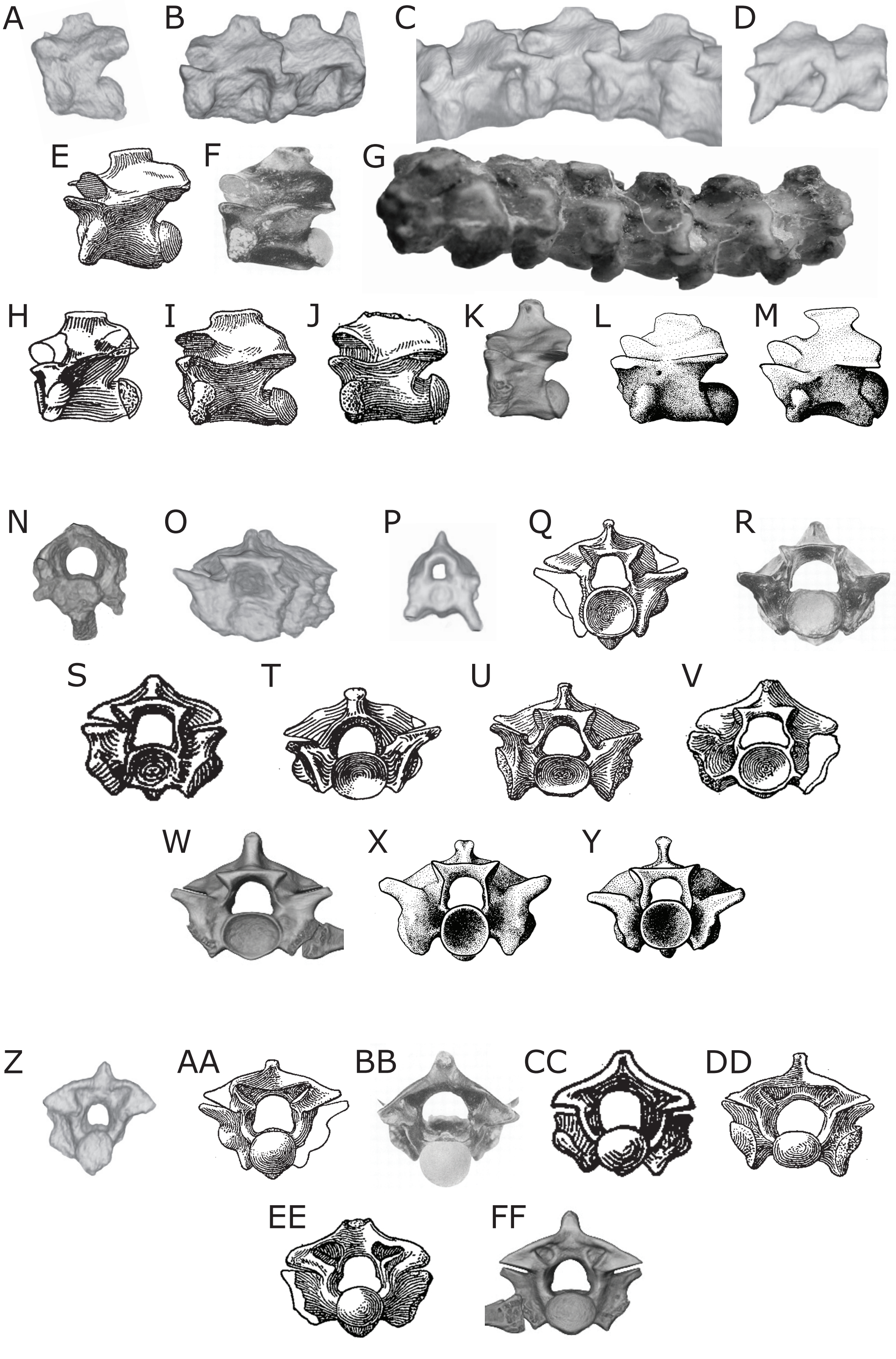
A
B
C
D
E
F
G
H
I
J
K
L
M
N
O
P
Q
R
S
T
U
V
W
X
Y
Z
AA
BB
CC
DD
EE
FF

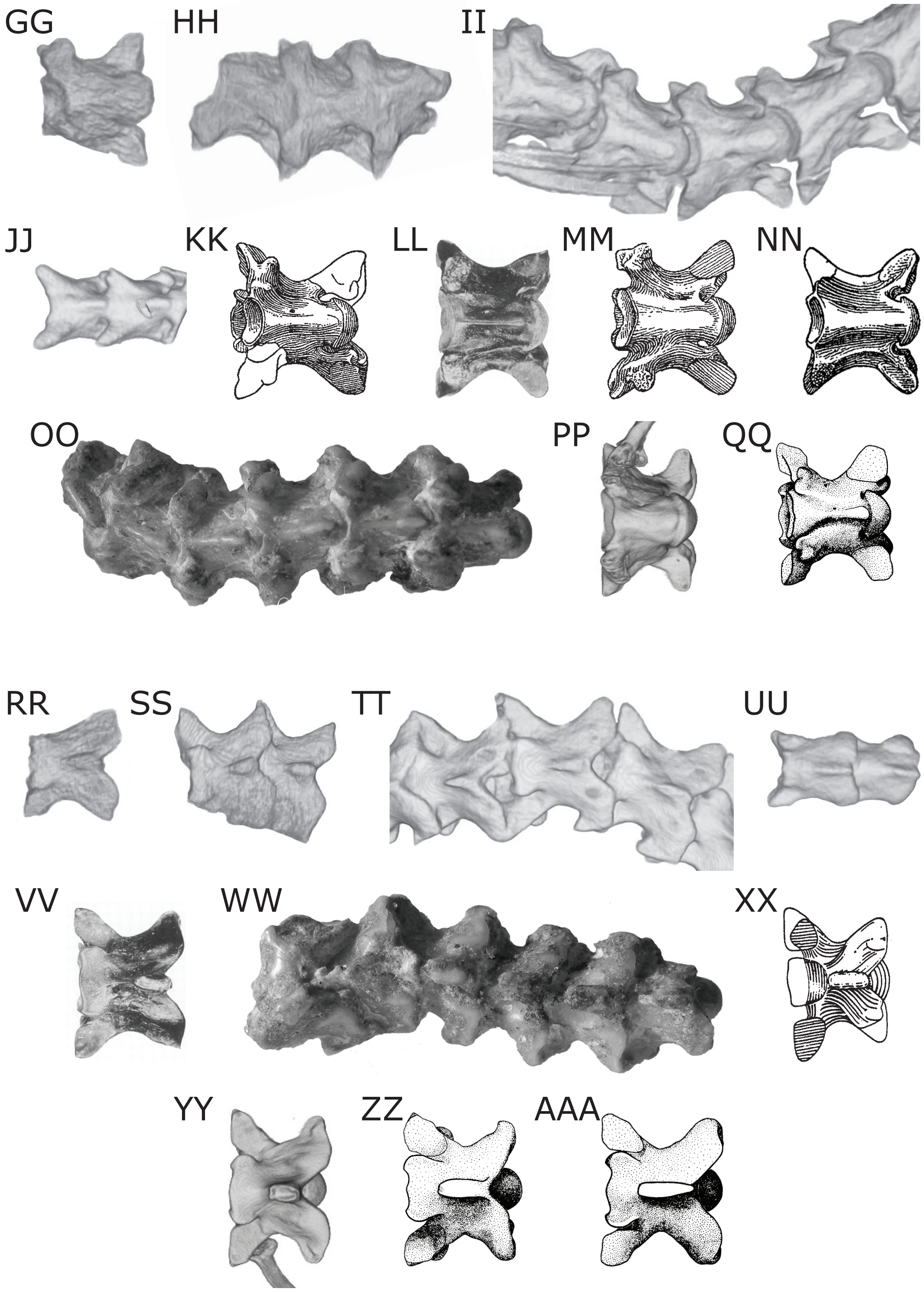
GG
HH
II
JJ
KK
LL
MM
NN
OO
PP
QQ
RR
SS
TT
UU
VV
WW
XX
YY
ZZ
AAA

# LITERATURE CITED

Auffenberg, W., 1963. The fossil snakes of Florida. Tulane Studies in Zoology 10:127-213.

Bogert, C. M., 1968. A new genus and species of dwarf boa from southern Mexico. American Museum Novitates 2354:1-38.

Breithaupt, B.H., and D. Duvall, 1986. The oldest record of serpent aggregation. Lethaia 19:181-185.

Cope, E.D., 1873. Synopsis of new vertebra from the Tertiary of Colorado, obtained during the summer of 1873. Washington, D.C. U.S. Government Printing Office 1-19.

Cope, E.D., 1883. The Vertebrata of the Tertiary formations of the West. Book I. Reports of the United States Geological Survey of the Territories, F. V. Hayden, United States Geologist-in-Charge 3:1-1002.

Gasc, J.-P. 1967. L'interprétation fonctionnelle de l'appareil musculo-squelettique de l'axe vertébrale ches les serpents (Reptilia). Mémoires du Muséum Nationl d'Histoire Naturelle (A)83:1-182.

Gilmore, C. W., 1938. Fossil snakes of North America. Geological Society of America Special Paper 9:1-96.

Head, J., & Holroyd, P. (2008). Assembly and biogeography of North American Paleogene snake faunas based on an expanded fossil record. Journal of Vertebrate Paleontology 28:90A.

Hecht, M. K., 1959. Amphibians and reptiles *in* McGrew, P. O. (ed.). The geology and paleontology of the Elk Mountain and Tabernacle Butte area, Wyoming. Bulletin of the American Museum of Natural History 117:130-146.

Hecht, M. K., and C. LaDuke, 1988. Bolyerine vertebral variation: A problem for paleoherpetology. Acta Zoologica Cracoviensia 31(24):605-614.

Holman, J. A., 2000. Fossil Snakes of North America: Origin, Evolution, Distribution, Paleoecology. Indiana University Press, Bloomington, Indiana.

Holman, J. A., 1979. Paleontology and geology of the Badwater Creek area, central Wyoming. Pt. 17. The late Eocene snakes. Annals of the Carnegie Museum 48:103-110.

Holman, J. A., 1977. Snakes of the Monroe Creek Formation (Lower Miocene: Arikareean) of Wyoming. Copeia 1977(1):193-194.

LaDuke, T. C. 1991. The fossil snakes of Pit 91, Rancho LaBrea, California. Contributions in Science 424:1-28.

Pyron, R. A., F. T. Burbrink, and J. J. Wiens. 2013. A phylogeny and revised classification of Squamata, including 4161 species of lizards and snakes. BMC Evolutionary Biology 13(93):1-77.

Rage, J.-C. 1984. Serpentes (Handbuch der Paläoherpetologie, v. 11), Gustav Fischer Verlag, Stuttgart, 80pp.

Smith, K. T., 2012. New constraints on the evolution of the snake clades Ungaliophiinae, Loxocemidae and Colubridae (Serpentes), comments on the fossil history of erycine boids in North America. Zoologischer Anzeiger 252(2):157-182.

Szyndlar, Z., 1984. Fossil snakes from Poland. Acta Zoologica Cracoviensia 28(1):1-156.

Szyndlar, Z., and J.-C. Rage, 2003. Non-erycine Booidea from the Oligocene and Miocene of Europe. Polish Academy of Sciences, Institute of Systematics and Evolution of Animals, Krakow, 109pp.

Szyndlar, Z., and W. Boehme, 1996. Redescription of *Tropidonotus atavus* von Meyer, 1855 from the Upper Oligocene of Rott (Germany) and its allocation to *Rottophis* gen. nov. (Serpentes, Boidae). Palaeontographica Abteilung A Palaeozoologie-Stratigraphie 240(4-6):145-161.

# CHAPTER 4

# GENERAL CONCLUSION

The remarkable preservation of UW11120 has provided the first opportunity to study the cranial and vertebral evolution of a New World fossil snake that is clearly not an Old World erycine snake, but a member of a new clade of North Amercian Cenozoic and modern snakes, the Charininae. Using the nearly complete vertebral columns of the invividuals preserved on UW11120, it is recognized here that different sections of the column display the variation used to distinuguish vertebral form genera and species assigned to the fossil taxa *Ogmophis* (Cope, 1873) and *Calamagras* (Cope, 1883). Thus, the argument has been made that the type material for these various form genera and species is insufficient to define and diagnose those taxa. For example, the holotype specimen for *Ogmophis oregonensis* has been lost for over a century, and all that remains is a poor image from Cope (1884); as an image cannot serve as a type, and as each new vertebra or vertebral string bears form taxon differences to Cope's (1884) illustration, the type should likely be considered a nomen dubium. Isolated or short strings of vertebrae do not provide enough morphological information to distinguish a biologically relevant taxon at the generic level, and often not even the familial level. Sampling from just one small area of the trunk of an extant snake axial skeleton does not serve to define and diagnosis that taxon, and certainly does not encompass the full morphological variation of vertebrae that is present in that individual. There is undeniably a long tradition of creating vertebral form taxa for fossil snakes, but it is not a tradition that can be justified either empirically or philosophically, and thus should be abandoned. Creating form taxa in open nomenclature (e.g., Taxon A, Taxon B) is far superior to creating formalized Linnean binomials that require complex taxonomic revisions in the face of new empirical evidence.

The type material of UW11120 is one such new and important piece of empirical evidence. Because the specimen UW11120 includes the full vertebral column and cranial material, within which the diagnostic features of both *Calamagras* and *Ogmophis* are found, the specimens assigned to these form taxa can now be referred to the new taxon, *Congerophis.* The taxonomic fate of *Ogmophis* and *Calamagras* are problematic in the extreme. As *Ogmophis* is the junior subjective synonym of *Calamagras*, it is possible to refer species of *Ogmophis* to *Calamagras.* However, it is also more sensible to refer species of *Ogmophis* to *Congerophis*, and certainly to reassign specimens, apart from the holotype specimens, to *Congerophis.*

Three species previously assigned to the new synonyms are transferred to a new combination: *Congerophis murivorous, C. angulatus,* and *C. arenarum.* Two species of great morphologic similarity but great temporal disparity with

*Congerophis lego, Calamagras primas* and *Calamagras floridanus,* must be considered cf. *Congerophis lego* until their temporal and geographic ranges are better resolved. All other species previously assigned to *Calamagrs* or *Ogmophis* that have not been otherwise assigned (ie. excluding *C. weigeli* and *O. compactus*, which were recently assigned to the Ungaliophiinae and Loxocemidae, Smith, 2012) must be considered *nomina dubia* until additional finds can describe the complete intracolumnar variability as distinct from *Congerohis lego* for these taxa.

The results of the phylogenetic analyses presented here make it very clear that the Erycinae s.l., including both Old and New World taxa, is not monophyletic. The characters that have traditionally been used to support this concept are not diagnostic of the group, and have thus depended on a single feature, the unique additional apophyses of the caudal vertebrae, a feature that is considered an anti-predatory mechanism (Greene, 1973). As has been recognized for some time, such a feature could easily be convergently evolved, a concept supported here by the results of my phylogenetic analyses. To recognize the new clade formed by the New World taxa, wehave proposed a new taxon, the Charininae, inclusive of *Congerophis* and *Charina,* while the Erycinae has been redefined to include only the Old World genus *Eryx.*

An unexpected result of this analysis, the close relationship of the Ungaliophiinae to the Charininae, is supported by the fossil record of both groups as it is distinctly North American. Smith (2012) recently reassigned an extinct North American taxon previously considered erycine s.l., *Calamagras weigeli,* to the subfamily Ungaliophiinae. *Congerophis lego* may represent an evolutionary intermediate between the Ungaliophiinae and the Charininae, though it does not present the character, "absence of hemopophyses through the caudal vertebral series" that is so characteristic of the Ungaliophiinae. The molecular support for the close relationship between the Ungaliophiinae and Charininae is strong, with some authors going so far as to reassign *Charina* to the subfamily Ungaliophiinae (Pyron, Burbink, and Weins, 2013), but this analysis is the first to support a close relationship using morphological data. The relationship certainly deserves further exploration, both phylogenetically and through the use of data from the fossil record.

It is clear from this study that an indept review of the fossil record of North American Cenozoic snakes is well overdue. Unfortunately, without complete specimens like UW11120 which can describe the full intracolumnar variation of a taxon, or detailed, locality-specific reviews like that of Smith (2012), it is difficult to assess the true, likely over-estimated, diversity of extinct snakes in North America. Studies like the present paper and Smith (2012) suggest that such assessments are possible, albeit dependent on spectacular new finds or museum "rediscoveries".

As an unfortunate limitation of molecular analyses of phylogenetic relationships, in the inability to sample extinct taxa; as a result, they are left out of the analysis and so the cladograms produce sistergroup relationships without the benefit of data from fossil taxa. However, on the positive side, molecular studies routinely examine relationships at the species level and thus have found the traditional concept of Erycinae to be polyphyletic. And as has been shown here, some morphological characters (i.e. the erycine s.l. tail) have been used as support for the traditional hypothesis of Ercyinae, but in fact are found to be convergently evolved. It seems, from the results of this investigation, that once again the fossil record, in the form of these beautifully preserved extinct snakes assigned to the new genus and species, *Congerophis lego,* is an excellent arbitrator of hypotheses derived from the extant, but often competing data sources of molecules and morphology. It is my hope that by providing detailed morphological descriptions and data on these new fossils, that old questions will be answered and new ones generated.

# LITERATURE CITED

Cope, E.D., 1873. Synopsis of new vertebra from the Tertiary of Colorado, obtained during the summer of 1873. Washington, D.C. U.S. Government Printing Office 1-19.

Cope, E.D., 1883. The Vertebrata of the Tertiary formations of the West. Book I. Reports of the United States Geological Survey of the Territories, F. V. Hayden, United States Geologist-in-Charge 3:1-1002.

Greene, H. W. 1973. Defensive tail display by snakes and amphisbaenians. Journal of Herpetology 7(3):143-161.

Pyron, R. A., F. T. Burbrink, and J. J. Wiens. 2013. A phylogeny and revised classification of Squamata, including 4161 species of lizards and snakes. BMC Evolutionary Biology 13(93):1-77.

Smith, K. T., 2012. New constraints on the evolution of the snake clades Ungaliophiinae, Loxocemidae and Colubridae (Serpentes), comments on the fossil history of erycine boids in North America. Zoologischer Anzeiger 252(2):157-182.

Appendix A:

List of morphological characters used in the first and second analysis. All characters are from Lee and Scanlon (2002) as modified by Palci et al. (2013).

(1) Premaxilla: anterior surface convex or straight (0); anterior surface concave (1).

(2) Ascending process of premaxilla: long and contacting frontals, i.e. extends entire snout-frontal distance (0); intermediate in length and not contacting frontals (1); extremely reduced or absent (2).

(3) Ascending process of premaxilla (excluding lateral flange, see next character): process transversely expanded, partly roofing external nares (0); process narrow or spine-like, separating but not roofing external nares (1).

(4) Ascending process of premaxilla: without lateral flange (0); with lateral flange forming dorsal margin of external naris (1).

(5) Nasal keel (process) of premaxilla: absent (0); moderately developed, short flange (1); well developed, long process (2).

(6) Palatal (vomerine) process of premaxilla: extensive overlapping contact with vomer (0); non-overlapping, point contact with vomer (1); not in contact with vomer (2); extensive sutural contact with vomer (3).

(7) Premaxillary palatal foramina: paired (0); single (1); multiple (2); absent (3).

(8) Main body of premaxilla: on anterior end of the snout (0); on ventral surface of snout (1).

(9) Snout shape: tapering anteriorly in front of orbits (0); spherical, expanded in front of orbits (1).

(10) Posterior margin of lateral process of premaxilla, in palatal view: oriented anterolaterally (0); oriented transversely, perpendicular to midline (1); oriented posterolaterally (2).

(11) Maxilla-premaxilla contact: close, suture or strong abutting contact (0); close but not abutting, connected by short ligament (1); loose, widely separated (2).

(12) Anterior (premaxillary) process of maxilla: well developed, forming ventral margin of external naris (0); poorly developed or absent, maxilla excluded from ventral margin of external naris (1).

(13) Dorsal (ascending or prefrontal) process of maxilla: well developed (0); poorly developed or absent (1).

(14) Anteromedial maxillary flange: present, small horizontal shelf on medial surface of anterior end of maxilla (0); absent, anterior end of maxilla

without such shelf (1). Note: *Varanus* exhibits state “1” (contra Lee and Scanlon, 2002).

(15) Lateral maxillary foramina: present (0); absent (1). This character refers to large discrete foramina on the middle part of the maxilla, and does not include any small indistinct foramina at anterior or posterior tips.

(16) Maxilla: alveolar (tooth) row oriented longitudinally (0); 1, alveolar (tooth) row oriented transversely (1).

(17) Maxilla-palatine articulation: located anteriorly, at or in front of anterior orbital margin (0); located beneath anterior half of orbit (1); located posteriorly, at same level as center of orbit or further posterior (2).

(18) Palatine process of maxilla: absent, medial margin of maxilla smooth or with (at most) indistinct swelling (0); present, medial margin of maxilla with distinct process (1). Note: *Haasiophis* exhibits state “1” (contra Lee and Scanlon, 2002).

(19) Palatine process of maxilla: does not approach pterygoid, palatine broadly enters suborbital fenestra (0); contacts pterygoid, excluding palatine from suborbital fenestra (1). Inapplicable in taxa lacking a well-developed palatine process.

(20) Palatine process of maxilla: dorsomedial surface pierced by a large foramen (0); not pierced (1).

(21) Ectopterygoid flange of maxilla: maxilla without distinct posteromedial (ectopterygoid) expansion or flange (0); maxilla with weak but distinct posteromedial (ectopterygoid) expansion or flange (1); maxilla with large posteromedial (ectopterygoid) expansion or flange (2).

(22) Posterior extent of maxilla: does not reach middle of orbit (0); reaches middle of orbit, or slightly further (1); extends past posterior margin of orbit (2).

(23) Nasal: does not closely approach lateral process of premaxilla (0); extends anteriorly to almost reach lateral process of premaxilla (1).

(24) Horizontal lamina of nasal: narrow anteriorly, tapering to a point beside premaxilla (0); horizontal lamina of nasal wide anteriorly, at most tapering only slightly to a blunt anterior end (1). Not applicable in taxa where the nasals are vestigial or absent.

(25) Horizontal lamina of nasal: posterior margin wide (0); posterior margin narrow, tapering to a posteromedial point (1). This character does not include the median vertical flange, which can extend past the wide posterior margin of the horizontal lamina.

(26) Nasal-frontal contact: horizontal laminae of nasals and frontals in contact (0); horizontal laminae of nasals and frontals not in contact (1).

(27) Nasal-frontal contact: nasals overlap frontals dorsally (0); frontals overlap nasals dorsally (1); clasping junction, nasal fits into anterior groove in frontal and is thus overlapped and underlapped by frontal (2).

(28) Nasal-frontal boundary: concave posteriorly in dorsal view (0); approximately straight and transverse (1); convex posteriorly (2); W-shaped, nasals project posteriorly into embayments in frontals (3).

(29) Descending laminae of nasals: not enlarged (shallow) anteriorly (0); distinctly enlarged (very deep) anteriorly (1); absent (2). *Varanus*, *Heloderma*, *Lanthanotus* and Mosasauroidea have been recoded as having state 2.

(30) Anterior process of prefrontal: moderately developed, triangular flange (0); greatly reduced (1); greatly elongated process (2).

(31) Anterodorsal lappet of prefrontal, extending along lateral margin of nasal: absent or indistinct (0); distinct process (1).

(32) Prefrontal-nasal contact: prefrontal separated from nasal by external naris (0); prefrontal contacts nasal (1); prefrontal separated from nasal by ragged fissure that is not part of external naris (2); prefrontal separated from nasal by frontal-maxillary contact (3).

(33) Prefrontal-maxilla contact: anterior process and ventrolateral margin of prefrontal contact maxilla (0); anterior process of prefrontal does not

contact maxilla and projects freely, only ventrolateral margin of prefrontal contacting maxilla (1); anterior process and ventrolateral margin of prefrontal do not contact maxilla (2).

(34) Prefrontal-maxilla contact on facial region: tight or interdigitating, relatively rigid (0); flat or slightly convex surfaces, allowing rocking or sliding motion (1).

(35) Antorbital buttress of prefrontal: lateral foot process does not contact palatine (0); lateral foot process contacts palatine (1).

(36) Antorbital buttress of prefrontal: medial foot process does not contact maxilla (0); medial foot process contacts maxilla (1). Not applicable in anomalepidids and typhlopids, which have a highly modified maxilla. *Varanus*, *Heloderma* and *Lanthanothus* were recoded as not applicable, because they lack medial and lateral "foot processes" of the prefrontal.

(37) Lateral process of palatine: does not reach lateral edge of maxilla (0); reaches lateral edge of maxilla (1).

(38) Outer orbital (lateral) margin of prefrontal, in lateral view: slants anteroventrally (0); vertical (1).

(39) Prefrontal lacrimal duct roof: absent (0); present, a horizontal flange extending anteriorly from lacrimal foramen (1).

(40) Prefrontal-frontal contact: approximately straight (0); curved, prefrontal fitting into deep embayment in frontal (1).

(41) Prefrontal-frontal contact: oriented approximately parasagittally, prefrontals contact only lateral margins of frontals and are widely separated (0); oriented anteromedially, prefrontals contact anterolateral margins of frontals and are moderately separated (1); oriented anteromedially or transversely, prefrontals closely approaching or contacting one another (2).

(42) Prefrontal-frontal contact: prefrontal sutured to or tightly buttressed against frontal (0); prefrontal moveably articulated to frontal (1).

(43) Antorbital (vertical) buttress of prefrontal: broad, extends medially underneath lateral descending flanges of frontal (0); narrow, does not extend medially to reach lateral descending flanges of frontal (1).

(44) Lacrimal foramen: completely enclosed by prefrontal (0); between prefrontal and palatine (1); between prefrontal and maxilla (2); between prefrontal and lacrimal (3).

(45) Jugal: present (0); absent (1).

(46) Postorbitofrontal ossification(s) in adults: one discrete ossification, conventionally termed the postorbitofrontal (0); two discrete ossifications,

conventionally termed the postfrontal and postorbital (1); no discrete ossifications (2).

(47) Postorbitofrontal ossification(s): forked medial margin, anterior and posterior rami tightly clasping frontoparietal suture (0); not forked medially, without distinct anterior and posterior rami, abutting skull roof (1). Not applicable in taxa lacking postorbitofrontal ossification(s).

(48) Prefrontal and postorbitofrontal ossification(s): widely separated, frontal broadly enters orbit (0); narrowly separated, frontal narrowly enters orbit (1); in contact, frontal excluded from orbit (2).

(49) Lateral process of parietal: lateral process distinct (0); lateral process absent (1). The lateral process of the parietal is situated immediately behind the posterior orbital ossification(s), when these elements are present.

(50) Posterior orbital margin: complete, closed by postorbital contacting jugal (0); complete, closed by postorbital contacting ectopterygoid-maxilla unit (1); incomplete (2).

(51) Frontal shape: 0, frontals gradually tapering anteriorly (0); frontals rectangular, at most slightly constricted in middle (1); frontals gradually tapering posteriorly (2); frontals greatly constricted in middle (3).

(52) Anterior tab of frontal: distinct and well defined (0); poorly defined or absent (1). This character refers to a transverse ridge on the anterior margin of the frontal which underlaps the prefrontal and nasal.

(53) Frontal-parietal contact (dorsal aspect): mostly straight and transverse, slight median notch in frontals at most (0); anteriorly concave, i.e. frontals extending posteriorly into broad median embayment in parietals (1); complex W or M shape (2).

(54) Subolfactory (lateral descending) processes of frontal: not contacting one another ventromedially (0); meeting ventromedially, below medial descending processes of frontal if present (1); absent (2).

(55) Medial descending processes of frontal: absent (0); present (1).

(56) Medial descending processes of frontal: meeting with subolfactory (lateral descending) frontal processes at the mesial frontal suture (0); fused to subolfactory frontal processes, mesial frontal suture obliterated (1).

(57) Mesial frontal suture: on ventral portion of interolfactory pillar (0); on middle of interolfactory pillar (1).

(58) Length of main body of parietal (i.e. excluding supraorbital or posterior processes): short, at most 40% skull (snout-occiput) length (0); intermediate, between 40 and 55%of skull length (1); long, at least 55% of skull length (2).

(59) Suture between frontal and parietal descending flanges: in lateral view, suture between frontal and parietal extends approximately vertically, or slightly anterodorsally (0); suture greatly inclined anterodorsally, i.e. closer to the horizontal than the vertical (1); suture curved, extending vertically in its ventral portion and becoming horizontal more dorsally (2).

(60) Optic foramen: posteriorly located, posterior border forming a deep notch in parietal(0); intermediate position, posterior border formed by straight margin of parietal (1); anteriorly located, posterior border within frontal (2).

(61) Optic foramen: opening faces anterolaterally (0); opening faces laterally (1).

(62) Anterior (supraorbital) process of parietal: absent or poorly developed (0); enlarged, extending along at least 50% of lateral margin of frontal (1).

(63) Posterior border of parietal: with distinct median notch (0); without distinct median notch (1).

(64) Posterior border of parietal: without median projection over supraoccipital (0); with median projection over supraoccipital (1).

(65) Posterolateral (supratemporal or suspensorial) process of parietal: well developed, posterolateral margin of parietal with a distinct flange (0);

reduced, posterolateral margin of parietal with a triangular corner (1); absent, posterolateral margin of parietal rounded (2).

(66) Descending flange of parietal: without horizontal crest (0); with very large horizontal crest, extending from orbital region towards prootic (1).

(67) Descending flange of parietal: does not contact anterior margin of base of basipterygoid process (0); broadly contacts anterior margin of base of basipterygoid process (1).

(68) Supratemporal: large, quadrate contacts supratemporal but not otic capsule (0); vestigial, quadrate contacts supratemporal and otic capsule (1); absent, quadrate contacts otic capsule only (2).

(69) Supratemporal: posterior end projecting greatly beyond otoccipital (0); posterior end projecting slightly beyond otoccipital (1); posterior end not projecting beyond otoccipital (2).

(70) Supratemporal: does not substantially cover dorsolateral surface of prootic (0); covers almost the entire dorsolateral surface of prootic (1). Not applicable in taxa with vestigial (or absent) supratemporals.

(71) Supratemporal: anterior tip well behind anterior margin of prootic (0); anterior tip slightly behind anterior margin of prootic (1); anterior tip in line with or in front of anterior margin of prootic (2).

(72) Quadrate: without small ossification (‘stylohyal’) on medial surface, contacting stapes (0); with such ossification (1).

(73) Dorsoposterior ( = suprastapedial) process of quadrate: distinct, large (0); indistinct, small or absent (1).

(74) Dorsoposterior (suprastapedial) process of quadrate: projects posteroventrally, forming acute angle with quadrate shaft (0); projects posteriorly, forming approximately a right or slightly obtuse angle with quadrate shaft (1); projects posterodorsally, forms very obtuse angle with quadrate shaft in lateral view (2). Cannot be scored in taxa lacking a prominent process.

(75) Length of quadrate shaft (i.e. excluding suprastapedial process): short, maximum length along shaft no more than 25% of snout-occiput length (0); long, more than 25% of snout-occiput length (1).

(76) Cephalic condyle of quadrate: situated dorsally, approximately level with dorsal margin of prootic (0); situated ventrally, well below level of dorsal margin of prootic (1). Note: *Lanthanotus*, *Varanus* and Dibamidae exhibit state 1 (contra Lee and Scanlon, 2002).

(77) Quadrate shaft: inclined slightly anteroventrally (0); inclined greatly anteroventrally (1); vertical (2); inclined posteroventrally (3).

(78) Septomaxilla: projects anterolaterally, overlapping lateral process of premaxilla and/or anterior tip of the maxilla (0); does not project anterolaterally, not overlapping lateral process of premaxilla or anterior tip of maxilla (1).

(79) Dorsolateral flange of septomaxilla: blunt, without spine, expansion or calcified ligament (0); with spine projecting posterolaterally (1); with posterior expansion projecting posteromedially towards frontal (2); with calcified ligament (3).

(80) Septomaxilla: maxilla, but not septomaxilla, contributes to posterior border of the external naris (0); septomaxilla with lateral flange contributing to the posterior border of the external naris (1).

(81) Septomaxilla-frontal contact: posteromedial flange of septomaxilla short, not contacting frontal (0); posteromedial flange of septomaxilla long, contacting frontal adjacent to midline on lower part of interolfactory pillar (1).

(82) Fenestra for duct of Jacobson's organ: faces ventrally (0); faces posteroventrally (1).

(83) Vomer: does not enter lateral margin of fenestra for Jacobson's organ (0); forms posterior part of lateral margin of fenestra for Jacobson's organ (1).

(84) Vomeronasal nerve: does not pierce the ridge on the vomer forming the posterior wall of the vomeronasal organ (0); pierces ridge via a single large foramen (sometimes with one or two additional small foramina) (1); pierces ridge through a cluster of numerous small foramina (2).

(85) Medial fenestra in vomeronasal cupola: posterior ends of sagittal flanges of vomer and septomaxilla with small or no contact, and large intervening fenestra or embayment (0); posterior ends of sagittal flanges of vomer and septomaxilla in extensive contact, with small or no intervening fenestra (1).

(86) Palatine length (excluding posteromedial process): short anteroposteriorly (much shorter than vomer)(0); intermediate in length anteroposteriorly (as long as vomer)(1); long anteroposteriorly (much longer than vomer)(2).

(87) Horizontal (palatal) lamina of vomer: 0, posterior end narrow, tapering to a point, choana wide (0); posterior end expanded, choana narrow (1).

(88) Vertical (posterior dorsal) lamina of vomer: small or absent (0); well developed (1).

(89) Palatine-vomer contact: medial (choanal) process of palatine with extensive contact with vomer (0); tiny point contact (1); no contact (2).

(90) Palatine-vomer articulation: medial (choanal or vomerine) processes of palatines do not project ventromedially to separate vomers (0); medial processes of palatines project ventromedially to separate the posterior portions of the vomers (1).

(91) Medial (choanal or vomerine) process of palatine: anteroposteriorly broad plate of bone (0); narrow finger-like process (1).

(92) Medial (choanal or vomerine) process of palatine: without distinct, large anterior flange (0); with distinct, large plate-like anterior flange, abutting vomer posterolaterally (1).

(93) Anterior process of palatine: no anterior process, only medial (choanal or vomerine), lateral (maxillary) and posteromedial (pterygoid) processes present (0); narrow (`dentigerous') process present, in addition to medial, lateral and posteromedial processes (1); wide horizontal plate present (2).

(94) Anterior process of palatine: contacting vomer-septomaxilla complex (0); not contacting vomer-septomaxilla complex (1).

(95) Palatine-maxilla contact: palatine sutured to maxilla (0); palatine meets maxilla in a loose joint (1); palatine does not contact maxilla (2).

(96) Lateral (maxillary) process of palatine: situated in middle or anterior end of main body of palatine (0); at posterior end of main body of palatine (1).

(97) Lateral process of palatine: pierced by foramen (0); lacking foramen (1). This foramen carries the palatine ( = sphenopalatine, = maxillary branch of trigeminal) nerve in extant taxa.

(98) Articulation of palatine with pterygoid: 0, medial pterygoid process of palatine absent (0); medial pterygoid process of palatine present (1).

(99) Pterygoid tooth row curvature: concave medially (0); 1, straight to slightly convex medially (1).

(100) Ectopterygoid process of pterygoid: well developed, a large rectangular or triangular lateral process (0); poorly developed, a small rounded lateral flange (1); absent (2).

(101) Ectopterygoid attachment to pterygoid: anterior to basipterygoid process (0). lateral to basipterygoid process (1); posterior to basipterygoid process (2).

(102) Pterygoid quadrate ramus: robust, platelike (0); gracile, rod-like (1).

(103) Pterygoid medial margin: 0, with distinct medial spur in region of basicranial articulation (0); with smooth medial bulge (1); with straight margin (2).

(104) Pterygoid quadrate ramus: with a shallow groove along ventromedial surface, or no groove (0); with a very deep groove along ventromedial surface, becoming dorsomedial posteriorly (1).

(105) Pterygoid quadrate ramus: vertical or oblique sheet (0); approximately horizontal sheet (1).

(106) Pterygoid quadrate ramus: terminates near jaw joint (0); projects posteriorly well past jaw joint (1).

(107) Ectopterygoid: present (0); absent (1).

(108) Ectopterygoid-pterygoid contact: clasps pterygoid on both dorsal and ventral surfaces (0); simple overlap on only ventral surface of pterygoid (1); simple overlap on only dorsal surface of pterygoid (2); simple contact on only lateral edge only of pterygoid (3).

(109) Ectopterygoid-maxilla contact: 0, posterior tip of the maxilla abuts ectopterygoid (0); posterior tip of the maxilla is lifted off ectopterygoid and projects freely (1).

(110) Ectopterygoid-maxilla contact: anterior end of ectopterygoid restricted to posteromedial edge of maxilla (0); ectopterygoid invades significantly the dorsal surface of the maxilla (1).

(111) Ectopterygoid shape: distal end of ectopterygoid with single anterior process projecting dorsally along maxilla (0); distal end of ectopterygoid with two anterior processes projecting dorsally along maxilla (1). Not applicable in taxa where this region of the maxilla is invaded by the jugal,

or in amphisbaenians and dibamids (where the ectopterygoid either has a complex suture with the maxilla, or projects ventrally beneath the maxilla).

(112) Lateral edge of the ectopterygoid: straight or slightly curved, lacking distinct angulation (0); distinctly angulated, a distinct 'corner' present between the anterior (parasagittally oriented) and posterior (posteromedially oriented) portions of the lateral margin (1).

(113) Cultriform process: anterior one-third broad posteriorly and tapering anteriorly (0); anterior one-third narrow throughout (1). Not applicable in the outgroups, because they all possess a much shorter cultriform process (i.e., the part corresponding to the anterior one-third in snakes is not ossified).

(114) Interchoanal keel of cultriform process: absent (0); present, a sagittal flange extending ventrally between the medial processes of the palatines (1). Not applicable in taxa with a short cultriform process.

(115) Parabasisphenoid transverse width behind frontal descending flanges: narrow, without concave ventral surface (0); broad and ventrally concave (1).

(116) Basipterygoid process: prominent, i.e. a pedicel or flange projecting far laterally with distinct distal facet (0); 1, weak, consisting of a crest or mound without a distinct distal facet (1); absent (2).

(117) Distal surfaces (facets or crests) of basipterygoid processes: long axes oriented obliquely, or transversely in ventral view (0); long axes oriented parasagitally in ventral view (1).

(118) Parabasisphenoid ( = sphenoid): sphenoid wing absent, no triangular dorsolateral prominence lateral to alar process of dorsum sellae (0); sphenoid wing present as triangular prominence distinct from alar process, extending up anterior margin of prootic below the trigeminal notch (1).

(119) Ventral surface of parabasisphenoid: smooth posteriorly, lacking keel (0); with median keel in posterior region, at level of posterior openings of vidian canals (1); with pair of parasagittal keels (2). This character is distinct from the ‘interchoanal keel’ of the cultriform process, which is situated much more anteriorly.

(120) Basioccipital-parabasisphenoid suture: 0, positioned midway between fenestra ovalis and trigeminal foramen (0); posteriorly positioned, closer to fenestra ovalis than to trigeminal foramen (1); anteriorly positioned, closer to trigeminal foramen than to fenestra ovalis (2).

(121) Basioccipital: with short posterolateral flanges (0); with long posterolateral processes (1).

(122) Posterior opening of vidian canal: within basisphenoid, not bordered by prootic (0); partly bordered by prootic (i.e., on basisphenoid-prootic suture) or entirely within prootic (1).

(123) Vidian canal: does not open intracranially (0); opens intracranially, emerging on internal surface of sphenoid (primary opening) then emerging externally on sphenoid-parietal suture (secondary opening)(1).

(124) Vidian canals: symmetrical (0); asymmetrical, left larger than right or vice versa (1).

(125) Hypophysial pit (sella turcica): without distinct anterior bony boundary (0); bounded anteriorly by distinct ridge (1).

(126) Cerebral carotid artery: opens into posterior region of hypophysial pit, near posterior transverse wall (0); opens into middle region of hypophysial pit, well away from posterior transverse wall (1).

(127) Dorsum sellae (crista sellaris): well developed (0); greatly reduced (1).

(128) Dorsum sellae (crista sellaris): oriented anterodorsally, overhanging the posterior portion of hypophysial pit (0); oriented dorsally, not overhanging hypophysial pit (1). Not applicable if dorsum sellae is weakly developed. *Lanthanotus* has been recoded as having state 0.

(129) Laterosphenoid: absent, V2 and V3 exits of trigeminal foramen confluent (0); present, fuses to prootic forming vertical bar between exits of V2 and V3 (1).

(130) Alar process of prootic: long distinct process projecting anteriorly well past trigeminal (V) foramen/notch (0); short process not projecting past trigeminal (V) foramen/notch (1).

(131) Trigeminal foramen, anterior margin: closed by parietal at least medially, upper and lower anterior processes of prootic may touch superficially lateral to the parietal (0); closed by prootic, deep contact or fusion of prootic processes excludes parietal from opening (1).

(132) Exit foramen for the facial (VII) nerve (hyomandibular branch, if distinct): 0, located outside the opening for the mandibular branch of the trigeminal nerve (V3, or V2-V3)(0); located within the opening (1).

(133) Sulcus connecting exit foramen of palatine branch of facial (VII) nerve with posterior opening of vidian canal: weakly recessed, with shallow and smooth margins (0); deeply recessed, with sharply defined anterior and often also posterior margins (1); embedded, closed laterally forming a tunnel in prootic (2).

(134) Crista circumfenestralis: juxtastapedial recess bordered by crests which may extend directly laterally but do not converge (0); juxtastapedial recess

surrounded by crests which converge to partly enclose stapedial footplate, much of footplate remains exposed laterally (1); juxtastapedial recess surrounded by crests which converge to largely enclose stapedial footplate (2).

(135) Supratemporal-supraoccipital contact: supratemporal and supraoccipital separated by dorsal exposures of parietal and exoccipital (0); supratemporal and supraoccipital separated by dorsal exposures of prootic, parietal and exoccipital (1); supratemporal and supraoccipital in contact (2).

(136) Paroccipital process: long process (0); distinct flange (1); indistinct bump or absent (2).

(137) Supraoccipital: external (dorsoposterior) surface with no, or very weak transverse ridge (0); external surface with moderate transverse ridge (1); external surface with very high transverse ridge (2).

(138) Supraoccipital dorsal exposure: long, sagittal dimension more than 50% transverse dimension (0); short, sagittal dimension less than 50% transverse dimension (1).

(139) Supraoccipital-prootic contact: narrow, less than half supraoccipital-parietal contact (0); broad, subequal to or as long as supraoccipital-parietal contact (1).

(140) Exoccipital separation dorsal to foramen magnum: exoccipitals widely separated above foramen magnum (0); 1, exoccipitals with point contact above foramen magnum (1); exoccipitals in extensive median contact above foramen magnum (2).

(141) Exoccipital separation ventral to foramen magnum: exoccipitals separated below foramen magnum, not in contact along dorsal midline of occipital condyle (0); exoccipitals in contact below foramen magnum, along dorsal midline ofoccipital condyle (1).

(142) Occipital condyle: dorsal surface deeply concave, i.e. with deep 'fovea dentis' (0); dorsal surface slightly concave at most, i.e., with shallow or no 'fovea dentis' (1).

(143) Stapedial shaft: straight (0); angulated (1).

(144) Stapedial shaft: slender and longer than diameter of stapedial footplate (0); thick and not longer than diameter of footplate (1).

(145) Distal end of stapes: associated with dorsal tip of suprastapedial process of quadrate (0); associated with ventral end of suprastapedial process and dorsal end of quadrate shaft, i.e. cephalic condyle (1); associated with middle or ventral half of quadrate shaft (2).

(146) Dentary length: dentary long, more than 40% of main mandible length, i.e., length excluding retroarticular process (0); dentary short, less than 40% of main mandible length (1).

(147) Mental foramina on lateral surface of dentary: two or more (0); one (1).

(148) Posterolateral margin of dentary: notch absent, posterolateral margin of dentary straight or slightly concave, dorsoposterior and ventroposterior processes indistinct (0); with shallow notch, processes short (1); with deep notch, processes long (2).

(149) Dentary posterior margin: dorsal posterior process does not extend much further than ventral posterior processes (0); dorsal process extends much further posteriorly than ventral process (1).

(150) Posteromedial shelf of dentary: not exposed medially (0); exposed medially (1).

(151) Meckel's canal (groove): lacks floor anteriorly, open ventrally anterior to level of anterior inferior alveolar foramen (0); floored by a horizontal ventral lamina for its full length (1); enclosed anteriorly, with ventral and medial lamina (2).

(152) Splenial: splenial present as discrete element (0); splenial not present as discrete element (1).

(153) Splenial size: small, extends no more than 50% of distance from intramandibular joint to symphysis (0); large, extends more than 50% of distance from intramandibular joint to symphysis (1).

(154) Splenial-angular joint: vertical in medial view (0); highly oblique in medial view (1). Only scorable in taxa with a straight, simple joint.

(155) Foramen within splenial ( = inferior alveolar foramen): present (0); absent (1).

(156) Dorsal margin of splenial: deeply notched, posterior region of notch bordered dorsally by anterodorsal spine (0); moderately notched, posterior region of notch not bordered dorsally by anterodorsal spine (1); smooth, not notched (2).

(157) Splenial-coronoid contact: posterior end of splenial in broad contact with coronoid (0); posterior end of splenial only just reaches coronoid (1); posterior end of splenial does not contact coronoid (2). Not applicable in taxa lacking either element.

(158) Splenial lateral exposure: anterior portion of splenial not exposed laterally (0); anterior portion of splenial greatly exposed laterally (1).

(159) Coronoid: coronoid large and distinct (0); coronoid greatly reduced and sometimes fused to compound (1); coronoid never present as distinct element (2).

(160) Coronoid: with posteroventral process or expansion (0); without posteroventral process or expansion (1).

(161) Coronoid lateral exposure: coronoid overlaps lateral surface of surangular and is exposed in lateral view (0); coronoid does not overlap lateral surface of surangular, but projects dorsally beyond it and is thus well exposed in lateral view (1); coronoid entirely medial to surangular and is largely covered in lateral view (2).

(162) Coronoid-angular contact: coronoid and angular separated by prearticular, or prearticular portion of compound bone (0); coronoid contacts angular (1).

(163) Coronoid dorsal process: well developed, distinct projection (0); poorly developed or absent, smooth rounded crest at most (1).

(164) Surangular eminence: compound postdentary element without dorsal eminence (0); surangular portion of compound with dorsal crest or process lateral to adductor fossa (1); prearticular portion of compound with ascending process medial to adductor fossa (2).

(165) Adductor fossa: posterior region exposed medially, prearticular dorsal margin lower than surangular dorsal margin (0); posterior region exposed dorsally only, prearticular about equal in height to surangular (1);

posterior region exposed laterally only, prearticular higher than surangular (2).

(166) Anterior surangular foramen: situated posteriorly, below apex of coronoid process or more posterior (0); situated anteriorly, between apex and anterior limit of coronoid process (1); situated far anteriorly, in front of anterior limit of coronoid process (2).

(167) Lateral crest of compound element, extending anteriorly from articular cotyle along ventrolateral surface of mandible: absent (0); present (1). The crest represents the attachment of superficial adductor and/or pterygoideus muscles.

(168) Articular-surangular fusion: articular and surangular not fully fused in region of articular facet (0); articular and surangular fully fused in region of articular facet (1).

(169) Retroarticular process length: long, longer than articular facet (0); short, not longer than articular facet (1).

(170) Dorsal flange of retroarticular process: absent (0); present (1).

(171) External grooves and ridges on tooth bases: present, surface of bases of mature tooth crowns with vertical ridges and grooves (0); absent, surface of bases of mature tooth crowns smooth (1).

(172) Premaxillary teeth: present (0); absent (1).

(173) Premaxillary tooth number: three or more alveoli on each side of the midline (0); one or two alveoli on each side (1).

(174) Maxillary teeth: nearly uniform in size, at most only slightly larger in middle of tooth row, with uniform gradation (0); distinctly larger near middle of tooth row, smaller anteriorly and posteriorly (1); distinctly larger near anterior end of tooth row, smaller in middle and posteriorly (2); larger posteriorly (3).

(175) Maxillary teeth: nine or more alveoli (0); eight or fewer alveoli (1).

(176) Dentary teeth: eight or more alveoli (0); seven or fewer alveoli (1).

(177) Alveoli (in middle of maxilla and dentary): not expanded transversely (0); wider transversely than anteroposteriorly (1). Note: because true alveoli are not present in pleurodont taxa, this character was coded as inapplicable in *Heloderma*, *Lanthanotus*, *Varanus*, Amphisbaenia, Dibamidae and scolecophidians.

(178) Palatine teeth: absent (0); present (1).

(179) Palatine teeth: nine or more alveoli (0); eight or fewer alveoli (1).

(180) Pterygoid teeth: present (0); absent (1).

(181) Pterygoid teeth: twelve or more alveoli (0); eleven to nine alveoli (1); eight or fewer alveoli (2).

(182) Median (basihyal) element: present, uniting hyoid cornua (0); absent (1).

(183) First branchial arch elements: present (0); absent, replaced by caudal extensions of the lateral edge of the basihyal (if present)(1).

(184) Hyoid cornua: diverging sharply posteriorly (0); diverging only slightly posteriorly (1); parallel (2).

(185) Number of presacral vertebrae: less than 120 (0); 120–160 (1); 160–200 (2); over 200 (3).

(186) Number of caudal vertebrae: more than 20 (0); fewer than 20 (1).

(187) Dorsoposterior process on atlas neural arch, overlying axis neural arch: present, well developed (0); absent or very weak (1).

(188) Second (axis) intercentrum: not fused to anterior region of axis centrum, suturally connected at most (0); fused to anterior region of axis centrum (1).

(189) Neural spine height: well-developed process (0); low ridge, or absent (1).

(190) Posterior margin of neural arch: shallowly concave in dorsal view (0); with deep, V-shaped embayment in dorsal view exposing much of centrum in front of condyle (1). Comparisons are restricted to mid-trunk elements, in order to avoid intracolumnar variability.

(191) Zygosphene buttress: with deeply concave anterior edge, i.e. deeply notched between zygosphenes (0); with shallowly concave anterior edge, i.e., slightly notched between zygosphenes (1); with straight or slightly

sinuous anterior edge, i.e., not uniformly concave between zygosphenes (2).

(192) Condyles of mid-trunk vertebrae: oval, sagittal dimension much less than transverse diameter (0); round, sagittal dimension similar to transverse dimension (1). Comparisons of this and the next character are restricted to mid-trunk elements, in order to avoid intracolumnar variability, which remains inadequately described for all taxa.

(193) Condyles of mid-trunk vertebrae: facing very dorsally, ventral edge (at most) of condyle surface exposed in ventral view (0); facing posteriorly, or posterodorsally, much of condyle surface exposed in ventral view (1).

(194) Precondylar constriction of centrum: absent or very weak (0); moderate (1); strong (2).

(195) Orientation of zygapophyses of mid-trunk vertebrae: steeply inclined medially, 30° or more from the horizontal (0); moderately inclined medially, between 15° and 30° from the horizontal(1); not inclined medially, less than 15° from horizontal (2).

(196) Paracotylar foramina (foramen on anterior surface between cotyle and transverse process): present on most or all vertebrae (0); absent or present only on a few vertebrae (1).

(197) Parazygantral foramina (foramen on posterior surface of neural arch, between zygantrum and postzygapophyseal facets): absent on all vertebrae (0); numerous small pits in parazygantral area (1); large, single foramen present on each side (2).

(198) Subcentral foramina: uniform throughout column, small and paired in most vertebrae (0); irregular, being either small and paired, absent, or single and large, in different vertebrae (1).

(199) Prezygapophyseal process: absent (0); present as a small process extending laterally from prezygapophyseal facet (1); present as a prominent process extending laterally from prezygapophyseal facet (2).

(200) Hypapophyses: present on anterior eight cervicals or fewer (0); present up to at least cervical ten, but absent in mid- and posterior trunk (1); present throughout trunk, but poorly developed in posterior trunk (2); present throughout trunk, well developed throughout (3).

(201) Ventral surface of centra: mid-trunk vertebrae with smooth, transversely convex ventral surface (0); mid-trunk vertebrae bearing single median hemal keels, this keel may merge posteriorly with the hypapophysis, if present (1).

(202) Lymphapophyses: fewer than three forked free ribs or lymphapophyses (0); three or more freeending cloacal vertebrae with lymphapophyses (1); absent (2).

(203) Caudal vertebrae: with posteroventral projections (0); without posteroventral projections (1). *Eupodophis* and *Haasiophis* possess typical chevron bones (contra Rieppel and Head, 2004) and they have been coded accordingly for this and the next two characters. The "sagittal, unpaired pedicels" reported in *Eupodophis* by Rieppel and Head (2004) are nothing else than the anteroventrally directed transverse processes of the caudal vertebrae and do not represent unique neomorphic structures to which the chevrons would articulate.

(204) Posteroventral elements of caudals: articulate with centrum (0); fuse with centrum (1).

(205) Posteroventral elements of caudals: distally fused (chevrons)(0); distally separated (hemapophyses)(1); single median element (caudal hypapophyses)(2).

(206) Ribs: tuber costae ( = tuberculum, tuberculiform process, dorsal process) of rib absent or weakly developed (0); tuber costae well developed (1). Note: *Haasiophis* was coded as having state "0".

(207) Ribs: slender throughout body (0); thickened and heavily ossified (pachyostotic) in middle region of body (1).

(208) Pelvic girdle: three elements present (0); two elements present (1); single element present (2); no elements present (3).

(209) Pelvis: external to sacral or cloacal ribs (0); internal to sacral or cloacal ribs (1).

(210) Hind limbs: hind limbs present, with distinct femur, tibia and fibula (0); hind limbs vestigial, with one bone (femur) only, sometimes with a single distal spur (1); hind limbs absent (2).

(211) Sacral vertebra/ae: present (0); absent (1).

(212) Cervical intercentra posterior to the axis: fused to centrum (0); not fused to centrum (1).